The fate and transport of nutrients in shallow groundwater and soil of an urban slum area in the city of Kampala, Uganda.

MSc. Thesis (2012)

J.C.N.Havik, Utrecht University.

Under supervision of:

ir. P.M. Nyenje (UNESCO-IHE institute for water education)

dr. J.W.Foppen (UNESCO-IHE Institute for Water Education)

dr. S.M.Hassanizadeh (Utrecht University)

Universiteit Utrecht

UNESCO-IHE
Institute for Water Education

Abstract

The absence of proper sanitation in urban slum areas in African mega cities is a multi-faceted problem where a socio-economic as well as a technical approach is required to come to a sustainable solution. Consequences of the lack of sanitation in slums can be the deterioration of groundwater and surface water quality by an increased input of nutrients such as nitrogen and phosphate species and an input of bacteria/viruses. Additionally the deterioration of surface water quality can lead to eutrophication. This research focused on the presence of nutrients in groundwater and the processes governing their fate. A monitoring network of 26 wells was installed in the Bwaise III slum area in the capital city of Uganda, Kampala. Water levels were registered weekly and slug tests were performed to determine the horizontal hydraulic conductivity. Parameters measured in the field on water samples were EC, pH, temperature, alkalinity, orthophosphate, nitrate and ammonium. In the laboratory, samples were analyzed for all cations and anions. Soil samples were analyzed for grain size and geo-available metals. Additionally, a phreeqc model was set up in order to validate the groundwater flow velocity and the possibilities for cation exchange occurring in the soil.

A NE-SW hydraulic gradient of approximately 3 m/km was derived from the groundwater level measurements with a hydraulic conductivity of 3.43 m/day. The groundwater flowing through the region ended up in Nsooba channel. Chemical analyses showed Bwaise acted as an effective nitrate reducing system where, in the southwestern parts, iron was also being reduced. Ammonium was well established in the region with values up to 1 mmol/l. Orthophosphate presence was 2-10 µmol/l in groundwater which was markedly less than the calculated input of 26.3 µmol/l. The geo-available metal content of the soil combined with the coarse grain sizes encountered showed that sorption to metal oxides is an unlikely mechanism for the marked decrease in orthophosphate. Mineral saturation indices revealed that hydroxyapatite could regulate orthophosphate concentrations in the nitrate reducing part of Bwaise and vivianite in the iron reducing part of Bwaise. The phreeqc model showed that different values for the assumed porosity and cation exchange capacity can produce the same pattern seen in the chloride and sodium values in the field.

Contrary to conclusions raised by other researches, our study showed that under the right circumstances, pit latrines as a means of managing waste in slum areas can be a favourable option from a nutrient management point of view especially in relationship to disposal of waste in drains that discharge in surface water.

Acknowledgements

First of all I would like to thank ir. Philip Nyenje and our field assistant Dirisa without whom I would not have been able to carry out this research. Through their guidance I was able to understand the different way of life in Uganda compared to the Netherlands and especially the proceedings in the slum. I can only imagine how utterly improbable it must have been for the residents of the slum to see a Muzungu march into one of the poorest regions of the capital asking (uncompensated) permission for the installation of a monitoring well. It is here that these people are greatly acknowledged for their hospitality.

The laboratory staff at UNESCO-IHE do a wonderful job in helping the students process samples from field research and many thanks are in order here. Additionally, laboratory personnel at Makarere University and the Utrecht geochemistry laboratory contributed to the analysis and I am grateful for their support.

I am also indebted to dr. Jan Willem Foppen and dr. Majid Hassanizadeh for their assistance in conducting the analysis and writing this report. In fact, I would like to thank all teachers at Utrecht University who have invested time in progressing my academic skills throughout the years.

My special thanks I would like to extend to the ICU guesthouse and their wonderful staff for looking after me in Uganda. Occasionally when a researcher gets caught up in his/her work the attention for his own well being diminishes. It is here that the ICU guesthouse played its part. Additionally, all of the new friends I made at the guesthouse are gratefully acknowledged for their good company and the ability to exchange experiences.

Utrecht University, UNESCO-IHE and my family are very much acknowledged for their financial and moral support during my travels.

Finally, my gratitude goes out to God for allowing me to pursue the Msc. course and the completion of this research. Only few people get the opportunity to experience a beautiful country like Uganda the way I have and this I will never forget.

Table of Contents

List of assumed parameter values

Parameter	*Description*	*Value*
$n\,[-]$	Porosity	0.3
$\alpha[m * s^2/kg]$	Compressibility of aquifer material	Min: 5E-8 Max: 1E-7
$\beta[m * s^2/kg]$	Compressibility of water	4.4E-10
$\rho[m^3/kg]$	Density of water	1000
$g[m/s^2]$	Acceleration due to gravity	9.81
$CEC[mmol/l]$	Cation exchange capacity	Model 1: 0.05 Model 2: 0.35
$\alpha_L[m]$	Dispersivity	2
$D_e[m^2/s]$	Effective diffusion coefficient	3E-9

List of abbreviations

CEC	Cation Exchange Capacity
dS	Storage
EC	Electrical Conductivity
IAP	Ionic Activity Product
IC	Ion Chromatography
ICP-MS	Inductively Couple Plasma Mass Spectrometer
IDW	Inverse Distance Weighting
IT	Inflow Transect
OT	Outflow Transect
LS	Latrine Site
MASL	Meter above sea level
SCUSA	addressing the Sanitation Crisis in Unsewered Slum areas of African Mega-cities.
SI	Saturation Index
SSA	Sub Saharan Africa
SW	Solid Waste site
TOP	Top of Pipe
TP	Total Phosphorus
Qlsi	Lateral Subsurface Inflow
Qlso	Lateral Subsurface Outflow
Qprec.	Recharge

1. Introduction

1.1 Setting and environment

Around the year 2000, 47% of the world's population lived in urban areas. Projections are that in the year 2030, this figure will have risen to 60% globally [UN-HABITAT, 2002]. Africa may have had a relatively low percentage of people living in urban areas in the year 2000 (38%), but predictions are that it will have the fastest increase in percentage of people living in urban areas with an expected 55% in 2030 [UN-HABITAT, 2002]. The rate of rapid urbanization will therefore most likely put a lot of stress on the settlements to which it applies. Besides the high rate of urbanization, Africa is also recognized to have the largest population growth rate as such and given the fact that only 9% (UNEP, 2007) of the world's freshwater is available for Africa, one can see the problems related not only to the production of clean drinking water, but also to the adequate service deliveries by local governments that prevent pollution of the limited water available [UNEP, 2002]. These problems have been affecting city life in Africa in the past, they do so in the present and will continue to pose a threat in the future especially with the projected increase in urbanization.

The majority of the people migrating to the city and thus contributing to urbanization are likely to end up in informal settlements or slums. These areas are characterized by poor housing, poor infrastructure, insufficient service deliveries such as electricity, piped water and sewage systems and a lack of legal status. The lack of service delivery inevitably leads to the uncontrolled disposal of waste. The disposal of waste can take on several forms such as solid waste dumps where remains such as plastics, papers and organic waste are disposed. Wastewater from kitchen, laundry or bathing applications, also called grey water is disposed of over the land or in small scale tertiary drains. Human excreta also needs to be managed accordingly, however many residents of slum areas only have the option of traditional unimproved latrines. Data from Sub Saharan Africa (SSA) show that a large portion of urban residents are living in these types of settlements (71.9%) (Warah, 2003).

1.2 Problem statement

One of the main drivers for the concern of water quality is the contamination of shallow groundwater with viruses and bacteria as well as nutrients. It has been shown by previous studies undertaken that an improper disposal of human waste and excreta can lead to contamination of springs that find are fed by shallow aquifers (Haruna et. al., 2005). However not only springs can become contaminated as at some locations people are also forced to rely on shallow groundwater wells for their daily water. These shallow groundwater wells have also been shown to become polluted by the presence of pit latrines (Argoss, 2001; Kiptum and Ndambuki, 2012). Nitrate concentrations often exceed the WHO drinking water limit of 50 mg/l (WHO, 2008a). In these quantities, nitrate is an unwanted presence in drinking water, because it causes methemohemoglobinemia in children (Robillard et. al., 2003). Additionally, concentrations of viruses and bacteria often exceed the WHO limit of nil counts per 100 ml (Kiptum and Ndambuki, 2012). There is therefore a need to take faeces, that have been disposed of improperly, out of the environment (Foppen and Kansiime, 2010).

Another cause for the interest in improving groundwater quality and sanitation is the risk of eutrophication of surface water bodies. Eutrophication is not a problem unique to Africa as estimates are that 54% of the lakes/reservoirs in Asia are impaired by eutrophication, in Europe this is 53%, in North America 48%, in South America 41%, and in Africa 28% (Nyenje et al., 2010). Even though these facts show that Africa has the lowest percentage of affected surface water bodies, we are still interested in preventing further decay especially considering the rapid increase in urbanization of the continent. Marshall and Falconer (1973) were one of the first to link the eutrophication of a surface water body to sewage water discharge. Waste water can be disposed of either controlled or uncontrolled, but in both cases waste water is recognized to contain elevated concentrations of nutrients such as nitrate and phosphate that degenerate surface water quality. Effects of degeneration are severe and often lead to the adjustment of entire ecosystems. Effects include an increase in primary production of a lake which may then lead to an impairment of oxygen levels in the lake, significant growth of specific groups of phytoplankton and aquatic macrophytes, the ecological alteration of the environment with less resistant species possibly dying and finally, the total depletion of oxygen in the lakes which may lead to total anoxia and many macroinvertebrate species becoming extinct in the lake [Nyenje et. al., 2009]. Eutrophication has been found to occur in lakes such as lake Chivero in Zimbabwe, Lake Albert on the boundary between Uganda and Congo, the Zeekoevlei, Rietvlei and Lake Krugersdrift in South Africa, rift lakes in Ethiopia and freshwater bodies in Cameroon and Nigeria [Nyenje et. al., 2009].

Summarizing the above, it has been shown that the improper disposal of waste in unplanned settlements leads to a deterioration of shallow groundwater and spring water quality. Research has also shown that there is a need to use shallow groundwater and spring water by the populace of such settlements. There is however surprisingly little research done on the processes that govern the availability of selected contaminants after they have been discharged into aquifers underlying slums. It is here that the premise of this study lies. It was chosen to focus on nitrate and phosphate availability primarily in contrast to bacteriological analysis.

1.3 Research Objectives

The main research objective was to gain a better understanding in the fate of nutrients in groundwater originating from pollution input due to the lack of proper sanitation in Bwaise. To work towards this goal, the main objective was divided into a number of smaller targets that each contribute to the main question.

- **i.** Obtain a better understanding of the geology and soil types of the region.
- **ii.** Measure various hydrogeological parameters in the field.
- **iii.** Establish an understanding of the hydrological and chemical processes affecting the availability of nutrients in the soil and pore water.
- **iv.** Determine the relationship between groundwater and surface water and how this affects the transport of phosphorus and nitrogen phases.
- **v.** Quantify the fate of nutrients in the soil.

1.4 Framework

This research was carried out in the context of the research project 'Addressing the Sanitation Crisis in Unsewered Slum Areas of African Mega-cities' (SCUSA) which is a joined cooperation between UNESCO-IHE in Delft (the Netherlands), Makarere University in Kampala (Uganda) and the Kampala City Council (Uganda). The SCUSA project aims at researching the impact that the living conditions in the slums of Kampala city have on the environment and, if applicable, intervene and work towards improvement.

2. Literature review

2.1 Site description

2.1.1. Location

Uganda is located in central Africa, south of the Sahara. It borders Sudan to the North, Kenya to the East, Tanzania and Rwanda to the South and the democratic republic of the Congo to the West. A part of the country is actually made up of Lake Victoria. Uganda's capital, Kampala, is located in the South of the country near lake Victoria. Kampala is divided up into 5 major divisions of which Kawempe is the Northern most, the Bwaise III slum is located in Kawempe division. Bwaise is again divided into 6 administrative zones being Katoogo, St. Francis, Bugalani, Bokasa and Kalimali. The boundaries of the research area are approximately the Katoogo and St. Francis zones as indicated in figure 2.1. Also indicated in figure 2.1 is Wakiso district to the west of Kawaala road. From a management point of view, this is not Kampala city anymore, however plans have been made to expand into Wakiso district which is currently largely wetland area unaffected by the change in land use that goes hand in hand with the expansion of a city.

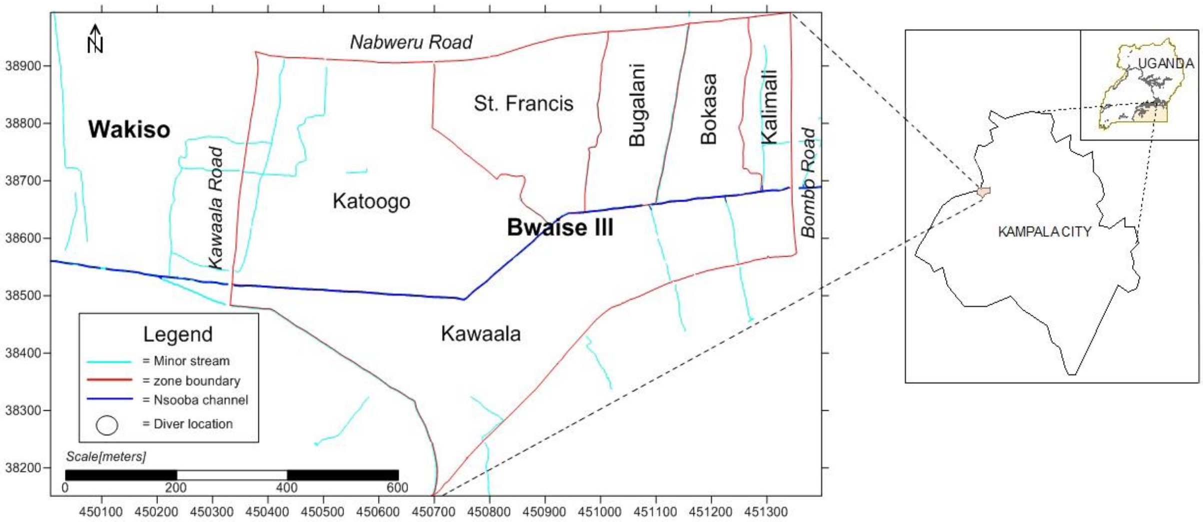

Figure 2.1: Geographical location of Bwaise III slum: modified from Nyenje et. al., (2012)

2.1.2. Climate

As Uganda lies near the equator, there is no profound distinction between the seasons similar to temporal climates as temperature is approximately 22-30 degrees year round. Instead, there are two rainy seasons that last from March through May and from October through November (figure 2.2). Uganda receives plenty of rainfall with a 1400 mm. yearly average, however, this rainfall tends to mostly fall within the rainy seasons. There is thus a monthly variation, but also inter-annual variability can be as high as 750-2000 mm. [UNEP 2002]. Therefore both water scarcity as well as a surplus can influence life in Kampala city. The climate also has a profound effect on life in Bwaise as the Nsooba channel is likely to flood its banks during the rainy season. Figure 2.2 confirms the deviation of rainfall patterns as the differences between monthly rainfall in 2010 and 2011 can be as large as 200 mm/month.

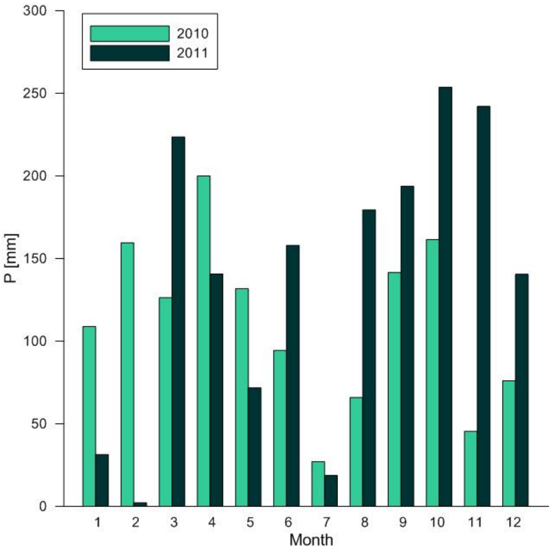

Figure 2.2: Monthly precipitation as recorded at Makarere weather station in mm.

2.1.3 Hydrogeology

The hydrogeology of the study area is similar to most places in equatorial Africa. It consists of a deeply weathered mantle that is underlain by fractured, but consolidated bedrock. Fractures in the bedrock are the result of decompression effects that are caused by the stripping of the overlying weathered mantle, by precipitation and runoff activity, and by the removal of overlying rock in solution (deep weathering) (Taylor and Howard, 2000). The fractured bedrock has been used to abstract groundwater from, but typically, yields have been low due to highly variable, but generally low transmissivity. Therefore, attention has shifted to shallow aquifers for the abstraction of suitable drinking water. The study undertaken by Kulabako et al., (2007) in the Bokasa and Kalimali district of Bwaise uncovered three distinct layers in a 2 meter soil profile where the first two layers were mostly sandy soils and the bottom layer was made up of smaller sized particles. The water table was mostly found in the middle layer.

2.1.4. Demographics

Historically, Bwaise was part of a wetland that drained into Lubigi swamp, but illegal habitation of the wetland reclaimed it. Figure 2.3 shows the physical expansion of Kampala city according to Nyaakana et. al., (2004) who compiled the image from historical atlas information. Kawempe division was being formed between 1955 and 1968 and was still in formation by 1968 as can be observed from the map. From the year 1980 onwards, the spatial extent of housing in Bwaise remained constant based on satellite image data (not shown here) also compiled by Nyakaana et. al., (2004). The Uganda bureau of statistics has held a population census of which the results were published in the year 2002. At that time, Bwaise experienced an annual population growth rate of 9.6% compared to 3.7% for the city of Kampala as a whole (UBOS, 2002). We can therefore say that the encroachment of the wetlands started around the 1960's and is still expanding up to this day. Additionally, with 27000 persons/km^2 (Foppen and Kansiime, 2010), Bwaise has one of the highest population densities in Kampala city. Its lack of legal status makes for very difficult service delivery by the authorities. There is a lack of infrastructure, lack of solid waste management and a lack of sewage facilities. It has been estimated that 90% of the population of Bwaise uses unimproved methods such as pit latrines or shared toilets as a sewage facility (Katukiza et. al., 2010) compared to 38% as the urban average in Uganda (WHO, 2008 b). This has subsequently lead to uncontrolled disposal of waste in the wetland area since 1955.

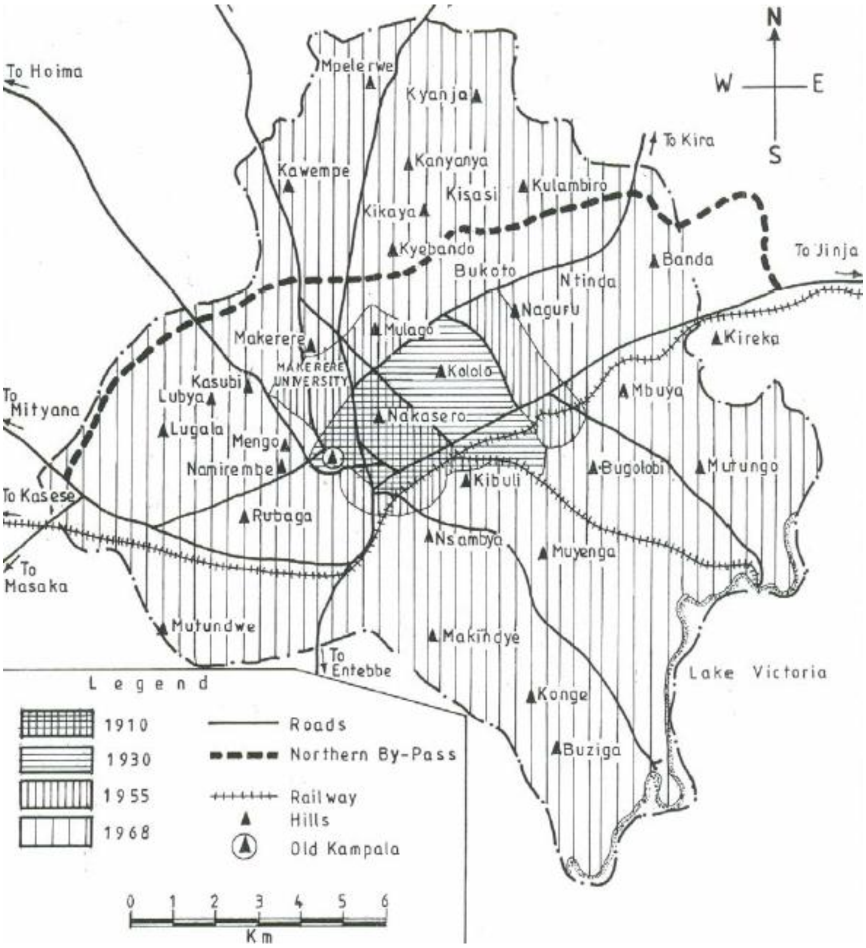

Figure 2.3: Physical expansion of Kampala city with time (adopted: Nyakaala et. al., ?)

2.2 Wetland hydrochemistry

Since Bwaise was built on a natural wetland, knowledge of the groundwater in wetlands may provide us with useful information on the unpolluted water that may be present in the study area. Wetlands can roughly be divided into two major categories based on the source of their water influx and therefore their pore water chemistry. Ombotrophic peatlands, which are also called bogs, receive their water influx only from rainfall whereas minerotrophic peatlands, which are also called fens, commonly receive water from both rainfall and groundwater influxes. One of the most common models for the formation of wetlands is that mineral rich fens may develop into mineral poor bogs. In this model, open water bodies are first filled with organic rich sediments that allow the growth of vegetation that is commonly associated with fens. Once this vegetation has been established, fen peat starts depositing until the land surface and water table rise above the regional water table which isolates the wetland from mineral rich groundwater (McNamara et. al., 1992; Reeve et. al., 1994;) From that point onwards the internal wetland chemistry changes and the 'bog' classification applies. This simple classification omits the fact that the progression from mineral rich fen to mineral poor bog is a gradual progression and studies have differentiated between fens that have mineral rich and mineral poor water content (Nicholson and Vitt, 1994; Wassen et, al., 1988). An additional subtype in wetland types is made based on vegetation. Areas where vegetation is present are either called swamps, where trees are present to variable extent or marshes where trees are absent, but grasses, reeds, cattails and other herbaceous plants flourish (McNamara et. al., 1992). The groundwater composition heavily influences the type of vegetation that grows on a wetland (Wassen et. al., 1988), however, once a certain type of vegetation is established and dead plant remains start to accumulate on the wetland, the degradation of different types of vegetation also affects the groundwater composition in turn .

Table 2.1 shows reported groundwater hydrochemical data from studies involving wetlands. What can clearly be seen is that a rich fen displays a larger quantity of major cations than a bog or poor fen. This is also reflected in the conductivity which is typically two or three times as high for rich fens than for a bog or poor fen. Additionally, pH is low in ombotrophic peatlands compared to minerotrophic wetlands. Ammonium and nitrate are given in µmol/l, so these are practically unavailable in the various wetlands described. Alkalinity is known to be low in ombothrophic wetlands (1 mmol/l) and high in minerotrophic wetlands (3 mmol/l). Phosphate is described to have relatively high concentrations in wetlands in low lying areas compared to non wetland pore water concentrations (Griffioen, 2005). Out of the researches reported in summary table 2.1, only Wassen et. al., (1988) and Schwindzer and Tomberlin (1982) reported an orthophosphate value which was 1.5 µmol/l for both mineral rich and mineral poor wetlands.

Table 2.1: Values for different hydrochemical parameters from wetland studies. All species are given in mmol/l except for NH_4^+ and NO_3^- and PO_4^{3-} which are given in µmol/l and conductivity is given in µS/cm.

Source	Type	HCO_3^-	PO_4^{3-}	Ca^{2+}	Mg^{2+}	Na^+	K^+	Cl^-	$NH4^+$	$NO3^-$	pH	Cond.
Schwindzer and Tomberlin (1982)	Bog	*	1.0	0.06	0.02	0.07	0.02	0.04	31.98	0.12	4.0	57
Schwindzer and Tomberlin (1982)	Fen	*	0.0	1.11	0.43	0.12	0.01	0.08	12.65	0.09	6.5	262
Schwindzer and Tomberlin (1982)	Thicket swamp	*	*	1.36	0.67	0.14	0.02	0.12	42.42	0.12	6.9	374
Nicholson and Vitt (1994)	Open bog	*	*	0.10	0.08	0.09	*	*	1.27	0.32	3.5	27
Nicholson and Vitt (1994)	Mod. Rich fen	*	*	0.82	0.41	0.22	*	*	9.00	0.13	6.2	162
Nicholson and Vitt (1994)	Shallow Marsh	*	*	1.02	0.41	1.35	*	*	7.37	0.26	6.4	478
Reeve et. al., (1994)	Wetland	3.76		1.71	0.27	0.39	0.04	0.31	*	34.7	6.2	*
Wassen et. al., (1988)	Poor fen	3.00	1.5	0.75	0.2	1.6	0.17	1.0	2.7	2.6	5.0	225
Wassen et. al., (1988)	Rich fen	0.80	1.4	1.8	0.25	2.2	0.02	2.1	14.7	3.9	6.4	440

** = not measured*

2.3 Anthropogenic influence on water chemistry

2.3.1 Bwaise III slum

In the Katoogo zone of Bwaise, research has already been done at an individual pit latrine (LS) and solid waste (SW) site. The locations of these two sites can be seen in figure 4.4. Monitoring wells were installed directly upstream and downstream of the sites on a presumed groundwater flow line. The results from Nyenje's work showed that solid waste sites do not significantly contribute to the presence of the selected hydrochemical parameters in shallow groundwater. The author attributed this partly due to the organic nature of the waste dumped at the site and partly because of polyethylene bags forming a pollutant seal. The latrine site on the other hand polluted heavily.

Table 2.2: Pollutant input from a pit latrine site and solid waste site (adopted: Nyenje et. al., 2012)

Parameter	**Latrine site**		**Solid waste site**	
	Upstream (n=4x5)	**Downstream (n=6x5)**	**Upstream (n=4x5)**	**Downstream (n=3x5)**
EC (µs/cm)	1306 (±306)	5061 (±1073)	859 (±141)	795 (±201)
pH	6.6 (±0.3)	7.5 (±0.2)	6.3 (±0.3)	6.5 (±0.2)
T (℃)	25 (±2)	25 (±2)	26 (±1.4)	26 (±1)
Cations:				
Na (mg/L)	48 (±19)	172 (±114)	37 (±20)	28 (±13)
K (mg/L)	42 (±28)	307 (±173)	22 (±17)	40 (±35)
Mg (mg/L)	16 (±21)	21 (±13)	6 (±4)	5 (±3)
Ca (mg/L)	22 (±10)	61 (±32)	25 (±16)	12 (±6)
Fe (mg/L)	0.02 (±0.02)	0.1 (±0.06)	0.04 (±0.06)	4 (±6)
Mn (mg/L)	0.9 (±0.7)	0.4 (±0.24)	0.8 (±0.5)	0.7 (±0.4)
NH_4 (mg/L)	4.9 (+5.1)	57 (±42)	2.9 (±1.7)	5.1 (±3.9)
Anions:				
Cl (mg/L)	110 (±45)	380 (±206)	67 (±20.7)	66 (±30)
HCO_3 (mg/L)	322 (±117)	1114 (±356)	171 (±71)	233 (±94)
NO_3 (mg/L)	85 (±(38)	228 (±237)	69 (±36)	16 (±12)
SO_4 (mg/L)	20 (±6)	127 (±86)	15.3 (±8.3)	7 (±6)
o-PO_4 (mg/L)	0.05 (±0.09)	2.4 (±3)	0.3 (±0.6)	0.2 (±0.3)
Others:				
SiO_2 (mg/L)	2.1 (±3.1)	4 (3.8)	1.1 (±1.9)	0.9 (±1.4)
TP (mg/L)	0.27 (±0.23)	3.2 (11.3)	0.5 (±0.7)	0.4 (±0.3)
DOC (mg/L)	5 (±3)	21 (±9)	2.8 (±1.4)	5 (±2.8)
***** Saturation indices (SI)***				
SI Hydroxyapatite	-6.4	1.2	-8	-6.7
SI Vivianite	-8.2	-5.1	-7.4	-2.6
SI $MnHPO_4$	1.2	2.2	2.0	-

In table 2.2, all nutrients increase in concentration as well as virtually all other constituents in the groundwater downstream of a pit latrine. Magnesium and manganese are the only parameters that do not increase significantly due to the discharge of pit latrine contents. Additionally, from saturation indices, Nyenje et. al., (2012) identified hydroxyapatite and MnHPO4 as possibly precipitating. Figure 2.4 shows a survey that was conducted by Kulabako et. al. (2007,2008) and shows the distribution of pit latrines in the entire Bwaise III slum. From this overview, it can be seen that on an area scale, contribution of contaminants by pit latrines can be regarded as a non-point source.

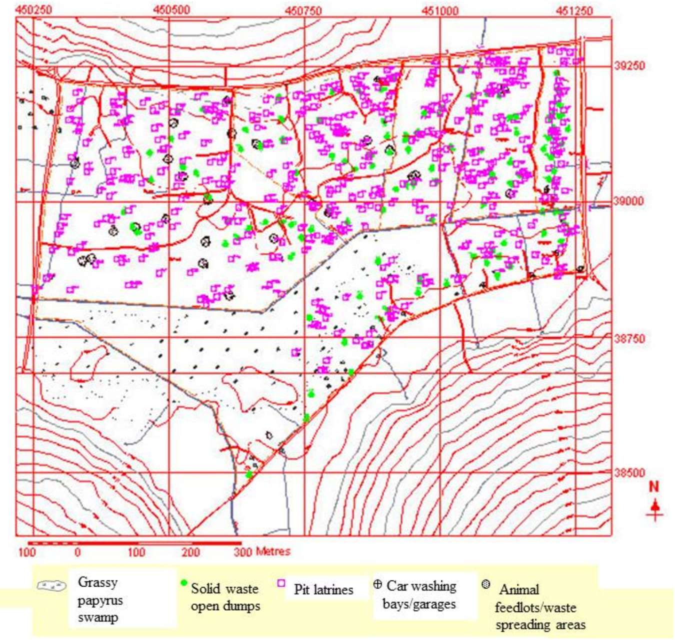

Figure 2.4: Distribution of pit latrines in Bwaise III slum as recorded roughly from 2006-2008. (adopted: Kulabako et. al., 2007, 2008)

The Msc. thesis conducted by Lisa Meijer in Bwaise III slum focused primarily on the water quality of Nsooba channel and a smaller tertiary drain (Meijer, 2011). The chloride and sodium values in Nsooba channel were quite variable during background sampling up to 2 mmol/l, during rainfall events the chloride values were fairly constant at 2 mmol/l. Sodium in Nsooba channel was variable during rainfall events, but did not exceed 2 mmol/l. It was found that filtered orthophosphate concentrations in Nsooba channel were in between 2-10 µmol/l during background sampling both near the inflow and the outflow of the channel through the slum. Orthophosphate concentrations in the tertiary drains exhibited much higher values going up to 50 µmol/l. Nitrate was found to be very low as well as Fe(II). It was therefore concluded that water in Nsooba channel was anoxic and capable of reducing nitrate, but iron oxides in the sediment were left intact. This was confirmed by the determination of geo-available metals in the sediment which yielded concentrations of up to 4000 mg/kg for iron. Generally, the effect of rainfall events was found to be diluting on the chemical components in Nsooba channel. In the tributary drain, concentrations of nutrients were linked to the disposal of grey water where the concentrations were higher during the day and lower at night. It is therefore likely that Nsooba channel polluted water consisted of disposed grey water from tertiary drains that had been diluted by water originating from further upstream and runoff due to rain events.

2.3.2 Nutrients in groundwater

There have been quite a number of studies that concerned themselves with the nitrate and phosphate concentrations in groundwater and the fate of those constituents. A myriad of pollution sources have been identified such as pit latrines, manure storages, fertilizer usage, septic tanks, industrial wastewater effluent, broken sewage pipes and general land use patterns. The research done has been found meaningful due to concerns about both drinking water standards and the risk to eutrophication.

Because of its use in fertilizer, nitrate is recognized as one of the most widespread groundwater contaminants in the world. The tolerable presence in groundwater was determined to be 50 mg/l by WHO (2008)a. There are generally two prevailing trends when it comes to the fate of nitrate in the literature, there are researches which report high presence of nitrate in groundwater and those that report a low presence of nitrate. Young et. al., (2010) report a high input of nitrate from overfertilization from the northwest of Sri Lanka. The subsequent values for nitrate in groundwater are found to be surprisingly low compared to the input. Corbett et. al., (1999) conducted field experiments where nutrients as well as conservative tracers were injected in a low discharge groundwater system in the Florida Keys. Nitrate uptake by the aquifer here was also found to be very high. Jayasingha et. al., (2011) document high values of nitrate in groundwater due to overfertilization from the Kalpitiya peninsula which is also located in the Northwest of Sri Lanka. Additionally, Young et, al., (2010) state that in the central province of Sri Lanka, nitrate values in the groundwater have also been found high. Kulabako et. al., (2008) reported increased values of nitrate further downstream on a well transect which is attributed to pollution from pit latrines and coincides with rainfall events. Krapac et, al., (2001) studied the contribution of excreta management from swine manure pits to the groundwater, but found no elevated nutrient concentrations.

In the literature, phosphate transport in groundwater has received less attention, because of the long held assumption that it would either adsorb onto the solid phase or precipitate and therefore, it would not be a threat (Holman et. al., 2008; Qian et. al., 2011). In recent years, the attention to phosphate transport in groundwater has seen an increase though. The increase in interest can be attributed to a number of causes. First of all, there has been a change in the amount of phosphate that has been deemed tolerable in groundwater. Whereas, in the past, the WHO guideline for drinking water was largely the scale of interest (0.05 mmol/l), in recent years it has been recognized that coastal waters and lakes in which nitrate is abundant need only little phosphorus to sustain an increase in eutrophication (2 µmol/l TP) (Dodds et. al., 1998). Indeed, the change in scale of interest can even be observed in the limit of detection of analytical equipment for phosphorus determination recorded in studies (Krapac et. al., 2001; Holman et. Al., 2008). Secondly, instances have been recorded where the phosphorus uptake by the aquifer system was less than expected (Kulabako et. al., 2008; Qian et. al., 2011). Also, the amount of phosphorus in groundwater was positively correlated to land use which would not be expected if adsorption and precipitation could account for all phosphorus input (Holman et. al., 2008; Qian et. al., 2011). Thirdly, researchers working in areas with particularly high nutrient loading have expressed concerns of saturation of the soil leading to breakthrough of contaminants (Corbett et. al., 1999). Besides the concerns raised, there are researches that report phosphorus concentrations to be effectively diminished in acceptable travel distances (Young et. al., 2010; Jalali et. al., 2010; Jayasingha et. al., 2011).

In addition to the studies that are mentioned above, Kulabako et. al., (2007, 2008) carried out research in the Bokasa and Kalimali district of Bwaise (figure 2.1) relating to nutrient presence in the subsoil. Therefore, the works of Kulabako are closely related to the work done in this research. Also, the capacity for several wetlands for buffering nutrient concentrations in the Kampala and Lake Victoria regions were studied (Kansiime and Nalubega, 1999; Kelderman et. al., 2007; Mugisha et. al., 2007; Kanyiginiya et. al., 2010). More specifically, in Kulabako et. al., (2008) the mechanisms of phosphate distribution were investigated at four different sites named MW1 through MW4. At each site a transect of three wells, 1.2 m. apart from each other, was designed to coincide with the groundwater flow direction. Groundwater samples were taken and analyzed in the lab for total phosphorus, total kjedahl nitrogen, and chloride. Additionally, soil samples from the mentioned locations were tested for, amongst other parameters, available phosphorus, geo-available iron, soil pH, organic carbon, grain size and exchangeable Ca^{2+}, Mg^{2+}, K^{+} and Na^{+}. To provide more insight into differentiation of soil phosphorus between different pools, Kulabako et. al., (2008) carried out fractionation experiments according to Furumai and Ohgaki (1982). The different pools of phosphorus (P) considered in the experiment were loosely bound P, Al and Fe bound P, Ca bound P, organic P and residual P. Batch studies were also carried out on the soil samples by equilibrating 5 g of air dried soil with 0.1, 1, 3, 5, 10 and 15 mg/l PO4-P standard solutions whilst sampling the solutions at 1, 2, 4, 8, 12 and 24 hours from the start of the experiment. During the batch experiments, adsorbed phosphorus was also determined using the ascorbic acid method at the selected times. Plotting the sorption data against different sorption isotherms showed that the Langmuir isotherm was most efficient at explaining the observed concentrations from the laboratory experiments. The batch studies also showed a fast initial response of adsorbing phosphorus that lasted for 4 hours followed by a slow decrease up to the 24 hour duration of the experiment. A multivariate statistical model showed that the maximum sorption capacity, C_{max}, of the soil was related to available phosphorus, Ca, organic carbon content and soil pH. Contrary to what would be expected, Fe content was not found to affect the sorption capacity of the soil. The concentrations of phosphorus measured in the well transects in the field show varying results. MW1 showed no attenuation of phosphorus whereas MW2 and MW3 did show a decrease in total phosphorus down the transect while MW4 actually showed an increase in total phosphorus concentration with distance. Furthermore, the observed attenuation at MW2 and MW3 was seemingly more pronounced in the dry season compared to the wet season. Also, concentrations of nutrients, EC and Cl^- were generally higher in the wet season compared to the dry season. Overall, the phosphorus attenuation at all locations was less pronounced than in the results from the batch studies. The author attributed the observed lack of attenuation and high total phosphorus values at MW1 to animal rearing activities in the vicinity of the transect. Additionally, flooding was observed here during the wet season which could have lead to anoxic conditions that may release phosphorus into groundwater through the reduction of iron oxides. The combination of high phosphorus content of the top soil layer and high organic matter content in the soil of the middle layer (figure 2.5a), which is known to block sorption sites, leads kulabako et. al., (2008) to conclude that leaching from the top soil during heavy rains plays a more important role than sorption at MW1 and MW2. The limited degree of attenuation that did occur at MW2 and MW3, according to Kulabako et. al., (2008), can be explained by the low flow velocities (figure 2.5b) at these locations. At MW4 flow velocity was also low, but the phosphorus concentrations themselves were very low here, because of low input and here Kulabako et. al., (2008) concluded that the increase in total phosphorus concentrations downgradient were again due to leaching playing a larger role than adsorption. The occurrence of macropores in the soil is referred to by the author as a factor contributing to the leaching process as there is less contact time between the dissolved species and the soil. The author would expect greater adsorption of phosphorus in the wet season due to increased dissolved oxygen concentrations and therefore increased iron oxide content of the soil. This was not the case, however and macropore flow was offered as a possible explanation for this (iron contents of the soil as seen in table 2.5b are said to be high). The phosphorus fractionation experiments yielded residual P as the highest contributor to the total phosphorus content of the soil followed by Ca bound P and Fe, Al bound P. Ca bound P was observed to be relatively more important in the top soil layer and Fe, Al bound P was observed to be more important in the middle soil layer. This is in line with the exchangeable metal and geo-available iron content as seen in figure 2.5. The high, mostly organic, residual phosphorus values were linked to animal rearing and dissolved organic phosphorus was suggested to be the main form of phosphorus in groundwater. Even though nitrogen and phosphorus species may leach from soils as described by Kulabako et. al., (2008), the wetlands through which wastewater passes before it reaches surface water bodies have the potential to take up nutrients through the growth of plants or adsorption on the wetland soil. Kanyiginiya et. al., (2010) found however that Natete wetland in Kampala did not have the capacity to take up phosphorus (0%). Nitrogen concentrations were reduced by 50%. Kelderman et. al., (2007) reported only 40-60% nitrogen uptake and 55% phosphorus uptake by Kirinya wetland and Kansiime and Nalubega reported 56% nitrogen uptake and 40% TP uptake by Nakivubo wetland. Overall, the determination of nutrients on dry weight showed that papyrus plants were most efficient in nutrient uptake. Biannual harvesting of plants in a wetland was advised to facilitate permanent nutrient removal in addition to the distribution of wastewater over a large area of the wetland in order to increase the nutrient uptake.

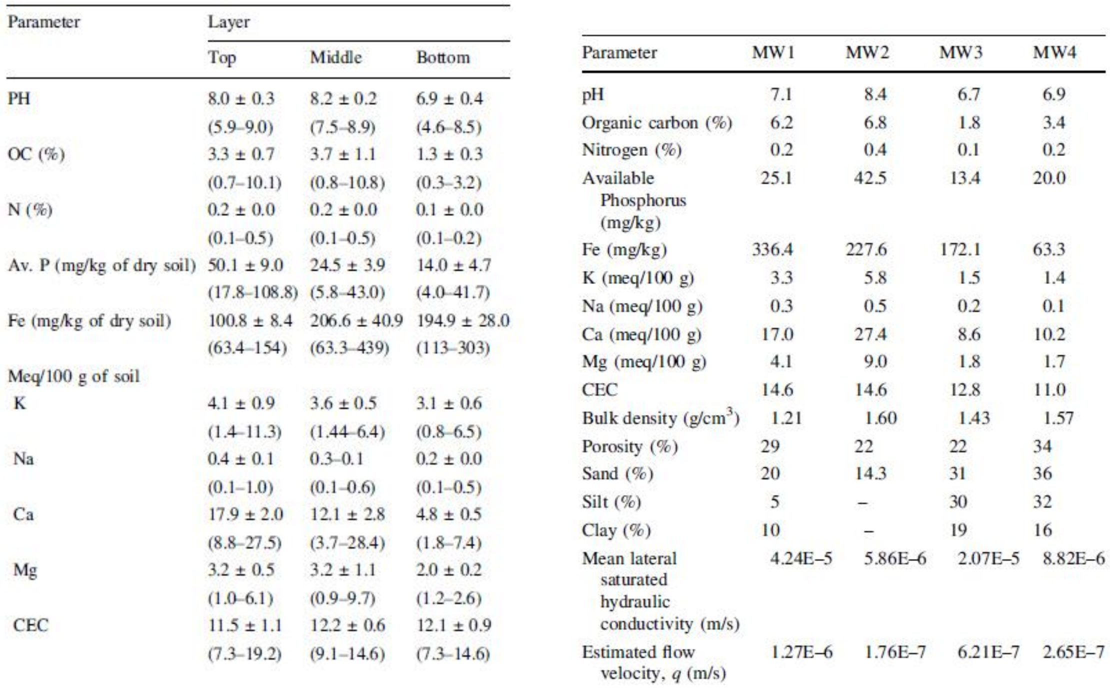

Parameter	Layer		
	Top	Middle	Bottom
PH	8.0 ± 0.3	8.2 ± 0.2	6.9 ± 0.4
	(5.9–9.0)	(7.5–8.9)	(4.6–8.5)
OC (%)	3.3 ± 0.7	3.7 ± 1.1	1.3 ± 0.3
	(0.7–10.1)	(0.8–10.8)	(0.3–3.2)
N (%)	0.2 ± 0.0	0.2 ± 0.0	0.1 ± 0.0
	(0.1–0.5)	(0.1–0.5)	(0.1–0.2)
Av. P (mg/kg of dry soil)	50.1 ± 9.0	24.5 ± 3.9	14.0 ± 4.7
	(17.8–108.8)	(5.8–43.0)	(4.0–41.7)
Fe (mg/kg of dry soil)	100.8 ± 8.4	206.6 ± 40.9	194.9 ± 28.0
	(63.4–154)	(63.3–439)	(113–303)
Meq/100 g of soil			
K	4.1 ± 0.9	3.6 ± 0.5	3.1 ± 0.6
	(1.4–11.3)	(1.44–6.4)	(0.8–6.5)
Na	0.4 ± 0.1	0.3–0.1	0.2 ± 0.0
	(0.1–1.0)	(0.1–0.6)	(0.1–0.5)
Ca	17.9 ± 2.0	12.1 ± 2.8	4.8 ± 0.5
	(8.8–27.5)	(3.7–28.4)	(1.8–7.4)
Mg	3.2 ± 0.5	3.2 ± 1.1	2.0 ± 0.2
	(1.0–6.1)	(0.9–9.7)	(1.2–2.6)
CEC	11.5 ± 1.1	12.2 ± 0.6	12.1 ± 0.9
	(7.3–19.2)	(9.1–14.6)	(7.3–14.6)

Parameter	MW1	MW2	MW3	MW4
pH	7.1	8.4	6.7	6.9
Organic carbon (%)	6.2	6.8	1.8	3.4
Nitrogen (%)	0.2	0.4	0.1	0.2
Available Phosphorus (mg/kg)	25.1	42.5	13.4	20.0
Fe (mg/kg)	336.4	227.6	172.1	63.3
K (meq/100 g)	3.3	5.8	1.5	1.4
Na (meq/100 g)	0.3	0.5	0.2	0.1
Ca (meq/100 g)	17.0	27.4	8.6	10.2
Mg (meq/100 g)	4.1	9.0	1.8	1.7
CEC	14.6	14.6	12.8	11.0
Bulk density (g/cm^3)	1.21	1.60	1.43	1.57
Porosity (%)	29	22	22	34
Sand (%)	20	14.3	31	36
Silt (%)	5	–	30	32
Clay (%)	10	–	19	16
Mean lateral saturated hydraulic conductivity (m/s)	4.24E–5	5.86E–6	2.07E–5	8.82E–6
Estimated flow velocity, q (m/s)	1.27E–6	1.76E–7	6.21E–7	2.65E–7

a *b*

Figure 2.5: Soil characteristics of a: the average of all samples taken for the three layers encounterd, b: the middle layer at the specific locations (adopted: Kulabako et. al., 2008)

2.4 Processes affecting the availability of nutrients

Nutrient concentrations in groundwater may be affected by a myriad of processes. The following section will outline the most likely mechanisms to be encountered in the study area.

2.4.1. Organic matter degradation

As discussed in section 2.2, organic material in wetlands often stems from plant material. Plant material consists mainly of lignins and carbohydrates. Compared to lignins, carbohydrate degradation is a more important process, because lignins are mostly inert (Appelo and Postma, 2005). The degradation of carbohydrates has several steps each with different microbiological mediators. The first step has fermenting bacteria hydrolyze the carbohydrates using enzyme excretions resulting in the production of fatty acids, alcohols and H_2. During the second step, other regulating bacteria degrade fatty acids and alcohols produced by the first step further into acetic acid, formic acid, H_2 and CO_2. In the final step, the products from the second step acetate, formate and H2 are oxidized. The specifics of the various oxidants that are involved in the final step are discussed in section 2.4.2. Equation (1) gives a shorthand representation of the breakdown of a carbohydrate in the presence of oxygen by various groups of micro-organisms.

$$C_{106}H_{180}O_{45}N_{16}P_1 + 118.5O_2 \rightarrow 106CO_2 + 66H_2O + 16NH_3 + PO_4^{3-} \qquad (1)$$

The rates of the degradation of organic matter are reported to vary widely (Appelo and Postma, 2005). One of the main causes for this is that either of the three steps described above can be rate limiting. When the first step is rate limiting then the amount of fatty acids and alchohols in groundwater will be low, when the second step is rate limiting, the amount of acetic acid, formic acid and the CO2 pressure in groundwater will be low. If the third step is rate limiting then CO2 pressure and the amount of acids in groundwater will be high and the quantity of reduced species such as Fe^{2+}, Mn^{2+} and H_2S will be low when compared to the amount of acids that are present in the water.

Oxygen and nitrate are also known to oxidize organic matter, however the micro-organisms governing these reactions can sometimes oxidize the products from the first step directly. The order in which oxidants are used for the breakdown of organic matter in natural environments is also called a redox sequence.

2.4.2. Redox sequence

Organic matter is typically seen as the driving factor in a natural redox environment. Several oxidants are reduced in the breakdown process of organic matter. The order in which this occurs is determined by which reaction is most energetically favorable. As oxidants are used up and reductants are created, the composition of groundwater changes accordingly. The most energetically favorable oxidant is oxygen which is available in all aquifers through the infiltrations of oxygen rich precipitation. The part of the redox environment that is oxygen rich is called the oxic zone. As depth increases, in most cases the oxygen content of the groundwater decreases as reducing substances are encountered. When oxygen is depleted, the redox environment is defined as anoxic. Many classifications exist that elaborate on the anoxic environment, most of which are based on a substance that is being reduced or formed. Berner (1981) defines a post-oxic, sulfidic and methanic zone. The post-oxic zone is dominated by the reduction of nitrate, Mn-oxide and Fe-oxide. This classification can be seen in figure 2.6.

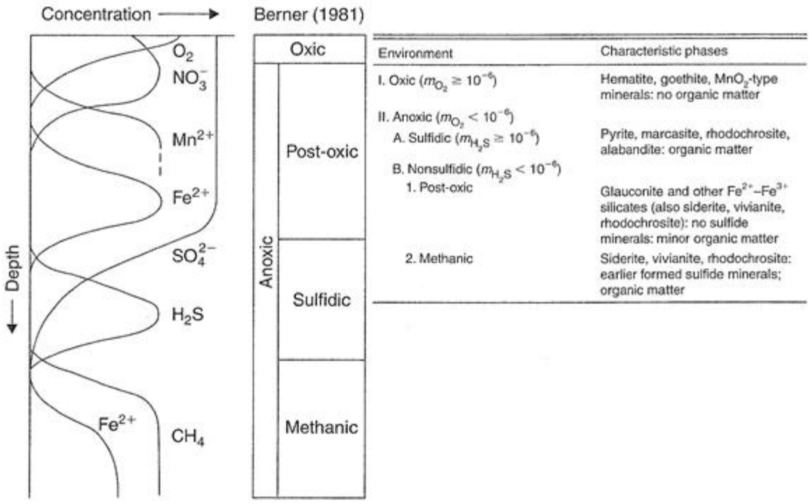

Environment	Characteristic phases
I. Oxic ($m_{O_2} \geq 10^{-6}$)	Hematite, goethite, MnO_2-type minerals: no organic matter
II. Anoxic ($m_{O_2} < 10^{-6}$)	
A. Sulfidic ($m_{H_2S} \geq 10^{-6}$)	Pyrite, marcasite, rhodochrosite, alabandite: organic matter
B. Nonsulfidic ($m_{H_2S} < 10^{-6}$)	
1. Post-oxic	Glauconite and other Fe^{2+}–Fe^{3+} silicates (also siderite, vivianite, rhodochrosite): no sulfide minerals: minor organic matter
2. Methanic	Siderite, vivianite, rhodochrosite: earlier formed sulfide minerals; organic matter

Figure 2.6: Redox classification according to Berner (1981) with expected minerals to form (adopted: Appelo and Postma, 2005)

Once oxygen has been consumed in the groundwater, nitrate is the next most energetically favorable oxidant. Nitrate does not form any insoluble minerals and it is not adsorbed to a great extent, so most nitrate that enters a groundwater system is available for the oxidation of organic matter. This reaction is shown in equation (2) where CH_2O is the schematic representation of organic matter (Rivett et. Al., 2008).

$$5CH_2O + 4NO_3^- \rightarrow 2N_2 + 4HCO_3^- + H_2CO_3 + 2H_2O \qquad (2)$$

This process is also called denitrification and is known to be the dominant pathway for the removal of nitrate under anoxic circumstances. Nitrate can also be assimilated to form NH_4^+, however, this has been found to occur to a far lesser extent than denitrification (Rivet et. al., 2008; Smith et. al., 1991). Denitrification is a permanent process, there are no conditions available in natural groundwater systems that allow the reversal of this reaction. Ammonium in the groundwater is able to undergo nitrification reactions in oxic soil. Additionally, in well aerated soil, part of the ammonium in groundwater may volatilize and be lost to the atmosphere. Recently, it has also been shown that under anoxic conditions, ammonium is able to be oxidized by hydroxylamine which is most likely derived from nitrite which is an intermediate product of denitrification. This process has been dubbed anaerobic ammonium oxidation or Annamox (Jetten et. al., 1998).

Manganese oxides are the next available species in figure 2.6 to facilitate the oxidation of organic matter. As Mn(IV) oxides are reduced, the concentration of Mn^{2+} should increase in the groundwater assuming no other reactions are taking place. Additionally, bicarbonate and H^+ ions are formed. Even though manganese oxides are typically reduced before iron oxides, they are much less abundant in most aquifers causing subsequent concentrations of Mn (II) to be lower than Fe(II).

Reductive dissolution of iron oxides is a common reaction in groundwater and adds ferrous iron as a product to the groundwater. Similar to the reduction of nitrate, organic matter is often the prime reductant in the dissolution reaction of iron oxide (Appelo and Postma, 2005):

$$CH_2O + 4FeOOH + 7H^+ \rightarrow 4Fe^{2+} + HCO_3^- + 6H_2O \qquad (3)$$

This process causes a strong increase in Fe^{2+} concentrations. As opposed to oxygen and nitrate, fermentation of organic matter, the first step in the degradation of OM, is not necessarily rate limiting in this reaction. Iron oxide reducing bacteria need to either make direct contact with a crystal surface or excrete complex formers in order to be able to take part in the dissolution reaction. Therefore, in the presence of highly reactive organic matter, the dissolution rate of iron oxide minerals can become rate limiting. The ascorbate and oxalate organic compounds have found to enhance the dissolution rate of iron oxide by forming a ligand at the exchange surface. Additionally, iron oxide minerals may be reduced by other oxidants than organic matter such as phenols, tannic acid, cysteine and H_2S (Appelo and Postma, 2005).

There is a variety of sources for sulfate in groundwater such as the dissolution of gypsum, oxidation of pyrite, acid rain deposition, fertilizer application or waste disposal. The sulfidic redox zone is characterized by the reduction of sulfate, again often by organic matter. This reaction produces H2S according to Massmann et. al., 2003:

$$2CH_2O + SO_4^{2-} \rightarrow 2HCO_3^- + H_2S \qquad (4)$$

H2S is a toxic component and also produces an undesirable smell which is why it should not be in drinking water. If iron oxides are present in the sediment, they may react with H_2S to form iron sulfide minerals. This can take both H_2S and Fe^{2+} out of the system again.

The methanic redox zone is the final stage in the redox environment and constitutes deep anoxic conditions. Methane can be produced either by biogenic or thermogenic processes. The methane produced thermogenically is often related to the production of oil taking place several kilometers down in the earth's crust. Biogenic methane production stems from two reactions; the fermentation of acetate and the reduction of CO2 by hydrogen. The former is dominant in freshwater sediments whereas the latter dominates in marine sediments. Methane, once formed, is quite stable and transports through an aquifer without undergoing much change. Only when it comes into contact with an aerobic environment, does it undergo an oxidation reaction.

2.4.3. Sorption

Sorption is one of the main mechanisms through which chemical constituents in groundwater can be immobilized. The term sorption refers to two processes actually; adsorption which is the adherence of a subject on a solid surface and absorption, which is the inclusion of the subject within the solid phase (Sposito, 2008). The tendency of a soil to retain phosphorus varies widely and is dependent on many factors and characterization of the phosphate sorption mechanism is therefore known to be difficult (McGechan and Lewis, 2001). The sorption of phosphorus is described to occur in two distinct stages that have been called "fast sorption" and "slow sorption". Sorption experiments onto sediments performed in laboratories therefore often yield dissolved phosphate concentrations that show an initial steep decline that lasts for a few hours followed by a much slower decline that can last for a few days (McGechan and Lewis 2002; Kulabako et. al., 2008). The processes involved in slow sorption are not yet well understood, however inclusion into the solid phase grains is expected to contribute to the observed slow decrease in phosphate concentrations. This process is regarded by some to be irreversible. The fast sorption process is recognized to be sorption onto available surface sites.

Sorption onto surface sites occurs when an ion in solution finds a surface site which has an opposite charge. The higher the clay and silt fraction in the soil, the higher the reactive surface area is and therefore sorption can be expected to increase with decreasing soil particle size. In general, clay particles have negatively charged surface sites and are therefore good receptors for cations. The total amount of cations that can be adsorbed to a given amount of soil is called the Cation Exchange Capacity or CEC of a soil and can be determined experimentally in a laboratory. In a steady state situation, the amount of cations in solution is in equilibrium with the amount of cations on the exchange complex. When the composition of water changes in a porous medium for instance due to intrusion of brackish water in a fresh water aquifer, cations start to equilibrate with the exchange complex and cation exchange is then said to take place (Appelo and Postma, 2005).

Apart from negatively charged particles, adsorption of anions can take place on positively charged surfaces such as iron and aluminum -oxides and -hydroxides. Equation (5) which was adopted from Holtan et. al., (1988) shows an adsorption reaction where hydrogen ions interact with an aluminum hydroxide surface site. This reaction also shows the effect of pH on the charge of metal hydroxide complexes. When pH increases, these complexes are likely to become positively charged which may inhibit anion adsorption, low pH may facilitate anion adsorption onto metal hydroxide particles in the soil.

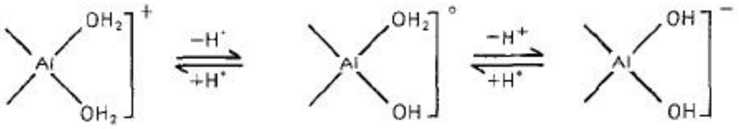

(5)

Organic matter is also known to facilitate the sorption of anions, the effects have been found ambiguous in the literature (McGechan and Lewis, 2002). On the one hand, since most substances which are derived from organic matter such as humic acid, fulvic acid and tannic acid are negatively charged, they may block positively charged surface sites on minerals which would otherwise be available to anions. On the other hand, the possibility exists for the formation of cation bridges. Iron has been found to act as an intermediate anion acceptor for orthophoshate leading to the formation of phosphate-Fe-humic complexes (McGechan and Lewis, 2002). In an attempt to explain the ambiguity, Hiradate and Uchida (2004) found that soil organic matter may buffer the pH dependency of phosphate sorption to metal oxides. In order to fully understand these concepts, further research is required.

Just as constituents in groundwater can be adsorbed onto the solid matrix, subsequent dilution due to heavy rainfall may facilitate desorption. Actual inclusion into the solid grains is an exception to this rule as no concensus has yet been found on the reversibility of this process. In the case of phosphate, it has also been proposed that the transport of mobile colloids with phosphates adsorbed to them can lead to a flux of phosphorus out of the soil. This observation was made by several studies after significant phosphate increase in groundwater after the occurrence of heavy precipitation was experienced (McGechan and Lewis, 2002).

2.4.4. Precipitation

The extent to which a mineral is soluble in water may control the presence of the constituents from which the mineral is built in the solution. In order to quantify to what extent this is happening the law of mass action with the corresponding solubility constant (K_{so}) can be used.

$$K_{so} = \frac{[A]^a[B]^b}{[C]^c[D]^d} \qquad (6)$$

Here capital letters denote molar concentrations and lower case letters give the stoichïometry of the reaction. Table 2.3 shows an overview of typical mineral formation processes in aquifers. Please note that the formation of strengite will not occur at low redox potential, because iron will only be present as Fe(II) in the groundwater.

Table 2.3: Mineral precipitation/dissolution according to the phreeqc minteq.v4 database.

Mineral	**Formation/dissolution**	**Log K_{so}**
Rhodochrosite	$MnCO_3^0 \leftrightarrow Mn^{2+} + CO_3^{2-}$	-10.58
MnHPO_4	$MnHPO_4^0 \leftrightarrow Mn^{2+} + PO_4^{3-} + H^+$	-25.4
Vivianite	$Fe_3(PO_4)_2{}^0 * 8H_2O \leftrightarrow 3Fe^{2+} + 2PO_4^{3-} + 8H_2O$	-36
Hydroxylapatite	$Ca_5(PO_4)_3OH^0 + H^+ \leftrightarrow 5Ca^{2+} + 3PO_4^{3-} + H_2O$	-44.33
Strengite	$FePO_4 * 2H_2O^0 \leftrightarrow Fe^{3+} + PO_4^{3-} + 2H_2O$	-26.4
Siderite	$FeCO_3^0 \leftrightarrow Fe^{2+} + CO_3^{2-}$	-10.24
Calcite	$CaCO_3^0 \leftrightarrow Ca^{2+} + CO_3^{2-}$	-8.48

When precipitation is invoked to explain behavior in hydrochemistry studies, one must be careful as there are factors that may inhibit the precipitation of a certain mineral. Reaction kinetics are therefore an important component of the discussion of mineral precipitation. Postma, (1981) described how high dissolved iron content, low H_2S presence and reducing conditions favor the precipitation of siderite and vivianite. Additionally, it was found that vivianite is more stable at lower pH with respect to siderite. The minerals were found to precipitate from strongly supersaturated solutions indicating slow reaction kinetics. Rhodochrosite was found to precipitate under high alkalinity and pH. A detailed discussion of another manganese mineral, MnHPO4, is not available as not much is known about this mineral (Hongve, 1997). The formation of hydroxyapatite is described as a difficult process with paradoxical effects under laboratory dissolution experiments (La Mer, 1962). Nevertheless, environments where alkalinity is high as well as pH are described to be favorable for hydroxyapatite precipitation (Richardson et. al., 1997). Cao et. al., (2007) showed evidence of humic acid as well as dissolved magnesium inhibiting the precipitation of hydroxyapatite. Laboratory studies such as those performed by Cao et. al., (2007) describe three distinct stages in the precipitation of minerals. The first one involves a slow rate of precipitation which has been associated with the initial formation of crystals on the surface of nuclei. The second stage is a fast stage of precipitation where the crystals formed in the initial stage are allowed to expand. The third stage is a very slow rate of consumption of constituents. During the second stage of precipitation it may be energetically favorable to form crystal structures that are not optimal, rearrangement of the crystal lattice in the third stage optimizes the shape of the formed minerals and facilitates an additional slow rate of precipitation.

3. Materials and methods

3.1 Overview

In order to gain an insight into the answers to our research targets described in section 1.4, several different kinds of data were gathered from the research area. The information gathered can be subdivided into soil data and groundwater data. In the months of January through April of 2011, soil samples and water samples were collected from the different well locations. These were mainly used for determining the hydrochemical parameters that govern the environment in Bwaise III slum. Several parameters were determined in the field directly from a fraction of the water sample taken whereas other parameters were determined from a fraction of the water sample that was put on transport and analyzed at UNESCO-IHE laboratory (Delft, the Netherlands). Soil sample analysis was carried out at Makarere University's soil science department (Kampala, Uganda).

In addition to the hydrochemical information gathered, from groundwater measurements both manual and automatic (through the application of divers at select locations and through slug tests), information was obtained pertaining to the hydrophysical characteristics of the site of study. The specifics of all analyses carried out can be seen in appendix II.

3.2 Hydrophysical data acquisition

3.2.1 Observation well installation

The observation wells used in this study were installed in the St. Francis and Katoogo administrative districts of Bwaise III Parish. These administrative zones were chosen because, from preliminary exploration, the local residents seemed willing to facilitate the space needed for installing the wells. Additionally these two zones cover a large surface area which allows possible areal trends to emerge from the research. The wells consisted of a simple PVC pipe which was closed at the bottom and screened with 2 mm slots over the length of the aquifer. The slotted part of the pipe was surrounded by a nylon screening cloth to prevent clogging of the slots. Typically these wells were installed 1 to 3 meters into the soil based on the hydrogeology at the site. The top 10 to 40 centimeters were reinforced with concrete to protect the well from damage. On top of the concrete, a cast iron casing with a padlock provided access and further protection. Figure 3.1 shows a schematic representation of a monitoring well. Following the installation of the wells, they were leveled with respect to mean sea level using a permanent benchmark that was located near the study area.

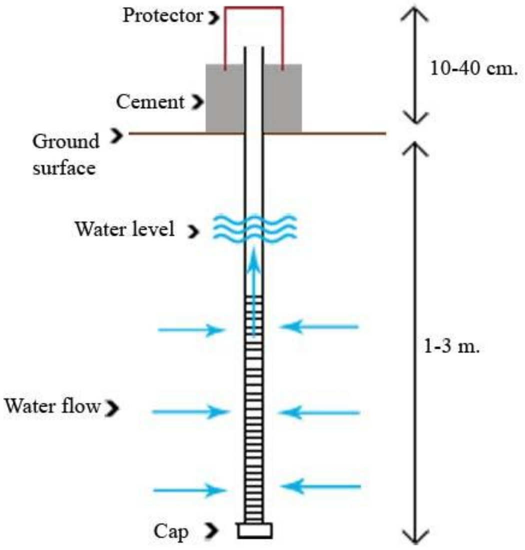

Figure 3.1: A monitoring well as installed in Bwaise III Parish.

3.2.2 Hydrological monitoring

The observation wells were monitored for water levels on a weekly basis for approximately two months using a measuring tape with a metal sounder at its end. In six of the observation wells, divers were installed to monitor the water level on a more frequent basis. The divers recorded the water level every ten minutes. Additionally, in order to monitor groundwater-surface water interaction in the area, special setups were made near the inlet of the Nsooba channel into the research area and near the outlet of the Nsooba out of our research area. Such a setup is henceforth referred to as a transect, the setup near the inlet is called the inflow transect (IT) and the setup near the outlet is called the outflow transect (OT). A transect consisted of a gauging station which was installed in the Nsooba channel itself, a well installed approximately 1 m. away from the channel and a well which was installed several meters away from the channel. All 3 wells in a transect were provided with a diver which recorded pressure once every 10 minutes.

3.2.3 Measuring hydraulic conductivity

Measurements of hydraulic conductivity were done based on the slug test method by Bouwer, (1989). This method employs Thiem solution to find a way of solving for hydraulic conductivity through the following equation:

$$K = \frac{r_c^2 ln(^{Re}/_{rw})}{2{*}Le} * \frac{1}{t}\ln\left(\frac{y0}{yt}\right) \qquad (7)$$

In this equation, $K\left[\frac{m}{day}\right]$ is hydraulic conductivity, $r_c[m]$ is the radius of the casing, $L_e[m]$ is the perforated section of the well, $r_w[m]$ is the radius as measured from the center of the well to the undisturbed portion of the aquifer, $t[s]$ is time, $y[m]$ is the difference between the water level in the well and the equilibrium groundwater level $y_0[m]$ and $R_e[m]$ is the effective radius over which the difference in water level y is undone. R_e is dependent on the geometry of the slug test setup. A typical slug test setup according to Bouwer and Rice (1976) is shown in figure 3.2.

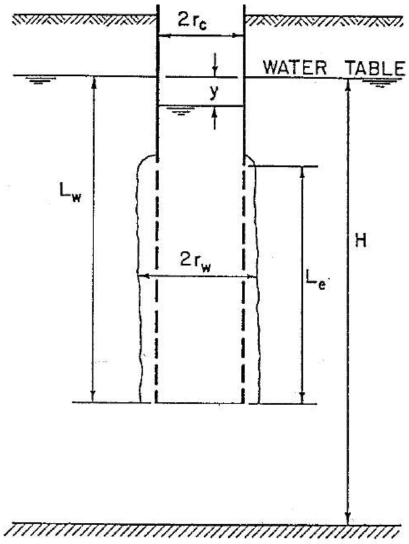

Figure 3.2: Slug test setup with parameters from equation (7) adopted: Bouwer and Rice, (1976)

The results of the analysis for the dependency of Re on the geometry yielded two equations, one that can be used if the setup penetrates the full length of the aquifer and one where it is partially penetrated. In this study all measurements of hydraulic conductivity were carried out with a fully penetrating setup, therefore the following equation from Bouwer, (1989) can be used:

$$ln\frac{R_e}{r_w} = \left[\frac{1.1}{ln(L_w/r_{w)}} + \frac{C}{L_e/r_w}\right]^{-1} \qquad (8)$$

where $C[-]$ is a dimensionless value that is plotted as a function of L_e/r_w in figure 2 from Bouwer and Rice, (1976) and $L_w[m]$ is the depth of the well with respect to the water table. Reading the C value from this graph and inserting it into equation (8) yields a value for $ln\,R_e/r_w$ which can then be used in equation (7) to obtain K. Our field setup consisted of a PVC casing with $r_c = 3.6\ cm$, which was closed at the bottom with a permeable nylon cloth to prevent sand from entering the pipe. Additionally, the casing was provided with 2 mm slots. The auger used for drilling the holes was an Eikelkamp open blade type auger with a radius of $r_w = 3.9\ cm$. After a hole was drilled up to the impermeable clay layer and the measurements of the different layers taken, the casing was taped so that possible macropore flow would be less of a problem in the field. After installing the pipe, the depth to the bottom was measured again to see if sand had entered during insertion of the pipe. The depth recorded with respect to the top of the pipe was also directly used in determination of the cable length for the diver. As a bailer, a PVC pipe of smaller radius was used where the bottom cap was modified to hold a valve that would open upon insertion into the PVC casing and close again on withdrawal. This system ensured quick and instantaneous bailing of approximately 20 cm. of water from the hole. Immediately after bailing the diver was inserted into the casing of our setup and subsequently the water level was recorded manually with a sounder for later confirmation of the readings taken by the diver. After recovery of the water level to its equilibrium value, the diver was removed from the casing and after a few minutes a duplicate measurement was taken.

3.3 Hydrochemical data acquisition

3.3.1 Initial sampling protocols

The field parameters were measured at the same time as the water samples were taken. A manual pump was used to extract the water from its well. After pumping the initial 3 well volumes, a 1 liter bottle was filled with the extracted groundwater. At times in the dry season, recovery of the water in the well was very slow to non-existent. At these locations less than 3 well volumes were extracted before collecting the sample. Temperature, pH, electrical conductivity (EC) and alkalinity were measured on the groundwater sample before filtering. Temperature and EC were measured using a WTW EC3330i portable EC meter, pH was measured using a WTW pH 340i portable pH meter and alkalinity was measured using a field titration kit from HACH where 0.2 M sulfuric acid was used to titrate a solution colored by 2 drops of bromocresolgreen from blue/green to orange/red. Additionally, in this research, it was opted to do orthophosphate and nitrate in the field. After filtering the groundwater sample into a separate plastic bottle, orthophosphate and nitrate were determined using a HACH DR 890 colorimeter (HACH company, 1997-2009). On a typical day in the field 5-8 samples were collected. The samples were also tested for ammonia which was done with the HACH colorimeter in the lab, because of the inconvenient 20 minute reaction time on the procedure. Analysis in the laboratory allowed us to carry out the colorimeter procedure for ammonia once for all the samples taken.

3.3.2. Revised sampling protocols

Throughout the sampling procedure, changes have been made in order to account for the situation specific to the research area. In the revised sampling procedure, the water was filtered as soon as possible out of the hand pump reservoir and orthophosphate was determined as fast as possible to prevent any iron precipitation from taking phosphorus out of the water. After phosphate, nitrate was determined. At the same time, the ammonia procedure was followed and alkalinity was determined. Reading pH, EC, and temperature and alkalinity was done after all other analyses. As the required reaction time on the ammonia reaction was progressing, the field setup was moved to the next location. Upon arrival at the next sampling location, ammonia was analyzed as soon as the required reaction time had expired and the sampling procedure commenced again for the new location. In contrast to our initial sampling protocol, determination of ammonium was done in the field to prevent any ammonium from undergoing nitrification reactions in the time it would take to analyze ammonium in the Makarere laboratory.

3.3.3. Water sample lab analysis

For each water sample taken, 50 ml was filtered and preserved in the field for cation and anion analysis. For cation analysis, upon departure into the field, the 25 ml. bottles used were provided with 2 drops of nitric acid which ensured the pH was 2 or less. For anion analysis the bottles were not acidified. After marking the bottles, they were stored in an ice box in the field and the same day, after transport, they were stored in a freezer at Makarere University. At the end of the fieldwork period in Uganda, the samples were still frozen and were wrapped in aluminum foil for transport to UNESCO-IHE in Delft, the Netherlands to do the laboratory analysis. Upon arrival in the Netherlands the water samples had defrosted, but were still cold and had been out of the fridge for approximately 16 hours.

Cation analysis of the water samples was done on the acidified sample. Dilutions of 10 and 50 times were made of all 118 samples and were subsequently acidified again with 2 drops of nitric acid to account for the dilution. The water sample dilutions were then tested on a Thermo Scientific x-series 2 ICP-MS machine for the presence of K^+, Mg^{2+}, Ca^{2+}, Fe^{2+}, Mn^{2+}. Anions were analyzed on a Dionex ICS-1000 machine using the non-acidified sample. Because iron had precipitated in these samples, they needed to be filtered through 0.45 micron filter paper again to prevent the IC from clogging. After filtering, the water sample was diluted 10 times before being run on the IC. Analyses was carried out for F^-, Cl^-, $SO4^{2-}$ and $NO3^-$.

3.4 Soil sample data acquisition

3.4.1. Soil Sampling protocol

The soil samples were collected right after digging each hole for the observation wells. A sample was taken from each distinctive layer encountered in the borehole profile and transported to Makarere university in polyethylene containers for soil sample analysis. Distinctions between layers were made based on qualitative observations in the field that showed a change in color, texture, moisture content and structure. The thickness of the distinct layers was measured using a steel tape every time a transition of soil properties was encountered. This sampling procedure yielded 56 unique soil samples from the 26 wells installed in the area for this research. After the analysis at Makarere university, the soil samples were transported to the Netherlands for the analysis of geo-available metals. All analysis was carried out on air dried samples that had already passed through a 2 mm sieve.

3.4.2. Soil sample lab analysis

Soil particle size analysis was done by means of the hydrometer method according to Okalebo et. al., (2002). The hydrometer method determines the fraction of sand, silt and clay sized particles present in the sample. It relies on the principle of differential settling velocity of the different categories of particle sizes within a water column. Approximately 50 grams of the air dried soil was suspended in 10 ml calgon solution (sodium hexametaphosphate 10%) after which the mixture was allowed to rest for 10 min. The calgon solution provided the dispersing properties needed in the solution to separate aggregates of different particle sizes. After the dispersion time the solution was transferred to a graduated cylinder which was filled up to 1 liter. For measuring the different particle sizes the cylinders were first inverted to establish that all of the soil mixture was in suspension. Then a hydrometer reading was taken for each soil sample after 40 seconds and two hours to determine the different particle size fractions. The first reading indicated the fraction of sand that had settled to the bottom of the cylinder whereas the second reading represented the fraction of silt on top of sand, which meant that the remainder of the 50 g. of soil was still in suspension. Percentage wise, the fractions were determined from the ratio of the hydrometer reading and the original sample weight.

Geo-available metals were determined using extraction with 0.43 M HNO_3. Approximately 2 g. of sample was weighed and 20 ml. of nitric acid was added. The solution was put on an orbital shaker for 22 hours. Subsequently, the metals that were dissolved in this process were separated from the soil by centrifugation at 3000 rotations per minute for four minutes. The supernatant solution from centrifugation was filtered using 0.45 µm membrane paper and analyzed using a Spectro Ciros ICP-OES machine.

3.5 Data interpretation

3.5.1. Hydrophysical climate

The groundwater flow velocity and the time it takes to flush the aquifer of the research area are prerequisite knowledge when discussing the fate and transport of nutrients in the slum. The groundwater flow velocity $v\left[\frac{m}{day}\right]$ was calculated by the use of the Darcy equation:

$$v = -\frac{K}{n}\frac{\partial \mathrm{h}}{\partial \mathrm{x}} \qquad (9)$$

In this equation $K\frac{m}{day}$ was determined from slug testing, the hydraulic gradient $\frac{\partial h}{\partial x}$ [-] from the water level measurements and a reasonable value was assumed for the porosity $n[-]$. Subsequently, when we know the travel distance of groundwater along a streamline we can calculate the time it takes for pollution to reach Nsooba channel from its source T (flush time):

$$T = \frac{dx}{v} \qquad (10)$$

In addition to velocity and flush time, a groundwater balance provides a basic insight into the different fluxes entering and leaving the domain. The groundwater balance equation used in this research is the following:

$$\left[Q_{prec} + Q_{lsi}\right] - \left[Q_{lso} + dS\right] = 0 \qquad (11)$$

where $Q_{prec}\left[\frac{mm}{day}\right]$ is the influx due to precipitation events also called recharge, $Q_{lsi}\left[\frac{mm}{day}\right]$ and $Q_{lso}\left[\frac{mm}{day}\right]$ are the lateral subsurface in and outflow through the aquifer due to the gradient in groundwater level that is present in the area. The storage term $dS\left[\frac{mm}{day}\right]$ is the water that is taken up or released from the aquifer.

The lateral subsurface inflow and outflow were calculated based on the hydraulic head difference over the in- and outflow boundaries of the area of interest, which can be seen in the results section, using equation (9) multiplied by the inflow and outflow area respectively. The change in storage was calculated based on equation (12) from Nonner (2001).

$$dS = S\frac{d\emptyset}{dt} \qquad (12)$$

Here $d\emptyset\ [mm]$ is the change in water level in a single well over the time interval $dt\ [days]$. $S[-]$ is the dimensionless storativity as defined in equations (14) and (15).

The recharge $Q_{prec}\left[\frac{mm}{day}\right]$ was estimated using the groundwater table fluctuation method from Nonner (2001). This method proposes that the recharge in the study area is a combination of water stored and water that is added to discharge. These effects are combined in the following equation which is modified from Nonner (2001).

$$Q_{prec} = S\frac{d\emptyset_{mod}}{dt} \qquad (13)$$

Here $d\emptyset_{mod}[mm]$ is the change in the groundwater table obtained from divers in the area and $dt[days]$ is the period of time over which there was a significant change in the groundwater level. $S[-]$ is again the dimensionless storativity which was calculated using a reasonable value for the selected parameters in the following two equations:

$$S = S_s b \quad and \qquad (14)$$

$$S_s = \rho g(\alpha + n\beta) \qquad (15)$$

where $S_s[1/m]$ is the specific storage coefficiënt, $b[m]$ is the aquifer thickness at the location of the diver reading which was measured at the time the wells were installed, $\rho\left[\frac{kg}{m^3}\right]$ is the density of water, $g\left[\frac{m}{s^2}\right]$ is the acceleration due to gravity, $\alpha\left[\frac{m*s^2}{kg}\right]$ is the compressibility of the aquifer and $\beta\left[\frac{m*s^2}{kg}\right]$ is the compressibility of water. The compressibility and density of water and the acceleration due to gravity are constant and well known. Porosity may vary, however since the compressibility of water is very low, the effect of porosity variations on the determination of the specific storage coefficient will be low. For α, a range of values was obtained by Freeze and Cherry (1959). The minimum and maximum values for loose sand were used to show the possible effects of the variation of this parameter on the outcome of the water balance.

3.5.2. Hydrochemical climate

The total number of 118 groundwater samples that were analyzed in the lab were subjected to an internal screening in the form of the ion balance concept. Phreeqc was used to calculate the percentage error resulting from the following equation according to Parkhurst and Appelo (1999).

$$percent\ error = \frac{\sum cations - \sum anions}{\sum(cations + anions)} * 100 \qquad (16)$$

Where Na^+, K^+, Mg^{2+}, Ca^{2+},$NH4^+$, Fe^{2+}, and Mn^{2+} constitute the cations and HCO_3^-, Cl^-, $SO4^{2-}$, NO^{3-}, $PO4^{3-}$ and F^- constitute the anions. All posts on this balance of ions were expressed in [meq/l]. Since the sampling and storage of water samples in Kampala and the subsequent transport to the Netherlands was difficult, an error of 20% in the analysis of the water sample was deemed to still be acceptable. The Stuyfzand classification was also determined using Phreeqc. The Stuyfzand classification is based on the division of water samples into main type, which is based on chlorinity, type which is based on the values for alkalinity and subtypes which denotes the most prominent cation and anion in a water sample. The coding system for the Stuyfzand classification can be found in tables 3.1 and 3.2.

Table 3.1: Main type classification according to Stuyfzand (1993).

Main Type	Main Type	Code	mg Cl/L	meq Cl/L
Fresh	Oligohaline	G	0-5	<0.141
	Oligohaline-fresh	g	5-30	0.141-0.846
	Fresh	F	30-150	0.846-4.231
	Fresh-brackish	f	150-300	4.231-8.462
Brackish	Brackish	B	300-1,000	8.462-28.206
	Brackish-salt	b	1,000-10,000	28.206-282.064
Salt	Salt	S	10,000-20,000	282.064-564.127
Hypersaline	Hypersaline	H	>20,000	>564.127

Table 3.2: Type classification according to Stuyfzand (1993).

		Alkalinity as HCO3-	
Type	code	mg/L	meq/L
Very low	*	<31	<0.5
Low	0	31-61	0.5-1
Moderately low	1	61-122	1-2
Moderate	2	122-244	2-4
Moderately high	3	244-488	4-8
High	4	488-976	8-16
Very high	5	976-1953	16-32
Extreme	6	1953-3905	32-64
Very extreme	7	>3905	>64

in order to separate this effect from any reactions taking place. Appropriate representations, or endmembers, of these water types were therefore made from averaging water samples from well GW15 for the polluted end member and GW24, 25 and 26 for the natural endmember and using the subsequent values obtained for Cl^- in the following equation obtained from Appelo and Postma (2005), where all masses were calculated in [mmol/l].

$$f_{pol.} = \frac{M_{Cl^-,sample} - M_{Cl^-,natural}}{M_{Cl^-,pol.} - M_{Cl^-,natural}} \qquad (17)$$

Here the $M_{cl-,pol.}$ and $M_{cl-,natural}$ components are Cl^- values from the respective chosen endmember and the $M_{cl-,sample}$ is the Cl^- value from a sample. The resulting $f_{pol.}$ ratio which lies between 0 and 1 gives an indication of the influence of either endmember in the chosen samples. This ratio can then be applied to predict the amount of other components, i, in a sample that would be there only because of conservative mixing ($M_{i,mix}$) between endmembers through the following equation from Appelo and Postma (2005).

$$M_{i,mix} = f_{pol.} * M_{i,pol.} + \left(1 - f_{pol.}\right) * M_{i,natural} \qquad (18)$$

The surplus or deficit ($M_{i,react}$) of a component i with mass M in a sample can then be quantified by the third reaction in this sequence which was also obtained from Appelo and Postma (2005).

$$M_{i,react} = M_{i,sample} - M_{i,mix} \qquad (19)$$

It was discussed that mineral formation can be an important control on the availability of ions in groundwater (section 2.4.4). The Saturation Index (SI) of minerals gives an indication of whether or not a specific mineral is liable to precipitate. The SI reads as follows from Sposito (2008)

$$SI = \log\left(\frac{IAP}{K_{so}}\right) \qquad (20)$$

In this equation IAP stands for Ionic Activity Product which is basically the mass action law that leads to the formation of the mineral based on the values for the different ions in the sample. $K_{so}[-]$ is the resulting value of that same mass action law if the mineral phase were in thermodynamic equilibrium with the ions in solution. If the SI > 0, the solution is saturated with respect to the mineral for which it was calculated, if SI < 0, the solution is undersaturated and if SI = 0, the solution is at equilibrium.

Appropriate surface plots of different chemical parameters were made using Golden Software's Surfer application if it was found they provided insight into the behavior of a chemical constituent of the soil. Any graphs were made using Grapher except for the borehole plot in the Geology results section which was made using Strater both also by Golden Software.

3.5.3. Phreeqc model

In section 3.5.2, we noted the calculation of the ion balance, saturation indices and Stuyfzand classification by using phreeqc. In addition to these parameters, a one dimensional reactive transport model was made in phreeqc in order to simulate the flow velocity with the parameters from equation (9) that were obtained during fieldwork. Assuming that the longest distance a dissolved component can travel is 800 m, the model can be looked upon as an 800 m column experiment where the domain is allowed to equilibrate with the natural water type endmember that is described in section 3.5.2 for $t = 0$. Subsequently, the polluted water type endmember is introduced at the far end of the column and transport starts at $t > 0$. For a chemical that is transported, phreeqc solves the following equation (Appelo and Postma, 1999) for the aqueous concentration $C\ [\frac{mmol}{l}]$:

$$\frac{\partial C}{\partial t} = -v\frac{\partial C}{\partial x} + D_L\frac{\partial^2 C}{\partial x^2} - \frac{\partial q}{\partial t} \qquad (21)$$

where $t\ [s]$ is time, $v\left[\frac{m}{s}\right]$ is pore water flow velocity, $x[m]$ is distance along a streamline, $q[\frac{mmol}{l}]$ is the concentration of the transported chemical in the solid phase, and $D_L\left[\frac{m^2}{s}\right]$ is the hydrodynamic dispersion coefficiënt according to:

$$D_L = D_e + \alpha_L v \qquad (22)$$

where $D_e\left[\frac{m^2}{s}\right]$ is the effective diffusion coefficient and $\alpha_L[m]$ is the dispersivity. The values used for dispersivity and effective diffusion coefficient can be found in the list of assumed parameter values. Figure 3.3 gives a schematic overview of the various terms in equation (21) where vC represents advective transport and $-D_L\frac{\partial C}{\partial x}$ represents dispersive transport into a domain cell. $\frac{\partial q}{\partial t}$ is the change in concentration of a chemical species in the solid phase due to all chemical equilibrium and non-equilibrium reactions considered by the phreeqc minteq v4 database.

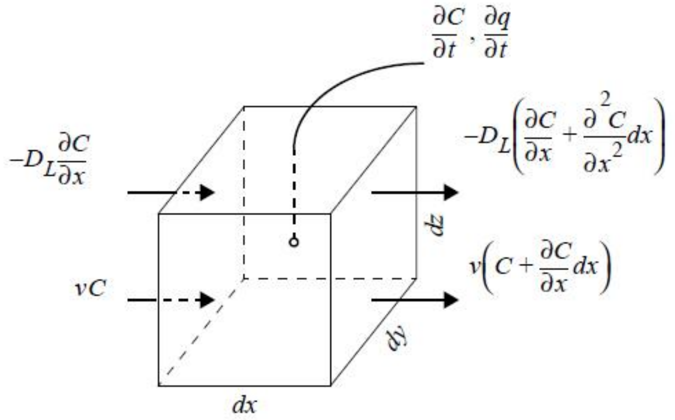

Figure 3.3: Representation of the advection-reaction-dispersion equation that is solved by phreeqc adopted: Parkhurst and Appelo (1999)

Using the initial conditions $C(x,0) = C_0 \neq 0$ and for the displacing solution $C = C_i$ and the third type or Cauchy boundary condition $C(0,t) = C_i + \frac{D_L}{v}\frac{\partial C(x_{end},t)}{\partial x}$ the solution becomes:

$$C(x,t) = C_0 + \frac{1}{2}(C_i - C_0) * A \tag{23}$$

where,

$$A = erfc\left(\frac{x - vt/R}{\sqrt{4\alpha_L\, vt/R}}\right) + \sqrt{\frac{x}{\pi\alpha_L}}exp\left[-\frac{(x - vt/R)^2}{4\alpha_L\, vt/R}\right] - \frac{1}{2}\left(1 + \frac{x}{\alpha_L} + \frac{vt/R}{\alpha_L}\right)exp\left(\frac{x}{\alpha_L}\right)erfc\left(\frac{x - vt/R}{\sqrt{4\alpha_L\, vt/R}}\right) \tag{24}$$

Here $R[-]$ is the retardation factor according to:

$$R = 1 + \frac{CEC}{C} \tag{25}$$

where $CEC\left[\frac{mmol}{l}\right]$ is the cation exchange capacity according to the list of assumed parameter values. To investigate the extent to which cations are exchanged in Bwaise was the second goal for building this model. Since the cation exchange capacity was not measured, two scenarios were used which will henceforth be referred to as model 1 and model 2. Model 1 assumes a low cation exchange capacity in Bwaise, model 2 assumes the value which was obtained from Kulabako et. al., (2008) which was a lot higher.

4. Results

4.1 Overview

The presentation of the results has been structured by the use of three subchapters: geology, hydrology and hydrochemistry. The results in the geology section provide an insight into the different stratigraphic layers encountered in the study area and their thickness, soil texture classification and geo-available metal content. The hydrology section consists of the results for the hydraulic gradient, horizontal conductivity and the inflow and outflow transect diver data. Additionally, the groundwater balance compares the relative importance of the recharge, storage and lateral subsurface fluxes. The analysis of the geology and hydrology results can then help us in the interpretation of the hydrochemical data gathered in the field and measured in the laboratory. In order to provide an insight into the large body of hydrochemical information available, zones of differing water type in the study area will be characterized. Subsequently, these zones are then used to explain the processes governing the spread of nutrients in the study area. Processes governing the spread of nutrients that are considered in this section are: conservative mixing, cation exchange, sorption and precipitation.

4.2 Geology

During the installation of the wells, soil samples were taken from the different stratigraphic entities that were encountered in the soil of the research area. In general, three different layers could be distinguished almost everywhere in the research area. The layers will henceforth be referred to as the top, middle and bottom layer.

In the field, the top layer could be observed as a layer consisting of a material that varies in grain size and colour. This makes sense, as Bwaise is largely wetland reclaimed by its inhabitants. Grain sizes varied from silty to sandy, but pebbles and pieces of concrete were also encountered. Additionally, the poor waste disposal in Bwaise made it so that in this layer, a lot of household waste was observed. The household material could be anything ranging from plastics to synthetic materials such as t-shirts or fishing nets. The middle layer was the part of the soil profile in which the water table was found in the field. After the initial encounter of the water table, typically, it would rise to a shallower depth indicating the semi-confined nature of the layer in which it was found. The middle layer consisted of poorly consolidated grey material that, from qualitative observations in the field, was deemed more sandy. This layer was therefore determined to be the aquifer. The bottom layer was made up of stiff material, decidedly better consolidated which, combined with the increased clay content made up for a very rigid/stiff layer. The material was almost white in colour with yellow/brown spots occurring randomly in the material.

The grain size analysis in the laboratory confirmed the distinction of the three layers based on field observations (table 4.1). Soil samples taken from the top layer contained grain sizes that fell in the loamy sand up to clay classifications according to the soil textural triangle (figure 4.1, 4.2). Additionally, grain sizes from the top layer were more varied between the different samples taken than the middle and bottom layer. The middle layer was made up of sandy loam to sandy clay loam and the confining bottom layer was made up of sandy clay to clayey material.

Considering the thickness of the 3 layers, the observation can be made that the top layer was roughly 0.5 m and the aquifer layer was roughly 1 m. in thickness (table 4.1). The exact thickness of the bottom layer is not known, because even though it was attempted, it was hard to drill deep into this layer with a hand auger. From the fact that the bottom layer was omnipresent and at least 20 cm. in thickness everywhere it was concluded that the bottom layer forms an effective confining layer in the geological makeup of the area even though the exact thickness is not known. During the fieldwork in Bwaise, the observation was made that the middle layer decreased in thickness closer to

Nsooba channel. The regional variation of layer thicknesses was therefore plotted on an approximate Ne-SW profile (figure 4.3).

From the analysis for geo-available metals, the three most prominent constituents of the soil solution were iron, aluminum and calcium which are shown in table 4.1, however even these three constituents together accounted for only 1 weight percent of soil dissolved during the analysis showing that the concentration of ions in the soil available for interaction with groundwater was very low. From the results for geo-available metals we therefore conclude that adsorption due to ligand exchange with metal oxides, which has often been described as the most effective way of retaining phosphorus can not play a major role in Bwaise.

Table 4.1: Average thickness and grain size percentages with standard deviations of the distinguished stratigraphic units in Bwaise. Only the wells of which three soil samples were taken were included in this analysis as those are regarded the most representative.

	Thickness[cm]	**%sand**	**%silt**	**%clay**	**Fe[mg/kg]**	**Ca[mg/kg]**	**Al[mg/kg]**	**n**
Top	53.5	56.9 ± 10.4	14.6 ± 5.2	28.5 ± 8.0	468.9	421.5	131.0	13
range	(20-90)	(38 – 74)	(4 – 22)	(14 – 40)	(185.4-1072.3)	(185.6-951.3)	(61.6-201.1)	
Middle	113.1	65.2 ± 12.5	13.2 ± 6.1	21.5 ± 8.8	379.6	371.7	110.4	13
range	(50-220)	(48 – 80)	(0 – 26)	(4 – 34)	(95.3-692.8)	(32.9-1164.8)	(19.3-228.3)	
Bottom	/	52 ± 7.8	11.5 ± 3.9	36.5 ± 7.4	276.3	103.7	60.1	12
range		(38 – 64)	(8 – 22)	(26 – 48)	(45.6-735.5)	(54.4-176.3)	(40.2-82.7)	

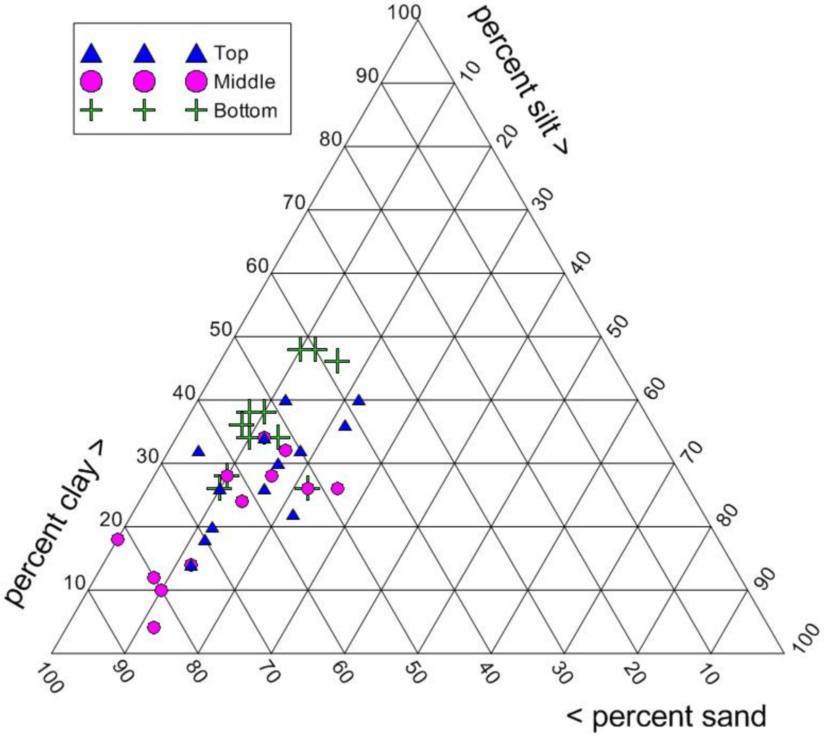

Figure 4.1: Soil texture classification of the three distinct layers encountered in Bwaise.

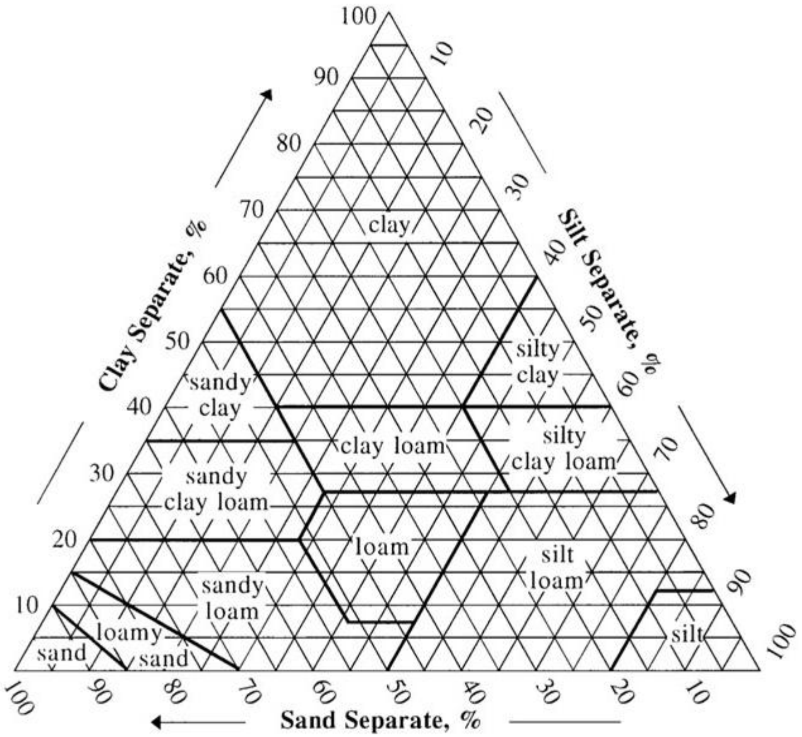

Figure 4.2: Soil texture triangle (Adopted: Okalebo et. al., (2002).

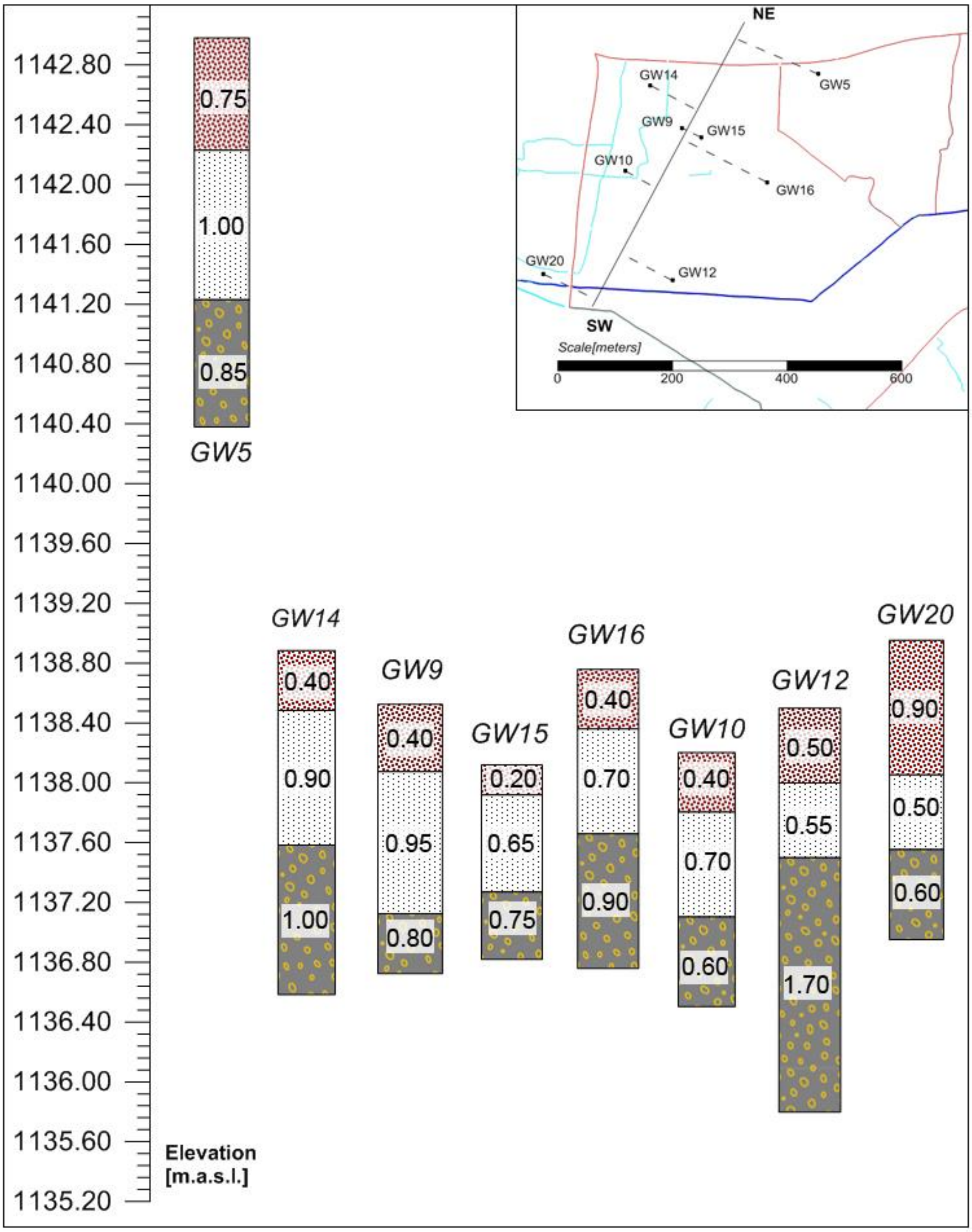

Figure 4.3: Borehole plots based on the measured depth of encountered stratigraphic units in groundwater monitoring wells indicated on the area plot [m.a.s.l].

The stratigraphic units shown are top, middle and bottom layer respectively with the thickness given in meters in each unit, note that the bottom layer's thickness is the minimum thickness observed in the field.

4.3 Hydrology

4.3.1 Groundwater contours

The installation of the wells yielded 26 individual wells in the study area (figure 4.4). The actual location of well no. 18-20 and 24-26 was not within Bwaise, but they formed an integral part of the study, because results for these wells could give an indication of how far contamination from human activity and land use might spread. The wells were given the names GW1 through GW26. Two locations named LS (latrine site) and SW (solid waste site) were included from a previous study from Nyenje et. al., (2012, in review) since the wells installed at these sites were already present in the area. The wells GW1 and GW23 together with a gauging station at the same location made up the inflow transect. The wells GW17 and GW21 with a gauging station formed the outflow transect. GW14 and GW16 were wells that held a diver for the purpose of continuously recording the groundwater level.

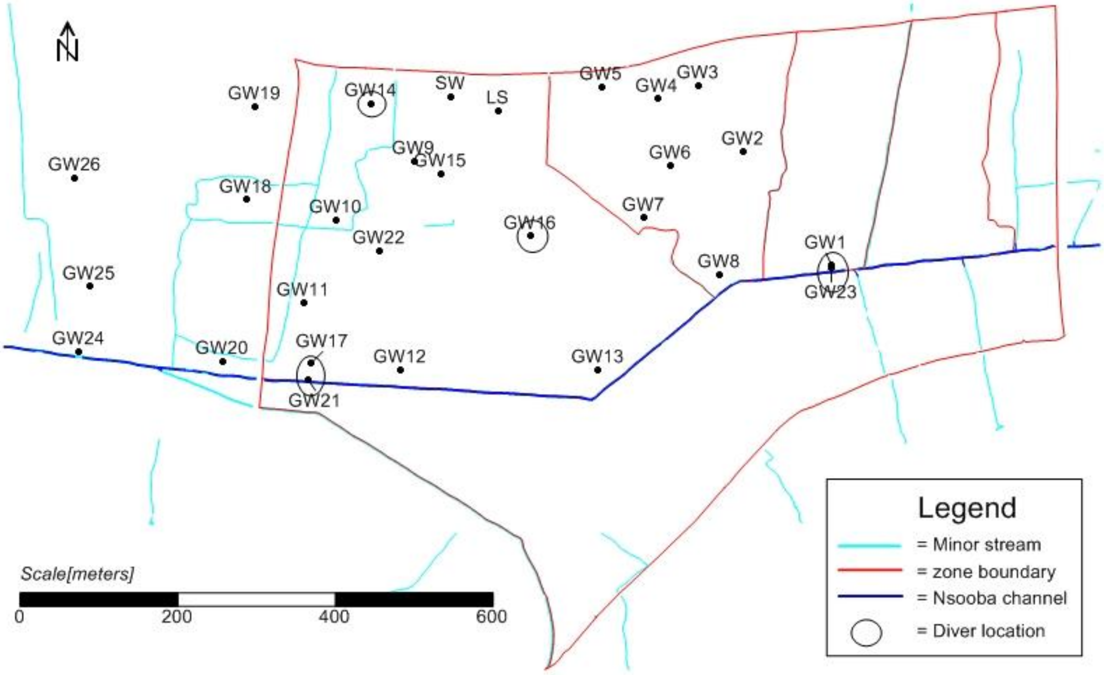

Figure 4.4: Groundwater monitoring well locations

The groundwater levels were recorded approximately once every week during the period of February to the beginning of April. During the period of measurement of these groundwater levels, an increase in rainfall marking a transition from a dry season to the rainy season was experienced in the field and this could also be observed in both the recordings from the divers and the manual data. From the experience in the field, the date at which the rainy season started was determined to be March 15th 2011. From the analysis of the groundwater contours, a groundwater flow pattern from Northeast to Southwest was observed (Figure 4.5, 4.6) both before and after the start of the rainy season. Over the entire research area during the time of measurement, there was a hydraulic gradient of approximately 3m/km. The gradient however was not continuous over the domain as the contours were more closely spaced in the St. Francis zone compared to the Katoogo zone. The shape of the contours did not change over time or with rainwater input. The height of the contours with respect to sea level (m.a.s.l.) did change however as the additional input of rainwater caused the groundwater table to rise approximately 0.5 m. higher than before the rains commenced.

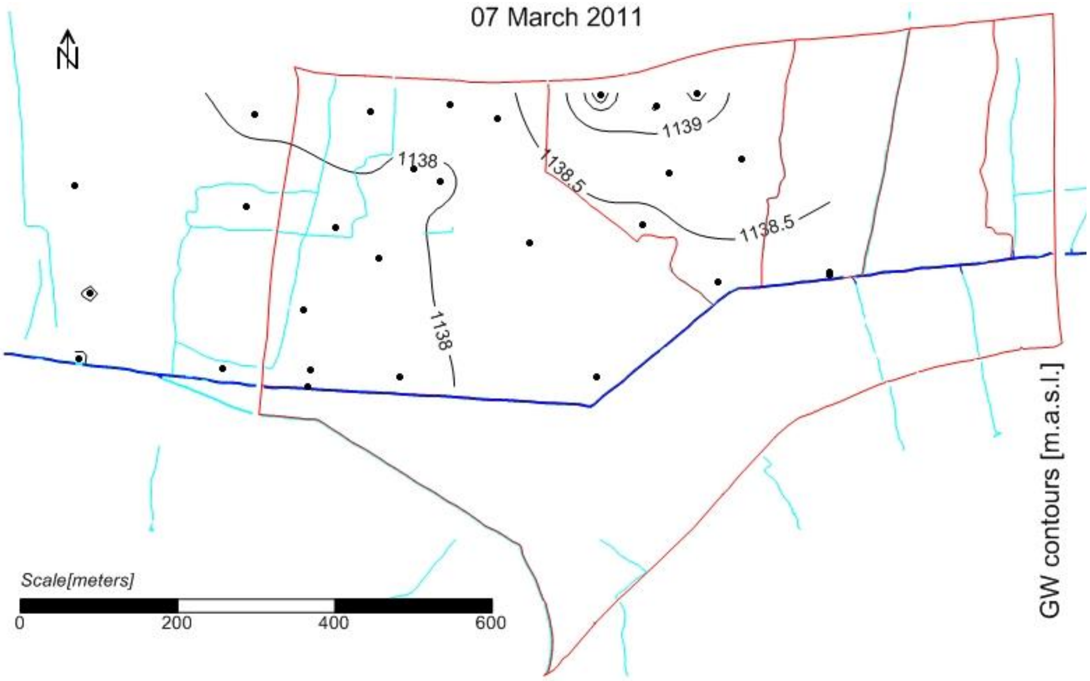

Figure 4.5: Groundwater contour levels as recorded before the start of the rainy season

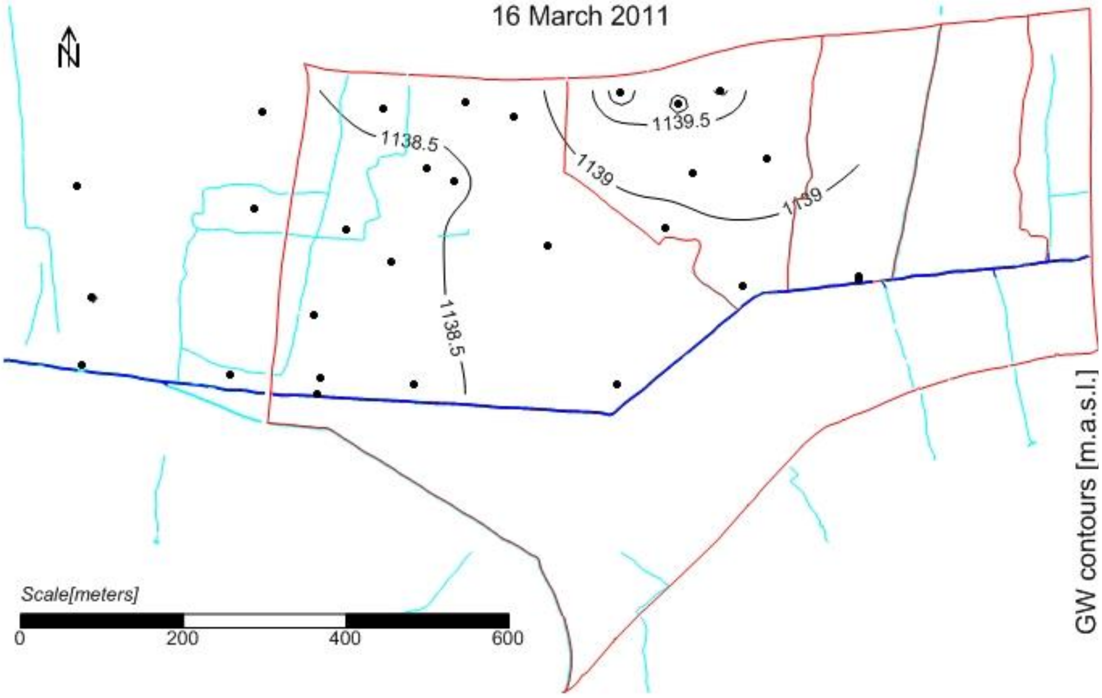

Figure 4.6: Groundwater contour levels as recorded after the start of the rainy season

Figures 4.5 and 4.6 give an accurate representation of the groundwater contours in the study area, however appendix I gives a complete record of all groundwater levels recorded during fieldwork.

4.3.2. Nsooba channel interaction

The divers were installed in the research area at the 12th of March, which is a bit later than the first manual measurement, but it was still before the start of the rainy season which was determined to be at the 15th of March. Similar to field observations, the water level recordings that were extracted from the divers showed that the start of the rainy season was indeed at March 15th.

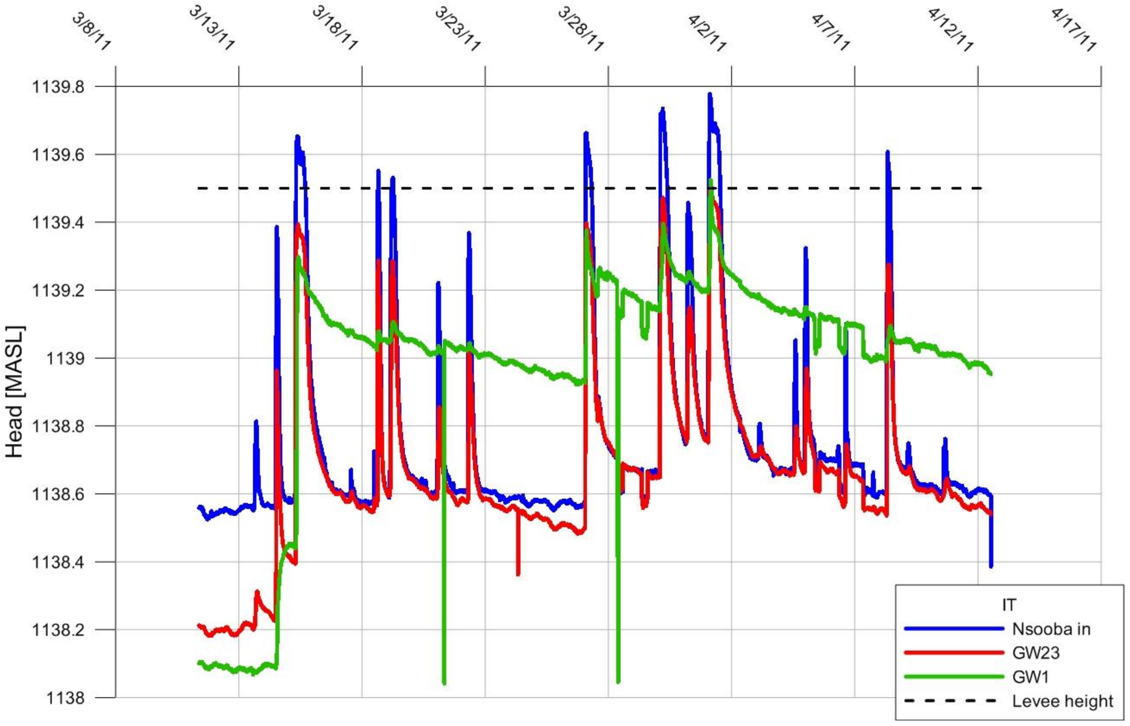

Figure 4.7: Groundwater levels in MASL at the inflow of the research area

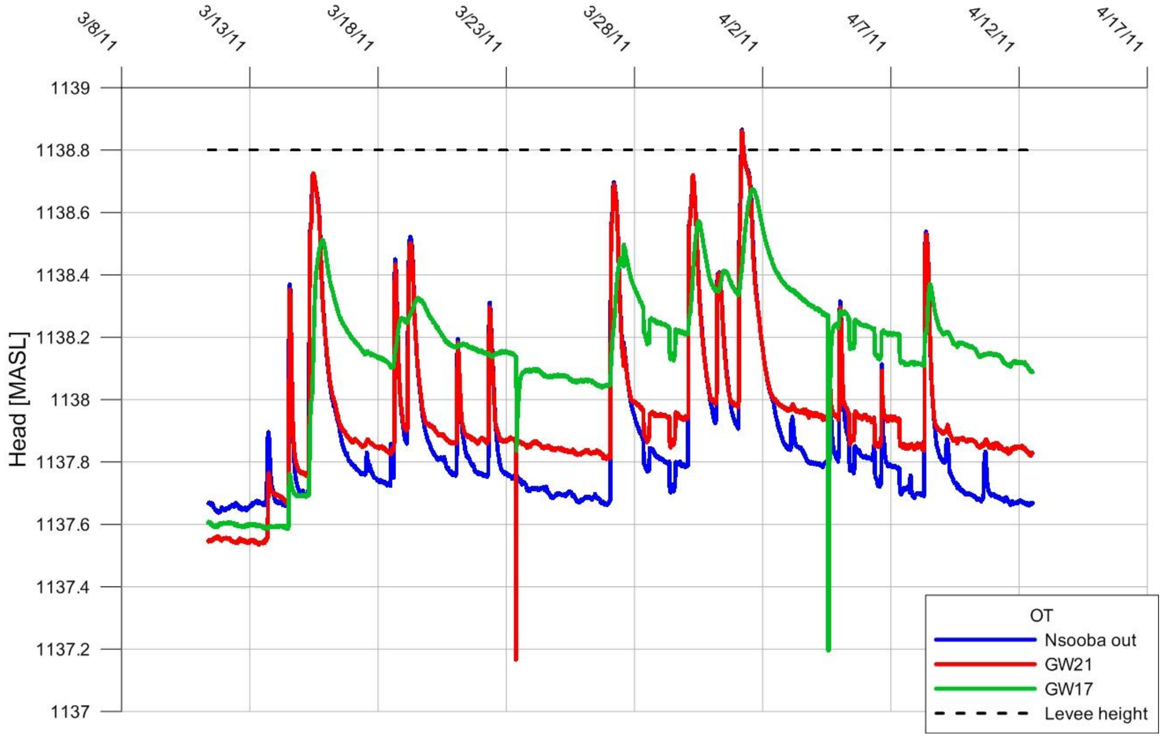

Figure 4.8: Groundwater levels in MASL at the outflow of the research area

The diver data plots (figure 4.7, 4.8) were constructed such that a sequence of gauging station (blue line), first well in the transect (red line) and second well in the transect (green line) would be conveniently shown for the inlet and outlet of the Nsooba channel respectively.

The few downward spikes recorded were instances where a diver measurement coincided with the extraction of a water sample from the well. From the baseflow water levels in the two transects we deduced that groundwater flowed towards and ended up in Nsooba channel. This effect was most pronounced at the outlet transect where the water level was highest at GW17 and going down progressively through the transect towards Nsooba channel. At the inlet transect, however, the water levels in the channel and GW23 coincided roughly during baseflow. From the fact that GW1 showed a consistently higher water level during baseflow, it was reasoned that water was still flowing towards Nsooba channel at the inflow transect.

For peak discharge due to heavy rainfall events we observed that for both the IT and the OT, the diver response was a fast increase in groundwater level irrespective of its location in the transect. During rainfall events, especially at the IT, the water level in Nsooba channel rose above the groundwater level for brief times. This suggests that the flow direction near Nsooba channel temporarily reversed during very high runoff. The ground surface elevation increased slightly near Nsooba channel (also visible in figure 4.3), which is why we call the ground surface elevation near Nsooba channel the levee height. The ground surface elevation for GW23 and GW21 was plotted in figures 4.7 and 4.8 respectively as the levee height. The water level in Nsooba channel exceeded the levee height once at the outflow transect and seven times at the inflow transect. Visual observations during fieldwork confirmed that sporadic inundation was indeed taking place. If inundation caused a significant contribution to the groundwater level in Bwaise then we would see the water levels at GW1 and GW17 for the inflow and outflow transects respectively increase steeply up to the water level of Nsooba channel. This didn't happen during the time of measurement (figure 4.7, 4.8) which lead us to conclude that the majority of the inundated water was subject to evaporation. Uganda is subject to a high annual evapotranspiration rate of approximately 1000 mm (Ateawung, 2010).

4.3.3. Slug tests

Hydraulic conductivity is the third component in this research contributing to the hydrological framework of the area. Slug tests in Bwaise were found to be difficult in part due to the nature of the top soil layer. Fragments of rock concrete and solid waste made it difficult to drill a proper auger hole.

Table 4.2: Measured hydraulic conductivities at selected well locations in Bwaise III parish

Site	K[m/day]	Site	K[m/day]
SW	5.30	GW4	0.62
SW	6.00	GW4	7.87
GW16	6.00	GW10	1.40
GW16	2.63	GW10	2.12
GW1	4.68	GW10	0.96
GW8	0.62		

During the slug testing, sites were chosen such that results would show the hydraulic conductivity at different parts of the domain. A duplicate of each measurement was taken for all locations except GW8. The duplicate from GW1 was found to contain an error in the diver recordings. From table 4.2 an approximate range of 0.6-7.9 m/day was established for locations SW, GW16, GW4 and GW10. An average of 3.43 m/day was calculated which we found a fair average despite the difficulties encountered and was used for the calculations of the Q_{lsi} flux in the water balance. For the Q_{lso} flux, a lower value for K was used to simulate the more densely packed nature of river bed sediments near Nsooba channel.

4.3.4. Water balance

This section shows the results of the quantification of the various terms on the water balance of the middle soil layer. A spatial representation of how the individual contributions Q_{lsi}, Q_{lso}, Q_{prec} and dS were considered was made (figure 4.9). The boundaries of the water balance were chosen according to the dotted line in figure 4.9. The surface area was calculated to be 1.66 km^2 in extent and the fluxes were calculated in mm/day per m^2 of surface area. Apart from these terms, there were no additional sources or sinks, groundwater was not abstracted from the area and from the geology results section we assumed that the confining bottom layer was omnipresent and effectively separated the shallow system this study focuses on from any deeper groundwater flow system that could be present. The lateral subsurface inflow was considered as a contribution to the water balance perpendicular to the hydraulic head contours presented in section 4.3.1. Four couples of two wells were chosen that formed gradients over the Q_{lsi} inflow boundary. The lateral subsurface inflow was calculated using the hydraulic head difference at a well couple dH, the hydraulic conductivity K and dx as the lateral distance between a well couple (table 4.3). The resulting Q_{lsi} value according to equation (9) for a specific time interval was calculated by averaging the Q_{lsi} values for all four well couples. The cross sectional area of inflow was calculated to be 431.1 m^2.

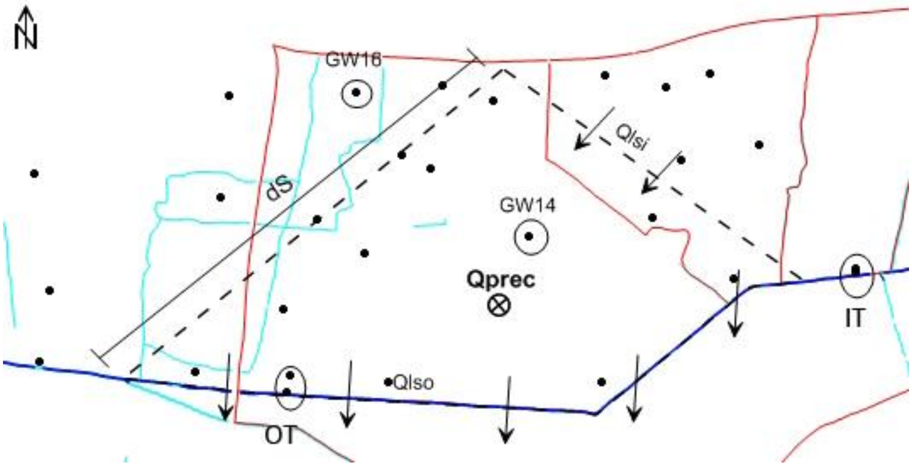

Figure 4.9: Fluxes of the water balance considered in the study area.

Table 4.3: Lateral subsurface inflow over the inflow boundary of the water balance.

Head[m]	07/03/2011	16/03/2011	24/03/2011	02/04/2011	dx[m]	K[m/day]
GW2	1138.78	1139.00	1139.05	1139.15		
GW8	1138.44	1138.98	1138.90	1139.12		
dH	-0.34	-0.02	-0.15	-0.03	158.86	3.43
GW6	1138.87	1139.06	1139.01	1139.06		
GW7	1138.07	1138.73	1138.61	1138.78		
dH	-0.79	-0.32	-0.39	-0.27	74.24	3.43
GW4	1139.80	1140.82	1140.73	1140.77		
GW16	1138.28	1138.48	1138.54	1138.67		
dH	-1.52	-2.34	-2.19	-2.10	237.06	3.43
GW5	1141.34	1141.38	1141.52	1141.68		
GW15	1137.61	1138.27	1138.27	1138.31		
dH	-3.73	-3.11	-3.25	-3.37	231.77	3.43
Qlsi[mm/day]	0.078	0.062	0.065	0.061		

On March 7th the lateral subsurface inflow was 0.078 mm/day, but it decreased to 0.062 mm/day after which it remained approximately stationary. This decrease was caused by the sudden increase in rainfall between the 7th and the 16th of March having a more pronounced effect on the wells downstream of the inflow boundary than on those upstream causing the hydraulic head difference over the boundary to decrease. The results for Q_{lsi} were also added to summary table 4.6.

Since the spatial scale of the study area was small compared to the area over which rainfall occurs, recharge was considered as a contribution that is constant over the area and perpendicular to the paper as shown in figure 4.9. Two divers were present in the study area in wells GW14 and GW16, their recordings along with daily rainfall and the time interval over which equation (13) was solved (dotted line) were combined in figures 4.10 and 4.11.

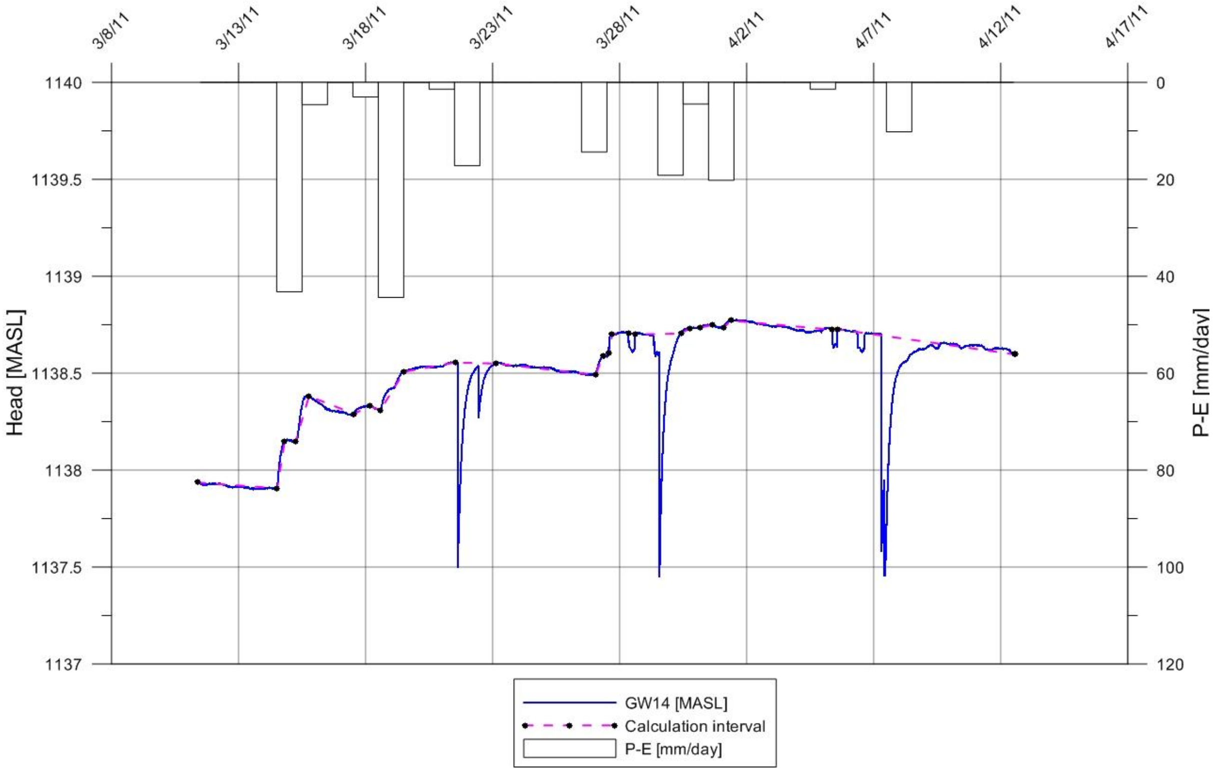

Figure 4.10: Groundwater level response to rainfall as seen in well GW14

The sudden downward spikes observed in the graphs were, like in the transect water level plots, instances where the measurement of groundwater level coincided with the abstraction of a water sample from the well. The response of the water level in the two wells with rainfall was found significant when plotted against the rainfall data obtained from Makarere weather station. Even though both wells displayed an increase in groundwater level at the same times, there were some differences between the two locations. The increases and decreases in GW16 were a lot more sudden creating a graph with an almost 'sawtooth-like' shape whereas plotting GW14 showed a response of similar magnitude, but with more dampening in the increases and decreases. This effect could even be seen in the groundwater sampling instances where GW16 seemed to recover instantly on this timescale and GW14 took a good day or two to recover its water level from sampling. The amount of recharge Qprec. resulting from a rainfall event was plotted in figures 4.12 and 4.13 for GW14 and GW16 respectively. The different behavior noted in the rainfall-response graphs 4.10 and 4.11 was also observed in the results from the calculations (eq. 13) where figure 4.12 shows a more detailed recharge pattern when compared to the more dampened response in figure 4.13.

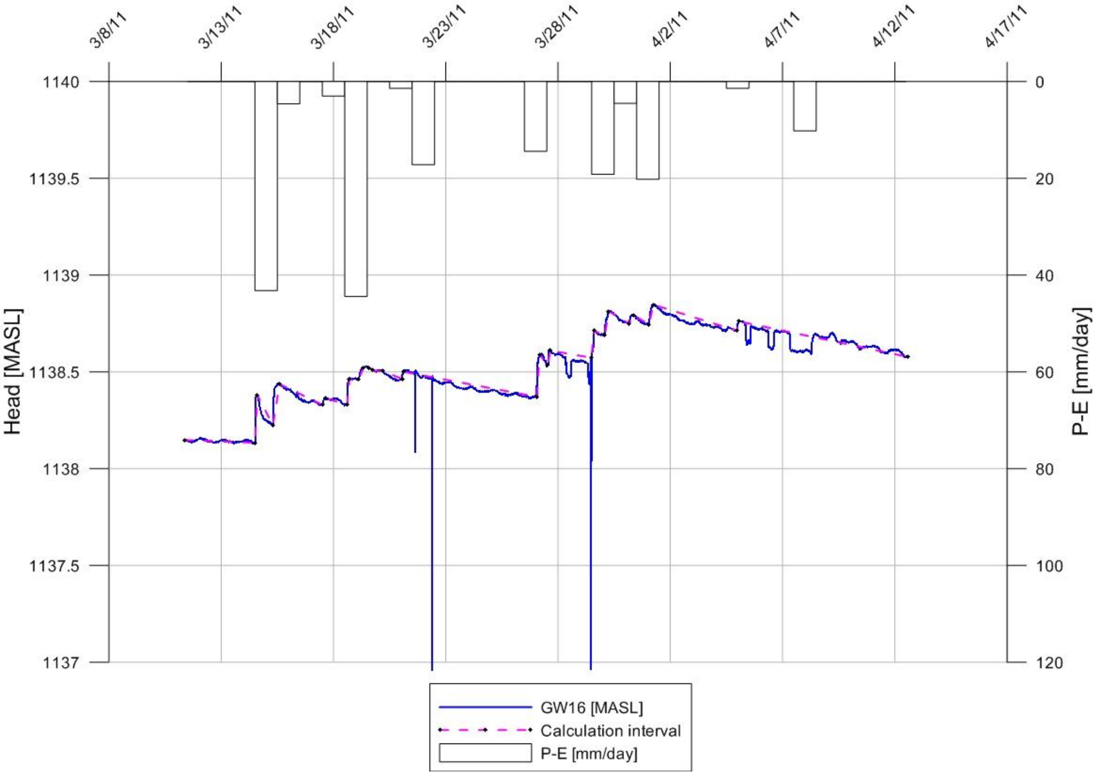

Figure 4.11: Groundwater level response to rainfall as seen in well GW14

The actual maximum amount of recharge in response to high magnitude rain events was also observed to be lower in GW14 (0.7 mm/day) compared to GW16 (1.8 mm/day). The resulting values for the recharge obtained from the recharge calculation were summed for the respective time period and were added to summary table 4.5.

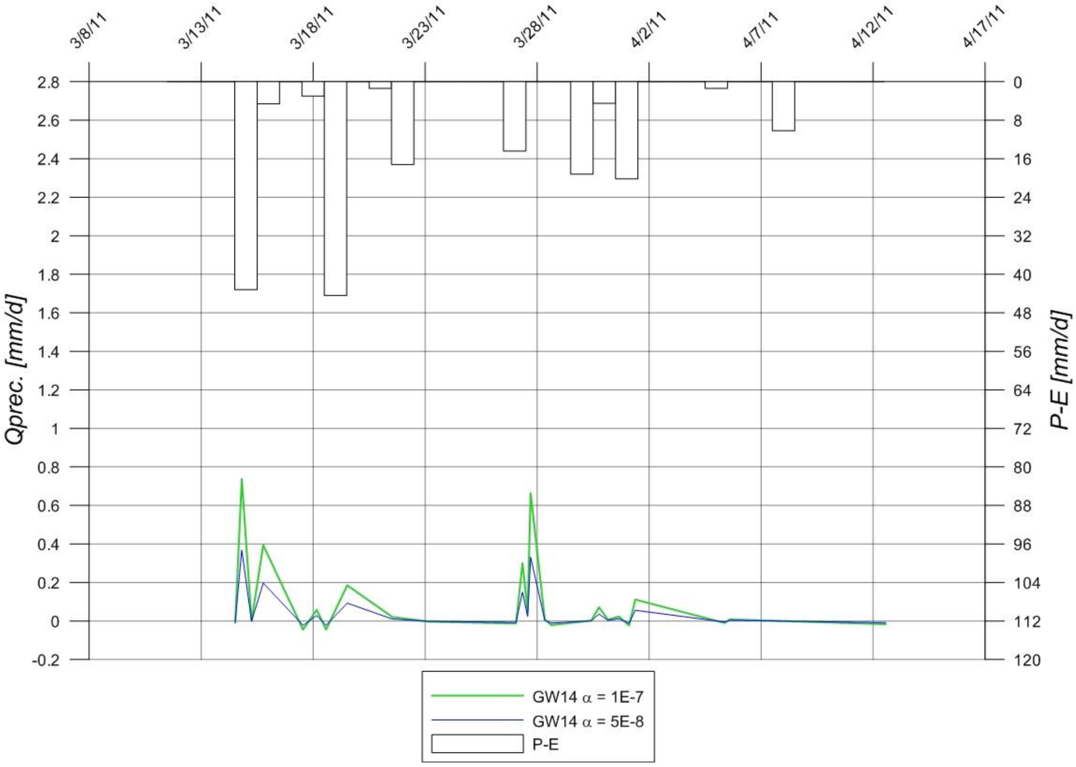

Figure 4.12: Amount of recharge entering the aquifer at well GW14

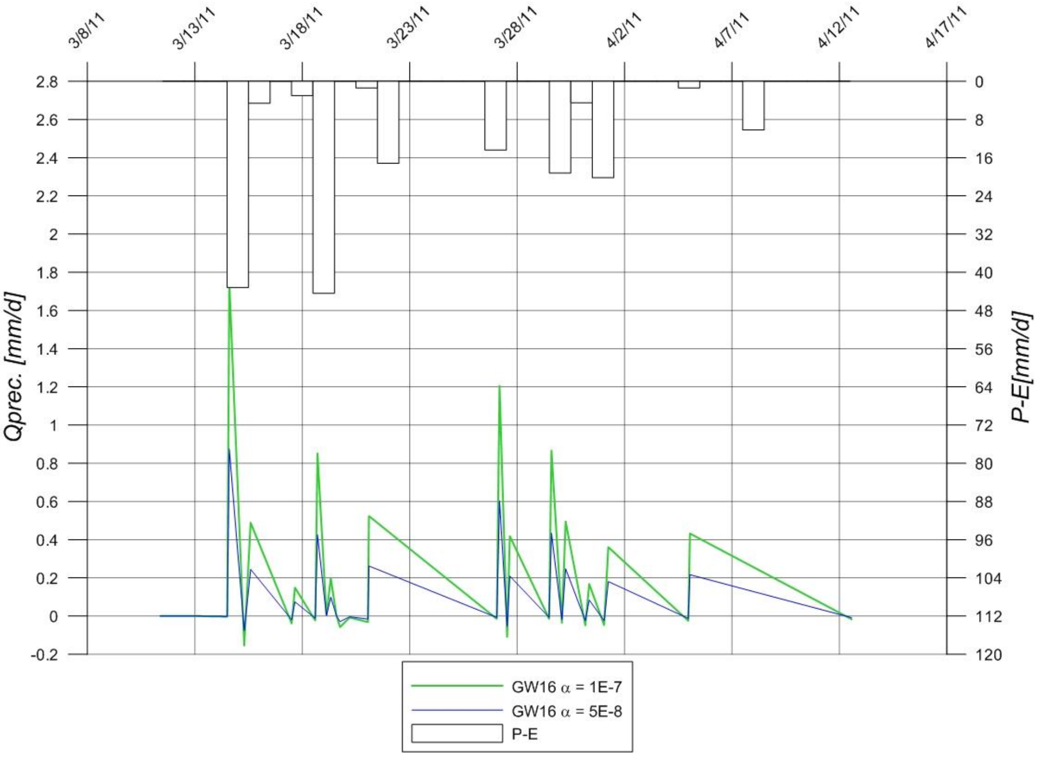

Figure 4.13: Amount of recharge entering the aquifer at well GW16

The change in storage was determined using the change in hydraulic head with time in selected wells that were deemed representative for the water balance area and were approximately evenly spaced. A weighted average for the change in storage dS was calculated using the change in hydraulic head $d\emptyset$ at a specific time dt for the wells in table 4.4. Additionally, the two end member values for α from Freeze and Cherry (1959) yielded different values for dS (table 4.4). The dS values for the appropriate time intervals were also added to the summary table 4.5.

Table 4.4: Calculated dS values as weighted averages based on the change in water level with time in the individual wells.

date	**11/02/2011**	**16/02/2011**	**25/02/2011**	**07/03/2011**	**16/03/2011**	**24/03/2011**	**02/04/2011**
dt[days]	8	5	9	10	9	8	9
dϕ[mm]							
GW7	-110	-60	-100	-80	660	-120	170
GW8	-90	-30	-50	-80	540	-80	220
GW10			-40	-40	20	110	150
GW11	-100	0	-70	-60	810	-300	320
GW12	-120	0	-60	20	590	-280	340
GW13	-110	-80	-120	-90	500	20	-240
GW15	-190	-90	-100	-170	660	0	40
GW16	-80	-10	-60	-50	200	60	130
GW20	-120	-30	-70	-60	570	-150	340
α=1E-7 dS[mm/day]	-0.0104	-0.0058	-0.0058	-0.0051	0.0412	-0.0074	0.0138
α=5E-8 dS[mm/day]	-0.0052	-0.0029	-0.0029	-0.0026	0.0206	-0.0037	0.0070

The lateral subsurface outflow was calculated using the water level recordings from the divers installed at the two transects for the selected periods of time in table 4.5. A resistance was applied in the calculation of Q_{lso} to account for the more resistant riverine deposits. The K value used here is 0.8 m/day. The outflow area was determined to be 423.4 m^2.

Table 4.5: Summary of contributions to the groundwater balance of the aquifer in mm/day

	Date	Qprec.	Qlso	Qlsi	dS	Err
α=1E-7	24-3-2011	0.0141	0.0829	0.0655	-0.0074	0.0041
	2-4-2011	0.0213	0.0677	0.0605	0.0139	0.0002
α=5E-8	24-3-2011	0.0070	0.0829	0.0655	-0.0037	-0.0067
	2-4-2011	0.0107	0.0677	0.0605	0.0070	-0.0035

From the summary table we concluded that the lateral subsurface in and outflow constituted a much more significant component than any contribution due to rainfall or change in storage during the times of measurement.

Ideally, the closing error on the water balance should be the 0 displayed in equation (11). From table 4.5 we concluded that Err < 10% of the input fluxes which we found an acceptable error on the aquifer water balance. Only two periods were displayed in the summary table, because the times at which the divers were recording only partially overlapped with the manual recordings. Variation of the compressibility of the solid matrix yielded an increase or decrease in the recharge into the aquifer. Even though the effect of varying the matrix compressibility displayed a significant increase for short but heavy downpours (figure 4.12, 4.13), the actual effect on the overall water balance was not large enough to affect the dominance of lateral subsurface flow as the major contributor.

4.4 Hydrochemistry

4.4.1. Water type zonation

Typically, EC has been an indicator for the total amount of ions in suspension and chloride was used as a conservative tracer that is indicative of human induced pollution in many researches (figure 4.14, 4.15). An overview of the water types present in different wells in Bwaise was calculated using phreeqc (figure 4.17). Also, the redox state discussed in section 2.4.2 possibly afected many processes in contaminant spread (figure 4.18). Plotting these parameters provided us with an initial overview of the hydrochemical water quality in Bwaise. Additionally, all water samples for which the ion balance was within the 20% limit were summarized in table 4.6 along with their determined field parameters and cation and anion content (phreeqc output for the percentage error calculation was listed in table 4.8). The samples in the table were ordered first on well number and secondly, within samples of a single well, on the date the samples were taken. Since more than one sample was taken per well and it was opted not to average any hydrochemical data, not all samples from table 4.6 could be presented on a map. A mid-of-the-range EC sample was therefore selected amongst the samples for each well for display on a map.

A wide variety of EC values were measured (figure 4.14). Within Bwaise, there were a number of wells with high EC values approaching 2000 µS/cm and even some going up to 3000 µS/cm. Interestingly enough, the ranges measured for EC from different wells could also show a large variation where wells like GW6, GW12, GW19 or GW26 showed a variation of 50 µS/cm or less whereas wells like GW5, GW10, GW18 or GW20 displayed a variation more than 500 µS/cm between samples. The location of wells with higher EC value was seemingly random since locations GW5, GW7, GW15 and GW17 were well spread across the study domain, but they all contained EC values higher than 2000 µS/cm. The EC values in the Wakiso area of this research tended to be lower than in the rest of the area (1500 µS/cm or lower).

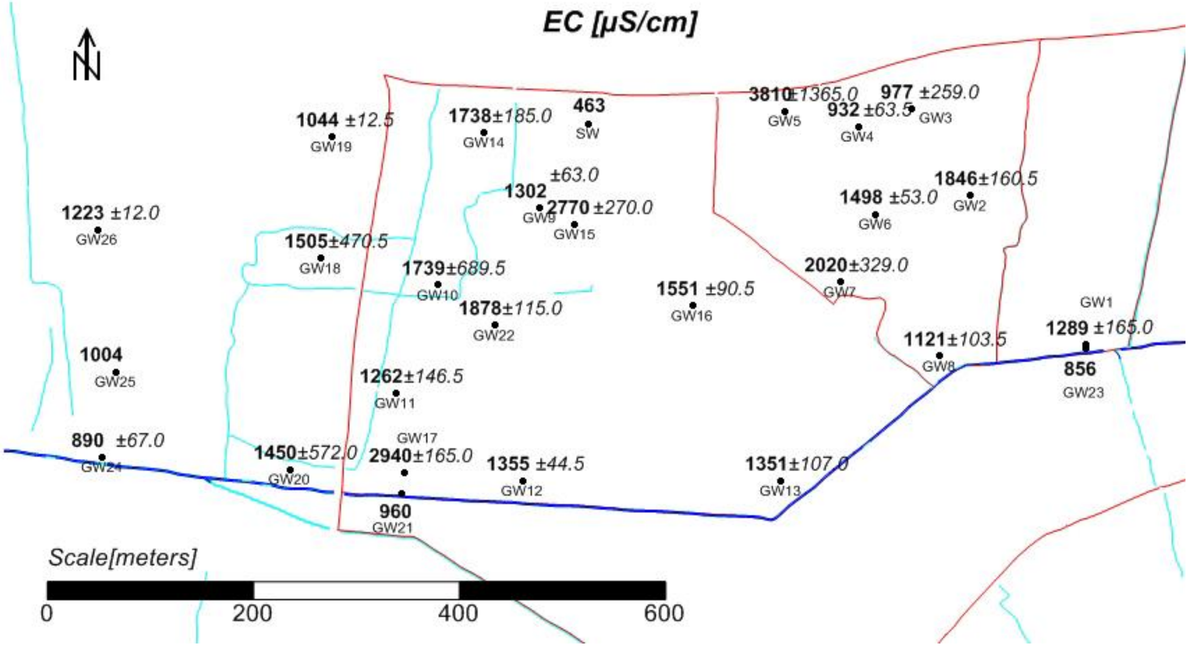

Figure 4.14: EC, EC range and well number. Wells that do not show a value for range have one sample represented in the dataset.

When comparing EC values with chloride values in Bwaise, the observation of a lower pollution input in Wakiso district based on EC was partly supported by chloride in the area (figure 4.15). Chloride in wells GW24, GW25 and GW26 showed values up to 1.4 mmol/l with low ranges. Chloride for wells

GW18, GW19 and GW20 was higher though. The values in the Katoogo part of Bwaise showed a large variation in results ranging from 1.5 (GW11) up to 9 mmol/l (GW15). St. Francis also showed a remarkable variation in chloride values of 1.2 (GW4) up to 8.4 mmol/l (GW5). In terms of variation of chloride samples within a single well, we observed that the higher the chloride content, the higher also its range would be. The wells along the Nsooba channel were an exception to this however as their values were approximately 2-2.8 mmol/l, but the range was relatively high showing a larger variation in obtained values here.

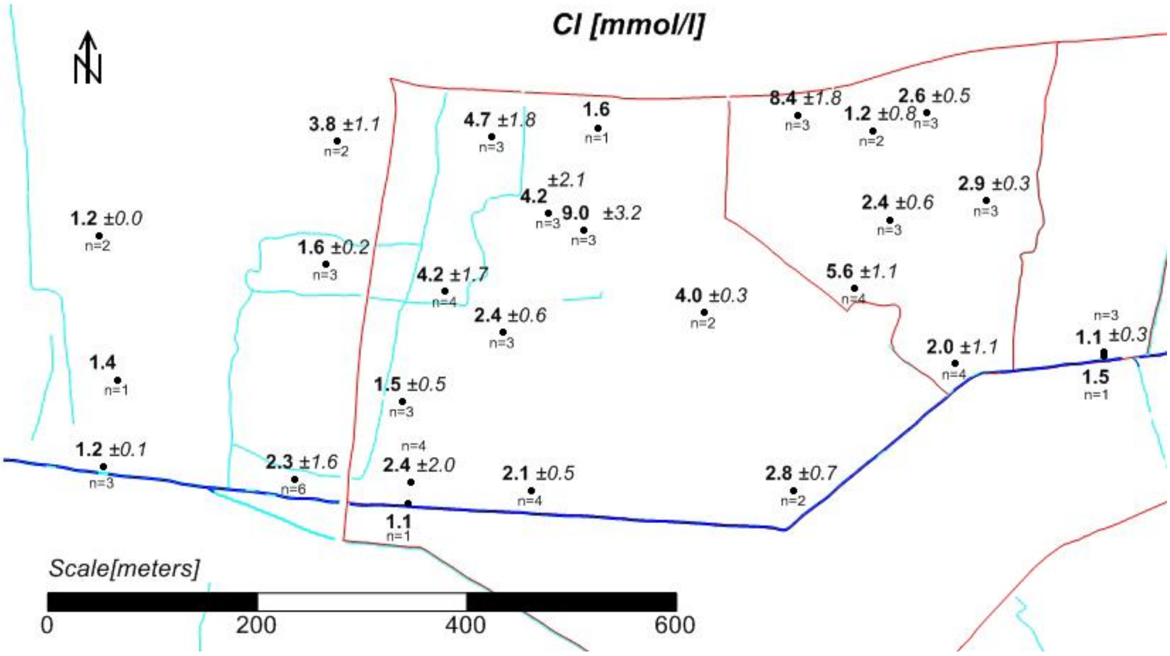

Figure 4.15: Chloride values in Bwaise slum including range and the number of samples. Wells that do dot display a range have one sample represented in the dataset.

One of the first things that stood out from the results of the Stuyfzand parameters was the constant 'high'classification according to table 3.2 for alkalinity (figure 4.17). There were two instances in GW17 and GW5 where the water could be classified as very high and a few where a moderate to moderately high class applied. The moderate values for alkalinity were usually found in the Northern most part of the area, however well GW8 was an exception to this observation. Subtype classification based on prominent cation and anion types was also interesting as we saw that the high alkalinity type values returned in the subtype classification as bicarbonate was the most prominent anion in every well. GW15 was the only exception to this as no anion exceeded the criterion for dominance and thus MIX was displayed. The most prominent cation in the Stuyfzand classification was less constant than the most prominent anion. Wells in Wakiso district constantly contained Ca^{2+} as their most dominant cation, moving to the East however in Katoogo Na^{+} classified samples started to appear. Moving into the St. Francis zone, two wells yielded samples with K^{+} as the dominant cation. Along Nsooba channel there were two wells which had NH_4^+ as their most prominent cation presense in some samples. For the main type, we saw that the chloride values fall into the F or f types, so water samples were classified as fresh, but they were in the upper part of the fresh class and especially the wells that produce samples with f main types started to become brackish. Well GW15 could even be counted into the brackish main type B according to table 3.1.

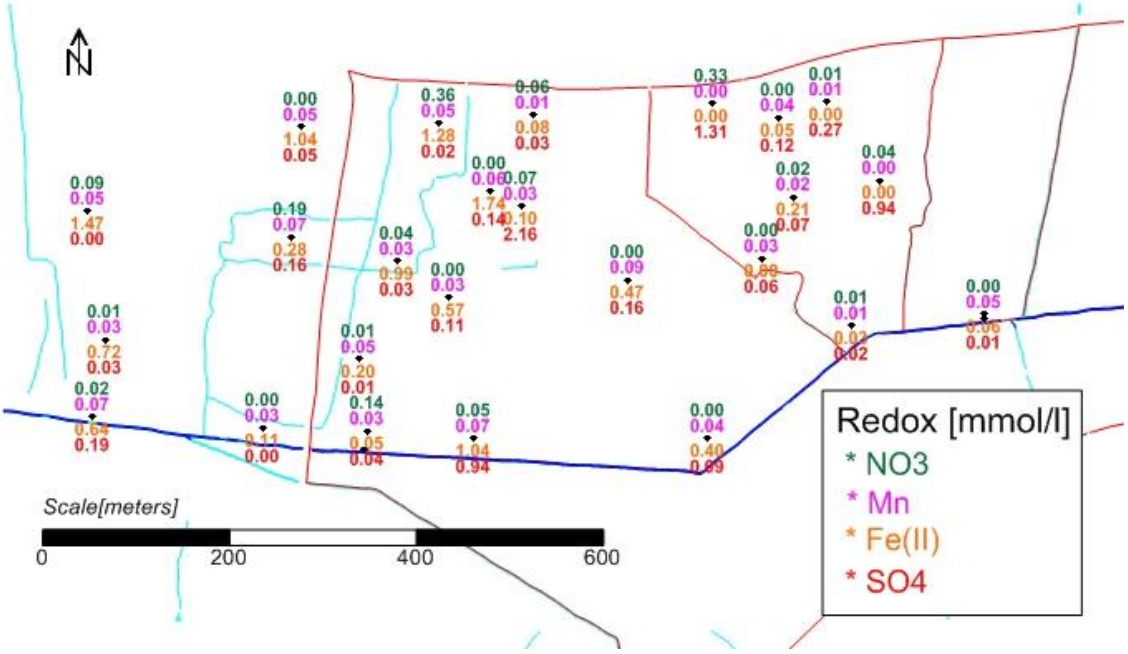

Figure 4.16: Distribution of redox species in Bwaise III

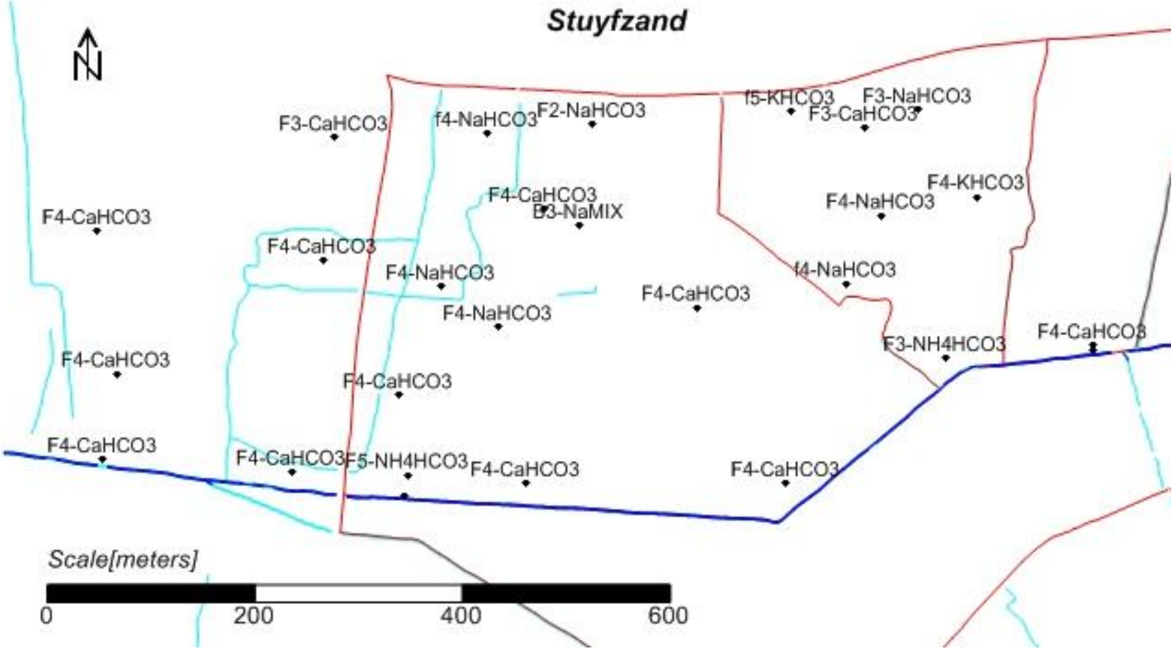

Figure 4.17: Stuyfzand classification

An overview of the redox species was made (figure 4.16). Nitrate values ranged from about 0 to 0.36 mmol/l, but in general, they were observed to be very low. There were two significant values in wells GW14 and GW5 in the Northern most parts of the study area. Additionally, GW18 and GW17 showed elevated levels of nitrate as well. Manganese ions fell in a range of 0 – 0.09 mmol/l where the wells installed in St. Francis mostly showed values below 0.05 mmol/l and the wells of Katoogo displayed values mostly above 0.05 mmol/l. Iron values yielded the most remarkable results as they showed a strong contrast between St. Francis and Katoogo zones. In St. Francis, only one value for iron above 0.05 mmol/l could be found whereas in Katoogo most values were higher than 0.2 mmol/l with values going as high as 1.74 mmol/l. Sulfate showed a variable pattern of concentrations that was relatively independent of location in the study area. The range of sulfate values found in Bwaise was 0-2 mmol/l. The highest values for sulfate were found in wells GW 2, 5, 12, 13 and 16 in the St. Francis and Katoogo zones. In Wakiso district the highest sulfate values were 0.19 and 0.16 mmol/l which is less, but still significantly above 0. From the plot of the redox species we derived that nitrate was only present in a limited amount of wells in the Northern most part of Bwaise and iron was present in the Katoogo zone whereas it was almost completely absent in the St. Francis zone. This indicated that Bwaise, at the time of sampling, was located on a boundary of nitrate reducing environmental conditions in the North to Northeast and iron reducing environmental conditions in the South to Southwest. Well GW14 was situated on the boundary of these two types of conditions and showed both high iron and nitrate values which shouldn't be possible. Possibly, the wells penetrated the full length of the aquifer and therefore no differentiation in depth specific groundwater was made when sampling which could lead to a mix of nitrate and iron rich water within the samples of a well. We also determined sulfate reduction not to take place, because of the sporadic occurrence of significantly high values in absence of the H_2S smell that occurs in sulfate reducing environments.

When looking carefully at water quality in the study area, we concluded that Bwaise was split into four zones as shown in figure 4.18 each with its specific class of groundwater:

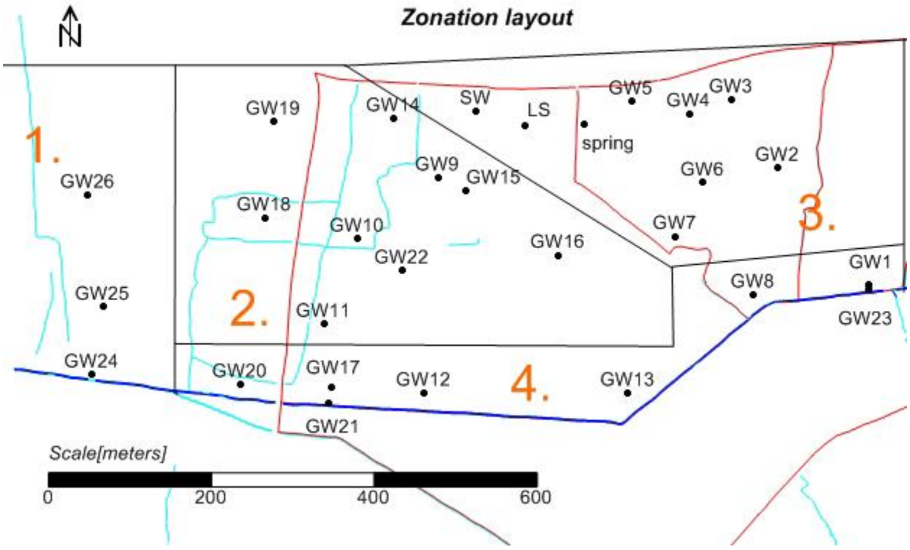

Figure 4.18: Subdivision of Bwaise into four segments based on water quality.

1. We called this segment the unpolluted zone mainly because of the lower chloride and EC values that were obtained from the water sampling.
2. This zone was heavily polluted with widely varying EC and Cl^- values. High iron values were found in this region as well for the redox analysis leading to the conclusion that this part of Bwaise contained polluted iron reducing groundwater.
3. This part was characterized by the sporadic presence of nitrate, but mainly by the absence of iron(II) in the groundwater. Additionally, both Cl^- and EC values were high and therefore we determined the water in this zone to be polluted nitrate reducing water.
4. The area near Nsooba channel showed chloride values consistently in a range of 2-2.8 mmol/l, but with relatively large variations within single wells, varying EC values and a sporadic presence of ammonium as the dominating cation. We therefore determined this to be an area of variable pollution circumstances.

Table 4.6: The complete set of hydrochemical parameters measured in the field and in the laboratory. The table is divided into a field parameter section and 3 ions sections. The major ions are generally most significant in their influence on the ion balance. Ions are shown in mmol/l except for phosphate which is in µmol/l.

sample no.	well no.	XCOORD	YCOORD	date	EC	pH	Temp.	Na	K	Mg	Ca	NH4	Cl	HCO3	SO4	NO3	Fe	Mn	o.PO4	F
Field parameters								Major cations					Major anions				Other ions			
23	GW1	451058	38664	15-02-11	1315	7.00	25.7	2.72	1.23	0.81	2.61	1.07	1.59	12.84	0.03	0.03	0.14	0.04	2.9	0.01
29	GW1	451058	38664	02-03-11	1289	6.41	25.8	2.95	1.72	1.10	3.81	1.36	1.06	10.86	0.01	0.00	0.06	0.05	1.9	0.01
79	GW1	451058	38664	28-03-11	985	6.91	25.3	1.10	0.78	0.42	2.00	0.00	1.40	7.44	0.28	0.02	0.14	0.03	14.2	0.01
19	**GW2**	450946	38808	10-02-11	1920	7.23	30.1	2.51	3.90	1.67	1.46	1.64	2.25	16.18	0.39	0.00	0.00	0.01	0.0	0.01
33	**GW2**	450946	38808	02-03-11	1599	8.94	30.4	3.20	4.97	1.87	1.58	1.00	2.58	11.88	0.09	0.02	0.00	0.01	306.5	0.03
54	**GW2**	450946	38808	21-03-11	1846	7.09	26	3.83	6.76	2.41	1.68	0.57	2.86	12.82	0.94	0.04	0.00	0.00	96.8	0.02
34	GW3	450889	38892	02-03-11	702	**	28.2	2.04	0.89	0.07	1.06	0.36	2.66	2.30	0.69	0.00	0.00	0.00	16.1	0.09
55	GW3	450889	38892	21-03-11	977	7.73	26	2.39	1.06	0.33	1.03	0.57	2.61	6.26	0.27	0.01	0.00	0.01	4.5	0.06
97	GW3	450889	38892	07-04-11	1220	7.98	27.8	5.03	2.68	0.76	2.28	0.57	3.71	8.58	0.25	0.04	0.00	0.02	1.0	0.04
35	**GW4**	450837	38875	02-03-11	805	**	30.3	2.64	0.86	0.05	1.67	0.29	2.85	1.82	0.47	0.02	0.00	0.00	0.0	0.02
56	**GW4**	450837	38875	21-03-11	932	7.11	26	3.13	1.01	0.49	1.92	0.00	1.23	5.06	0.12	0.00	0.05	0.04	3.5	0.00
16	GW5	450766	38890	10-02-11	3810	7.36	24.9	10.35	11.34	2.13	2.51	0.00	8.39	16.04	1.31	0.33	0.00	0.00	8.1	0.04
36	GW5	450766	38890	02-03-11	4970	7.91	28.4	11.24	14.88	1.22	1.22	18.56	7.29	32.47	0.87	0.91	0.00	0.00	7.1	0.10
57	GW5	450766	38890	21-03-11	2240	7.05	27	3.58	3.74	0.68	1.62	2.57	4.85	7.18	1.05	2.44	0.00	0.01	16.5	0.03
20	**GW6**	450854	38790	10-02-11	1461	7.04	25.1	3.37	1.63	0.56	2.10	0.57	3.36	10.22	0.04	0.20	0.14	0.02	3.2	0.07
53	**GW6**	450854	38790	21-03-11	1567	6.86	24.2	5.71	2.80	1.03	2.43	1.00	2.24	11.06	0.05	0.00	0.41	0.03	1.0	0.04
103	**GW6**	450854	38790	17-05-11	1498	7.13	23.9	12.49	1.50	0.48	1.16	0.64	2.39	10.38	0.07	0.02	0.21	0.02	7.1	0.00
21	GW7	450820	38724	10-02-11	2060	7.11	26	8.99	1.87	1.29	1.54	2.14	5.53	15.12	0.00	0.16	0.17	0.02	6.1	0.02
31	GW7	450820	38724	02-03-11	2020	8.63	27.4	6.30	3.39	0.97	3.02	2.28	5.62	12.70	0.06	0.00	0.00	0.03	2.9	0.00
52	GW7	450820	38724	21-03-11	1402	7.03	24.7	5.03	2.45	0.64	2.66	0.64	4.76	6.38	0.66	0.07	0.00	0.01	8.4	0.01
102	GW7	450820	38724	17-05-11	1697	7.17	25	3.25	2.65	0.47	2.32	0.79	3.45	12.60	0.23	0.02	0.06	0.03	3.2	0.00
24	**GW8**	450916	38652	15-02-11	1108	6.98	28	2.99	1.28	0.35	0.97	2.50	2.16	8.90	0.01	0.07	0.06	0.02	15.8	0.06
30	**GW8**	450916	38652	02-03-11	1121	7.57	27.5	1.76	0.56	0.29	1.03	2.86	1.96	7.92	0.02	0.01	0.03	0.01	6.5	0.03
80	**GW8**	450916	38652	28-03-11	1166	6.93	24.6	1.89	0.99	0.44	1.81	1.71	2.70	8.38	0.35	0.04	0.20	0.03	9.7	0.04
101	**GW8**	450916	38652	16-05-11	959	7.10	24.8	6.58	0.48	0.28	0.99	1.00	0.57	8.20	0.02	0.00	0.12	0.02	11.9	0.00
5	GW9	450528	38796	08-02-11	1404	6.74	25.1	2.94	0.65	1.16	3.29	0.57	2.33	12.84	0.01	0.51	1.38	0.07	0.0	0.04
71	GW9	450528	38796	23-03-11	1278	6.69	27.1	2.82	0.57	1.07	2.87	0.64	0.01	11.92	0.00	0.00	1.75	0.06	9.0	0.00
95	GW9	450528	38796	07-04-11	1302	6.70	27.4	3.77	0.89	1.26	2.87	0.71	4.19	10.46	0.14	0.00	1.74	0.06	1.9	0.08
26	**GW10**	450429	38721	16-02-11	1739	6.66	23.8	5.62	2.57	0.91	2.15	4.28	4.16	14.26	0.03	0.04	0.99	0.03	4.8	0.02
62	**GW10**	450429	38721	22-03-11	1791	6.64	25.3	3.32	1.86	0.55	1.31	3.64	2.57	13.80	0.00	0.00	0.54	0.02	5.8	0.04
93	**GW10**	450429	38721	07-04-11	2520	7.09	25.2	4.98	2.74	0.78	1.62	3.86	3.99	12.52	0.01	0.00	0.33	0.03	4.2	0.03
112	**GW10**	450429	38721	18-05-11	1141	6.98	27.2	2.57	1.35	0.37	0.93	1.71	0.81	7.78	0.01	0.16	0.04	0.01	2.6	0.00
8	GW11	450388	38616	08-02-11	1262	6.79	26.3	2.67	1.93	0.85	2.47	1.14	1.50	10.52	0.01	0.01	0.20	0.05	6.1	0.01

Table 4.6: (continued)

sample no.	well no.	XCOORD	YCOORD	date	EC	pH	Temp.	Na	K	Mg	Ca	NH4	Cl	HCO3	SO4	NO3	Fe	Mn	o.PO4	F
Field Parameters								Major cations					Major anions				Other ions			
67	GW11	450388	38616	23-03-11	1372	6.76	26.8	1.41	1.08	0.50	2.11	1.29	1.06	9.46	0.30	0.00	0.26	0.02	9.4	0.02
92	GW11	450388	38616	07-04-11	1079	7.86	24.7	2.92	2.47	1.09	3.48	1.93	2.12	10.62	0.54	0.00	0.00	0.05	0.3	0.02
2	**GW12**	450511	38531	07-02-11	1316	6.53	30.6	2.48	0.66	0.66	2.19	1.50	1.11	13.62	0.00	0.00	0.93	0.07	0.0	0.02
14	**GW12**	450511	38531	09-02-11	1318	6.51	25.9	1.93	0.54	0.50	1.71	1.36	1.42	10.64	0.00	0.66	0.56	0.05	0.0	0.02
63	**GW12**	450511	38531	22-03-11	1405	6.46	27.5	3.01	0.88	0.97	2.68	1.21	1.69	11.82	0.97	0.00	1.03	0.08	8.4	0.02
84	**GW12**	450511	38531	29-03-11	1355	6.67	28.4	3.30	1.10	1.09	2.96	1.50	2.11	12.34	0.94	0.05	1.04	0.07	26.1	0.04
15	GW13	450762	38531	09-02-11	1351	6.82	24	2.40	0.96	0.48	2.66	0.64	2.83	9.78	0.09	0.00	0.40	0.04	0.0	0.02
58	GW13	450762	38531	22-03-11	1137	6.88	22	2.21	0.61	0.30	1.47	0.29	4.25	4.68	0.61	0.16	0.13	0.02	1.0	0.04
4	**GW14**	450474	38869	08-02-11	1795	6.72	25.2	6.09	1.82	0.84	2.21	1.86	5.62	10.56	0.14	0.02	0.96	0.05	2.3	0.05
42	**GW14**	450474	38869	03-03-11	1738	6.75	31.6	5.96	1.65	0.91	2.31	2.21	4.67	8.20	0.02	0.36	1.28	0.05	16.5	0.06
94	**GW14**	450474	38869	07-04-11	1425	6.90	26.1	4.94	2.48	0.65	1.38	1.93	2.04	8.48	0.03	0.01	0.05	0.02	5.2	0.04
60	GW15	450562	38780	22-03-11	2290	6.74	25.3	9.56	2.20	0.87	2.40	0.50	9.02	6.94	2.16	0.07	0.10	0.03	2.3	0.04
87	GW15	450562	38780	29-03-11	2770	6.86	26.2	13.52	3.04	1.33	3.08	0.50	13.54	10.44	1.96	0.08	0.34	0.05	18.1	0.02
110	GW15	450562	38780	18-05-11	2830	6.93	26.1	10.98	2.28	1.10	2.65	0.71	7.05	11.92	0.73	0.76	0.28	0.04	6.5	0.00
12	**GW16**	450676	38701	09-02-11	1551	6.58	26.1	5.92	1.69	1.43	3.55	0.21	3.98	10.04	0.16	0.00	0.47	0.09	0.6	0.06
39	**GW16**	450676	38701	03-03-11	1370	7.10	27.1	4.31	1.58	1.06	2.65	0.43	4.56	8.74	0.14	0.01	0.26	0.07	1.9	0.02
25	GW17	450397	38539	15-02-11	2920	7.10	25.9	6.37	4.66	0.95	2.83	9.28	0.94	23.33	0.00	0.00	0.40	0.05	27.4	0.00
37	GW17	450397	38539	03-03-11	2980	7.20	25.9	5.13	4.21	0.81	2.77	12.14	4.99	21.01	0.00	0.25	0.50	0.04	0.0	0.01
66	GW17	450397	38539	23-03-11	2650	7.08	27	4.84	3.92	0.69	2.35	7.50	4.44	17.78	0.33	0.00	0.21	0.04	2.3	0.02
113	GW17	450397	38539	18-05-11	2940	7.46	26.2	5.64	4.38	0.75	2.06	10.35	2.45	23.09	0.04	0.14	0.05	0.03	2.9	0.00
3	**GW18**	450315	38747	07-02-11	1505	6.85	28.4	2.54	3.48	1.19	3.13	1.21	1.62	12.62	0.16	0.19	0.28	0.07	4.2	0.01
47	**GW18**	450315	38747	04-03-11	1807	6.81	27.3	2.25	3.41	1.12	2.46	2.93	2.22	17.06	0.01	0.01	0.54	0.04	18.4	0.00
91	**GW18**	450315	38747	04-04-11	866	6.94	23.3	1.78	1.89	0.59	1.70	0.50	1.75	7.62	0.09	0.00	0.07	0.04	4.2	0.02
48	GW19	450326	38865	04-03-11	1019	6.54	27.1	1.51	0.54	0.34	0.93	0.71	1.59	6.70	0.05	0.01	0.31	0.02	2.6	0.03
69	GW19	450326	38865	23-03-11	1044	6.30	26.5	3.33	1.01	0.75	1.55	0.50	3.80	6.92	0.05	0.00	1.04	0.05	2.9	0.04
1	**GW20**	450285	38542	07-02-11	1450	6.70	29.3	2.59	1.49	1.09	2.65	2.57	2.34	12.00	0.00	0.00	0.11	0.03	10.3	0.01
10	**GW20**	450285	38542	08-02-11	1403	6.57	25.4	2.03	0.97	0.70	2.91	1.86	2.13	10.46	0.00	0.14	0.90	0.03	3.9	0.01
43	**GW20**	450285	38542	04-03-11	1126	6.55	25.6	1.69	0.82	0.60	1.84	2.71	1.86	11.16	0.00	0.01	0.80	0.02	7.7	0.03
64	**GW20**	450285	38542	23-03-11	1815	6.55	26.9	3.20	1.31	1.21	3.74	2.28	2.23	10.62	1.93	0.01	1.36	0.04	21.9	0.02
88	**GW20**	450285	38542	04-04-11	2270	6.80	26.7	4.15	1.49	1.89	6.13	2.50	4.41	10.72	4.84	0.06	0.69	0.04	2.6	0.01
114	**GW20**	450285	38542	19-05-11	1657	6.90	25.8	2.29	1.20	1.10	2.69	2.50	1.21	13.12	0.15	0.04	0.71	0.03	3.5	0.00

Table 4.6: (continued)

sample no.	well no.	XCOORD	YCOORD	date	EC	pH	Temp.	Na	K	Mg	Ca	NH4	Cl	HCO3	SO4	NO3	Fe	Mn	o.PO4	0,18
Field Parameters								Major Cations					Major anions				Other ions			
65	GW21	450393	38519	23-03-11	960	6.56	26.2	1.81	1.37	0.57	1.94	1.14	1.13	7.92	0.32	0.00	0.44	0.04	10.3	0.03
13	**GW22**	450484	38682	09-02-11	1878	6.79	24.7	3.69	3.23	1.13	3.18	2.93	2.36	14.66	0.11	0.00	0.57	0.03	13.6	0.03
38	**GW22**	450484	38682	03-03-11	1883	7.16	25.9	3.68	3.50	1.11	2.38	3.21	3.60	15.12	0.01	0.23	0.29	0.02	6.5	0.01
78	**GW22**	450484	38682	26-03-11	1653	6.61	26	3.26	3.09	1.16	2.68	2.28	2.74	9.40	2.72	0.02	0.36	0.03	17.7	0.02
22	GW23	451058	38660	15-02-11	856	6.57	27.3	3.05	0.89	0.73	2.21	0.36	1.54	7.64	0.34	0.02	0.41	0.03	5.2	0.01
46	**GW24**	450103	38554	04-03-11	980	6.50	26.5	1.80	0.82	0.64	2.17	1.57	1.08	9.44	0.02	0.00	0.87	0.08	5.8	0.01
89	**GW24**	450103	38554	04-04-11	890	6.66	24.6	1.35	0.71	0.51	1.73	1.07	1.21	8.14	0.19	0.02	0.64	0.07	5.5	0.01
115	**GW24**	450103	38554	19-05-11	846	6.62	25	1.21	0.57	0.54	1.62	0.86	0.95	7.82	0.10	0.05	0.52	0.09	13.6	0.00
45	GW25	450116	38637	04-03-11	1004	6.66	27	2.76	0.64	0.38	1.41	1.43	1.40	8.38	0.03	0.01	0.72	0.03	1.6	0.02
44	**GW26**	450098	38775	04-03-11	1199	6.45	28.9	2.61	0.46	0.49	1.36	1.00	1.16	11.72	0.00	0.00	1.25	0.04	1.6	0.03
117	**GW26**	450098	38775	19-05-11	1223	6.48	26.1	2.89	0.41	0.50	1.16	0.71	1.18	11.16	0.00	0.09	1.47	0.05	7.1	0.00
11	Spring	450708	38862	09-02-11	519	4.66	25.7	0.51	0.17	0.05	1.23	0.00	1.90	0.00	0.04	1.97	0.01	0.00	1.6	0.00
77	Spring	450708	38862	26-03-11	455	4.64	26.1	1.56	0.30	0.24	0.77	0.43	1.49	0.00	0.02	1.58	0.00	0.02	9.7	0.00
49	**SW**	450575	38878	04-03-11	463	6.59	31.6	2.07	0.48	0.29	0.67	0.21	1.61	2.20	0.03	0.06	0.08	0.01	1.3	0.00

**=error in pH measurement

4.4.2. Phosphate

Phosphate was measured in the field during water sampling using the colorimeter (table 4.6, figure 4.19). GW2 showed remarkably high values for orthophosphate compared to the rest of the data. This well was installed near an organic waste dump subject to incineration, with charcoal encountered in the unfiltered groundwater. Wells GW13 and 16 contained the least amount of orthophosphate with 0 and 0.6 µmol/l respectively and showed a small range as well. When considering the 2.5 mg/l (26,3 µmol/l) orthophosphate input from the pit latrine site in the study of nyenje et. al., (2012), we can conclude that the amount of phosphate in groundwater in Bwaise during the time of measurement was surprisingly low. Upon close inspection of table 4.6, the majority of the samples had orthophosphate values below 10 µmol/l. There were a few exceptions for instance in wells GW12, 17 and 20. The exceptions on the general trend displayed no clear correlation with time or rainfall. Additionally, orthophosphate values were found to be independent of the zonation shown in figure 4.18. The conclusion was therefore drawn that the mechanism that governed the reduction of phosphorus in the aquifer operated in all hydrochemical zones identified in section 4.4.1. If multiple mechanisms were involved in the reduction of phosphate input then the achieved result was similar throughout the entire domain.

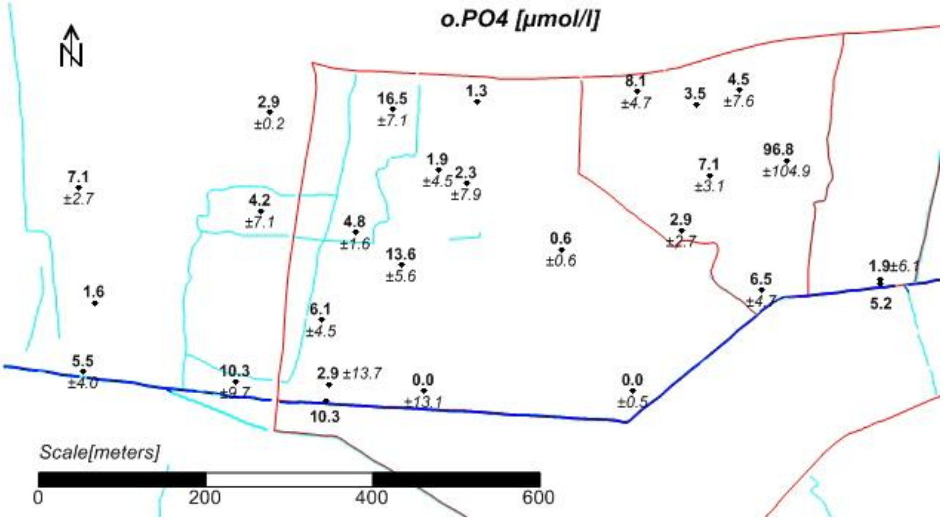

Figure 4.19: Distribution of orthophosphate values and ranges in the study area

4.4.3. Nitrogen

The results yielded low values for nitrate species as described in section 4.4.1.The results for ammonium showed a variable presence in the region (figure 4.20). The Northeast showed values mostly below 1 mmol/l although well GW5 showed a large variation in its ammonium contents. Being the less anaerobic part of the study area, nitrification may have played a role in the lower ammonium values here. In Katoogo zone, wells GW13 and 16 also yielded low values of ammonium and low ranges similar to the results for phosphate indicating that these two wells possibly received less nutrient input. Furthermore, Katoogo wells showed higher values for ammonium ranging from 1-2.8 mmol/l. These values were found to be lower than the input value of 57 mg/l (3.2 mmol/l) obtained by Nyenje et. al., (2012) though, indicating partial removal of ammonium by the Bwaise subsoil system. Anaerobic ammonium oxidation which is part of the nitrogen cycle as described in section 2.4.2 potentially played a part here. Well GW20 showed a very high input of ammonium as an exception on the lower values described above. The Wakiso district showed values above 1 mmol/l for ammonium as well except for wells GW19 and 26 which displayed lower ammonium concentrations.

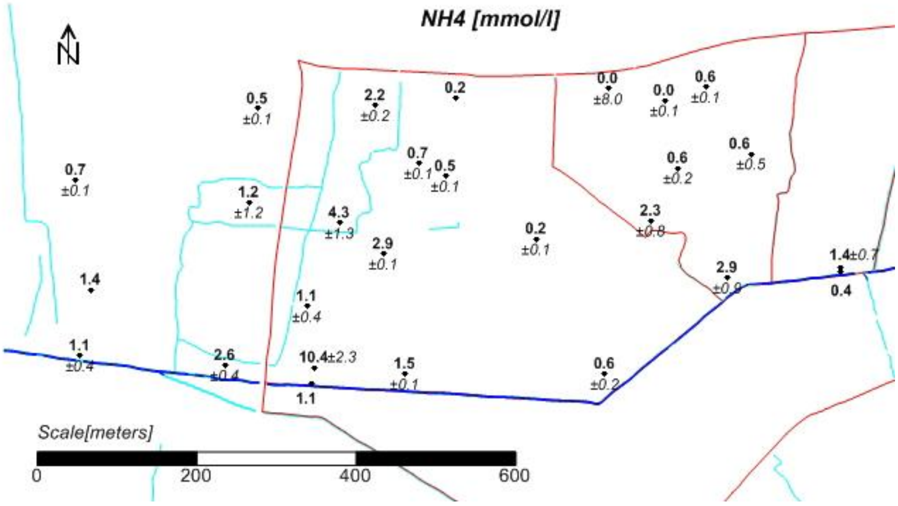

Figure 4.20: Distribution of ammonium values and ranges in the study area

4.4.4. Conservative mixing

We attempted to separate the contribution of conservative mixing from chemical reactions in the hydrochemical dataset obtained using the calculations described in section 3.5.1. Representative endmembers were compiled from the samples from well GW15 for polluted water and GW24, 25 and 26 for unpolluted (table 4.8).

Table 4.7: Endmember samples with components i given in [mmol/l]. PO_4^{3-} is shown in [µmol/l].

i	Na+	K^+	Mg^{2+}	Ca^{2+}	Fe^{2+}	NH_4^+	Mn^{2+}	Cl^-	HCO_3^-	SO_4^{2-}	NO_3^-	PO_4^{3-}
$M_{i,natural}$	2.10	0.6	0.51	1.58	0.91	1.11	0.06	1.16	9.4	0.06	0.03	0.6
$M_{i,pol.}$	11.54	2.62	1.1	2.74	0.21	0.50	0.04	11.28	8.69	2.06	0.07	10

The outcome of the calculations was processed in figure 4.21 for Ca^{2+}, Mg^{2+}, Na^+ and K^+. When interpreting this graph, one must note that the values calculated for $M_{i,react}$ in equation (19) do not differentiate between various chemical reactions such as adsorption or cation exchange. No clear trend towards enrichment or depletion was observed for the components Ca^{2+}, Mg^{2+} and Na^+. The absence of a trend could be due to multiple processes that lead to either enrichment or depletion simultaneously taking place. For K^+, a slight enrichment was observed as most values were above 0 and some values surpassed 2 mmol/l of reactive presence.

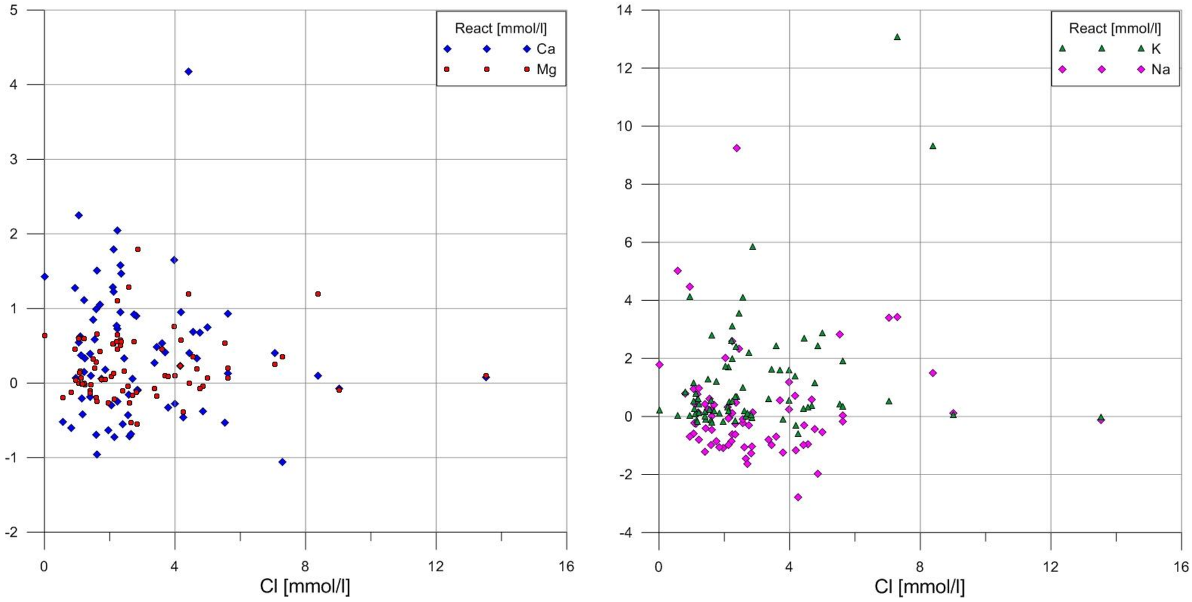

Figure 4.21: Outcome of React calculations according to equation (19) for Na^+, K^+, Ca^{2+} and Mg^{2+} plotted against Cl^-

4.4.5. Mineral solubility

The relevant mineral saturation indices from the phreeqc calculations were documented in table 4.8. One of the things that immediately came into view from table 4.8 is the CO_2 pressure which often ranged between -1 an -0.5. There was, at the time of sampling, thus a very high CO_2 pressure in the subsoil of Bwaise. Not only was Bwaise reclaimed from a wetland with decaying organic matter related to vegetation, but it also received a large input of organic matter through human waste disposal from the pit latrines over time. A high presence and also decay of composite organic matter could therefore explain the observed CO_2 pressures. Samples N34 and N35 (table 4.6) were not included in the analysis for mineral solubility, because their pH measurement was erroneous which affected the calculation for saturation indices too much. The saturation index for calcite strongly related to the CO_2 pressure of the soil and for higher CO_2 pressures, we observed higher saturation indices (table 4.8). Furthermore, calcite showed no clear trend towards either over or undersaturation within the samples. A distinction can be seen for calcite solubility based on water class discussed in section 4.4.1. where class 1 and 2 samples were more likely to be undersaturated than class 3 samples (table 4.8). An oversaturation of the samples with respect to rhodochrosite and $MnHPO_4$ was observed from table 4.8, however there was no clear trend related to area.

Since the groundwater class played an important role in the analysis of the results, the data in figure 4.22 (siderite and vivianite) and 4.23 (hydroxyapatite) were plotted using the four water classes. A strong correlation was found for the saturation index of siderite and vivianite indicating that Fe(II), which is a constituent in both minerals, played a major role in the saturation state of the water with respect to these minerals (figure 4.22). For some samples, Fe(II) content was found to be below the detection limit of the ICP-MS (table 4.6). These samples were therefore also undersaturated with respect to siderite and vivianite and would plot mostly in class 3, but are not shown in figure 4.22.

From figure 4.22, it was observed that samples found in class 3 were undersaturated for vivianite and samples with class 1 and 2 were mostly oversaturated for vivianite. Therefore, vivianite was inclined to precipitate in the Katoogo and Wakiso parts of the study area during the time of sampling. For siderite, some class 3 samples were also oversaturated in addition to the class 1 and 2 samples.

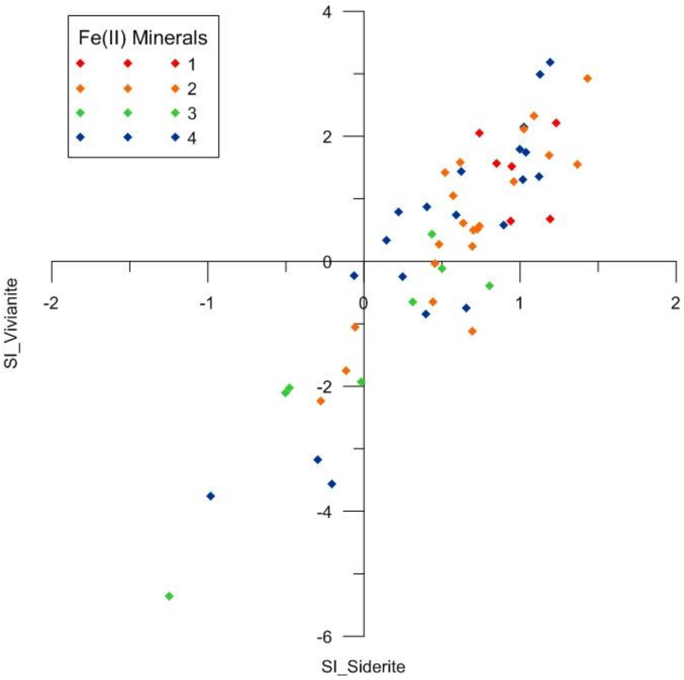

Figure 4.22: Saturation states of the samples w.r.t. siderite and vivianite. Different colors indicate the available water classes from section 4.4.1.

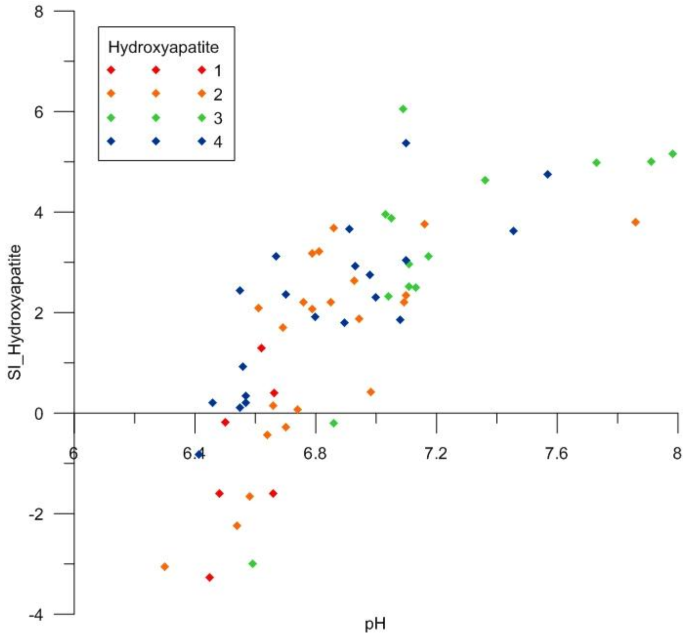

Figure 4.23: Saturation index of hydroxyapatite related to pH. Colors differentiate between the available water classes

The saturation state of the samples for hydroxyapatite showed large variations with samples being undersaturated up to -2.5 or oversaturated up to 5 (figure 4.23). Hydroxyapatite was positively related to pH and also showed a dependence on water class where class 1 tended more towards undersaturation and class 3 displayed the highest saturation index of all the water types for hydroxyapatite. Therefore, according to our data, hydroxyapatite was most likely to precipitate in the St. Francis zone of the study area while, from figure 4.22, it followed that vivianite was most likely to precipitate in the Katoogo zone and Wakiso district. Both are phosphate holding minerals and have the potential to regulate the orthophosphate concentrations in groundwater facilitating the decrease in phosphate concentrations observed in figure 4.19.

Table 4.8: PhreeQC output for all samples.

Sample No.	Well No.	Stuyfzand	pct_err	pCO_2	Calcite	Hydroxyapatite	Vivianite	MnHPO4	Siderite	Rhodochrosite
				Saturation indices						
23	GW1	F4-CaHCO3	-8.72	-1.14	0.34	2.31	-0.84	2.06	0.40	0.53
29	GW1	F4-CaHCO3	15.36	-0.63	-0.16	-0.83	-3.17	1.65	-0.30	-0.01
79	GW1	F3-CaHCO3	-15.00	-1.28	-0.05	3.66	0.79	2.70	0.22	0.17
19	**GW2**	F5-KHCO3	-15.08	-1.24	0.42	*	*	*	-1.26	0.20
33	**GW2**	F4-KHCO3	4.47	-3.21	1.81	14.80	*	3.75	*	1.86
54	**GW2**	F4-KHCO3	4.68	-1.23	0.18	6.05	*	2.57	*	-0.40
55	GW3	F3-NaHCO3	-17.28	-2.16	0.42	4.97	*	2.02	*	0.42
97	GW3	F4-NaHCO3	5.91	-2.30	1.10	5.16	*	1.47	*	1.01
56	**GW4**	F3-CaHCO3	17.32	-1.64	-0.01	2.97	-2.11	2.36	-0.50	0.36
16	GW5	f5-KHCO3	6.30	-1.42	0.65	4.63	-5.36	1.54	-1.25	-0.05
36	GW5	f6-KHCO3	8.04	-1.66	1.12	5.00	*	1.28	*	0.48
57	GW5	f3-KMIX	-6.81	-1.43	-0.07	3.87	*	2.05	*	-0.50
20	**GW6**	F4-CaHCO3	-11.34	-1.28	0.20	2.33	-0.65	1.80	0.31	0.13
53	**GW6**	F4-NaHCO3	13.11	-1.08	0.08	-0.21	-0.40	1.45	0.80	0.29
103	**GW6**	F4-NaHCO3	17.58	-1.37	0.01	2.50	0.44	2.23	0.44	0.26
21	GW7	f4-NaHCO3	-4.45	-1.18	0.25	2.52	-0.11	2.11	0.50	0.39
31	GW7	f4-NaHCO3	4.58	-2.85	1.89	9.09	*	2.03	*	1.95
52	GW7	f3-NaHCO3	8.42	-1.48	0.07	3.95	*	2.00	*	-0.30
102	GW7	F4-NaHCO3	-14.63	-1.32	0.44	3.11	-1.93	2.11	-0.02	0.61
24	**GW8**	F4-NaHCO3	-7.97	-1.25	-0.19	2.75	-0.24	2.60	-0.07	0.09
30	**GW8**	F3-NH4HCO3	-11.58	-1.90	0.38	4.76	-3.76	2.22	-0.98	0.43
80	**GW8**	F4-CaHCO3	-11.13	-1.25	-0.05	2.92	0.88	2.56	0.41	0.25
101	**GW8**	g4-NaHCO3	10.45	-1.42	-0.13	3.03	0.34	2.67	0.14	0.32
5	GW9	F4-CaHCO3	0.53	-0.89	0.14	*	*	*	1.35	0.50
71	GW9	G4-CaHCO3	14.31	-0.86	0.04	1.70	2.93	2.42	1.43	0.40
95	GW9	F4-CaHCO3	7.21	-0.93	-0.01	-0.28	1.56	1.74	1.37	0.34
26	**GW10**	F4-NaHCO3	5.67	-0.77	-0.10	0.14	1.69	1.87	1.19	0.09
62	**GW10**	F4-NaHCO3	-9.45	-0.74	-0.30	-0.43	1.27	1.84	0.96	-0.10
93	**GW10**	F4-NaHCO3	1.49	-1.25	0.20	2.20	0.51	2.12	0.72	0.47
112	**GW10**	g3-NaHCO3	-2.62	-1.31	-0.25	0.42	-2.24	1.74	-0.27	-0.04
8	GW11	F4-CaHCO3	3.35	-1.01	0.04	2.07	0.27	2.49	0.48	0.45
67	GW11	F4-CaHCO3	-7.94	-1.02	-0.08	2.21	1.04	2.34	0.57	0.05
92	GW11	F4-CaHCO3	9.67	-2.11	1.19	3.80	*	1.39	*	1.43
2	**GW12**	F4-CaHCO3	-9.47	-0.61	-0.13	*	*	*	1.18	0.41
14	**GW12**	F4-CaHCO3	-15.50	-0.72	-0.38	*	*	*	0.82	0.11
63	**GW12**	F4-CaHCO3	-3.14	-0.63	-0.24	0.20	1.75	2.43	1.04	0.28
84	**GW12**	F4-CaHCO3	-0.76	-0.82	0.03	3.12	3.18	3.03	1.19	0.48
15	GW13	F4-CaHCO3	-7.12	-1.08	0.05	*	*	*	0.75	0.33

** = Constituent species was below detection limit on ICP or IC.*

Table 4.8: (continued)

Sample No.	Well No.	Stuyfzand	pct_err	pCO_2	Calcite	Hydroxyapatite	Vivianite	MnHPO4	Siderite	Rhodochrosite
				Saturation indices						
4	**GW14**	f4-NaHCO3	4.00	-0.95	-0.12	-0.30	1.15	1.81	1.11	0.26
42	**GW14**	f4-NaHCO3	17.91	-1.06	-0.10	2.66	3.15	2.74	1.18	0.27
94	**GW14**	F4-NaHCO3	12.30	-1.21	-0.18	1.43	-1.53	2.14	-0.20	0.08
60	GW15	B3-NaMIX	-3.45	-1.15	-0.29	0.07	-1.76	1.71	-0.11	-0.12
87	GW15	B4-NaMIX	-2.67	-1.10	0.08	3.68	1.58	2.79	0.61	0.35
110	GW15	f4-NaHCO3	2.20	-1.11	0.18	2.64	0.61	2.38	0.64	0.46
12	**GW16**	F4-CaHCO3	14.00	-0.83	-0.08	-1.65	-1.12	1.47	0.70	0.36
39	**GW16**	f4-CaHCO3	2.84	-1.40	0.30	2.33	-0.65	2.20	0.44	0.75
25	GW17	F5-NaHCO3	8.63	-0.99	0.63	5.36	2.14	3.08	1.02	0.92
37	GW17	f5-NH4HCO3	6.22	-1.14	0.68	*	*	*	1.02	0.90
66	GW17	f5-NaHCO3	-0.12	-1.08	0.45	1.86	-0.75	1.92	0.66	0.68
113	GW17	F5-NH4HCO3	0.67	-1.35	0.85	3.61	-3.56	2.05	-0.21	1.07
3	**GW18**	F4-CaHCO3	5.96	-0.99	0.27	2.21	0.23	2.41	0.69	0.67
47	**GW18**	F5-KHCO3	-6.95	-0.82	0.22	3.22	2.33	2.74	1.09	0.49
91	**GW18**	F3-CaHCO3	-3.34	-1.31	-0.10	1.88	-1.06	2.29	-0.06	0.31
48	GW19	F3-CaHCO3	-16.97	-0.94	-0.74	-2.24	-0.04	1.68	0.46	-0.28
69	GW19	F3-CaHCO3	3.70	-0.70	-0.81	-3.06	0.56	1.74	0.74	-0.21
1	**GW20**	F4-CaHCO3	0.12	-0.85	0.05	2.36	-0.24	2.37	0.25	0.12
10	**GW20**	F4-CaHCO3	4.60	-0.80	-0.13	0.20	1.31	1.76	1.02	-0.08
43	**GW20**	F4-CaHCO3	-5.51	-0.75	-0.31	0.11	1.79	1.97	1.00	-0.17
64	**GW20**	F4-CaHCO3	8.38	-0.78	-0.10	2.44	2.99	2.51	1.13	-0.04
88	**GW20**	f4-CaMIX	1.66	-1.04	0.29	1.91	0.57	1.66	0.89	0.10
114	**GW20**	F4-CaHCO3	1.14	-1.03	0.24	1.79	1.35	1.89	1.12	0.29
65	GW21	F3-CaHCO3	3.21	-0.90	-0.40	0.92	1.43	2.42	0.63	-0.04
13	**GW22**	F4-NaHCO3	6.70	-0.89	0.22	3.18	2.12	2.42	1.02	0.23
38	**GW22**	F4-NaHCO3	-2.83	-1.23	0.49	3.76	0.50	2.22	0.70	0.53
78	**GW22**	F4-NaHCO3	-1.60	-0.89	-0.25	2.09	1.42	2.46	0.52	-0.14
22	GW23	F3-CaHCO3	6.15	-0.92	-0.34	0.34	0.74	2.01	0.59	-0.15
46	**GW24**	F4-CaHCO3	5.63	-0.76	-0.34	-0.18	1.52	2.40	0.95	0.31
89	**GW24**	F4-CaHCO3	-4.10	-0.99	-0.34	0.40	1.56	2.45	0.85	0.34
115	**GW24**	F3-CaHCO3	-5.57	-0.97	-0.41	1.29	2.06	2.93	0.74	0.39
45	GW25	F4-CaHCO3	0.29	-0.97	-0.39	-1.59	0.64	1.56	0.94	0.00
44	**GW26**	F4-CaHCO3	-11.61	-0.60	-0.47	-3.27	0.68	1.44	1.19	0.03
117	**GW26**	F4-CaHCO3	-10.40	-0.67	-0.56	-1.60	2.21	2.15	1.23	0.10
49	SW	F2-NaHCO3	10.94	-1.43	-1.20	-2.99	-2.03	1.04	-0.48	-1.14

4.4.6. Phreeqc model output

As stated in the methods section, CEC was the most important unknown for the model presented in this research. We opted to vary the CEC between 0.05 (model 1) and 0.35 (model 2) mol/kg. A groundwater flow velocity of 0.04 m/day was calculated using the parameters from equation (9) that were measured and a porosity of 0.3 for model 1. For model 2, a groundwater velocity of 0.08 m/day was calculated using the same measured parameters, but with an assumed porosity of 0.15. For model 1, a flush time (eq. 10) of 54 years was calculated whereas model 2 has a flush time of 27 years.

The values measured in the samples for chloride and sodium were plotted on the streamline distance from Nsooba channel where 0 is at the channel and 800 is the furthest point away from the channel (figure 4.24, 4.25). The field values showed a range of 0 to 3 mmol/l for chloride near Nsooba channel up to about x=400 m. After this point, a steep rise was observed in the field values going up to 11 mmol/l. A similar pattern for sodium was discovered where a steep rise occurs at the 400 m. mark. The model results for model 1 and model 2 were also displayed in figures 4.24 and 4.25.

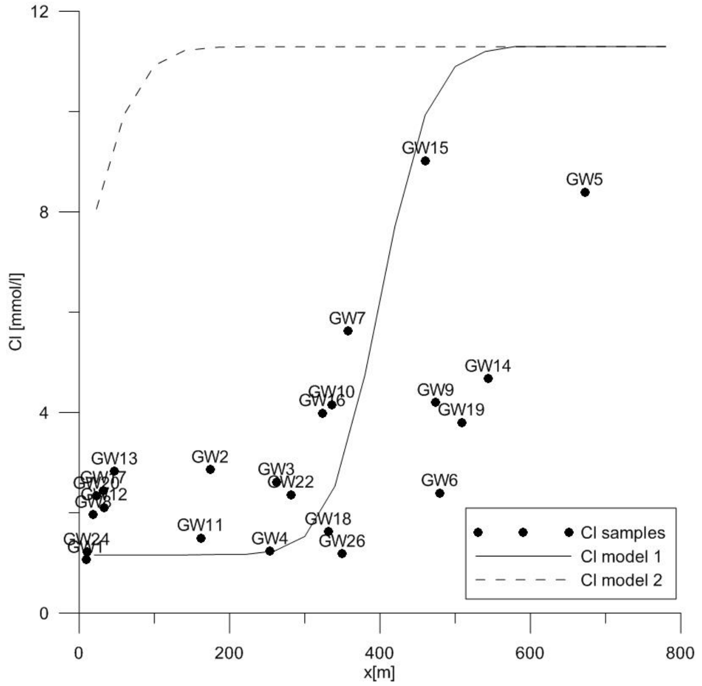

Figure 4.24: Sample values and model predictions for Chloride in the study area based on chosen endmember species. Model time = 27 years

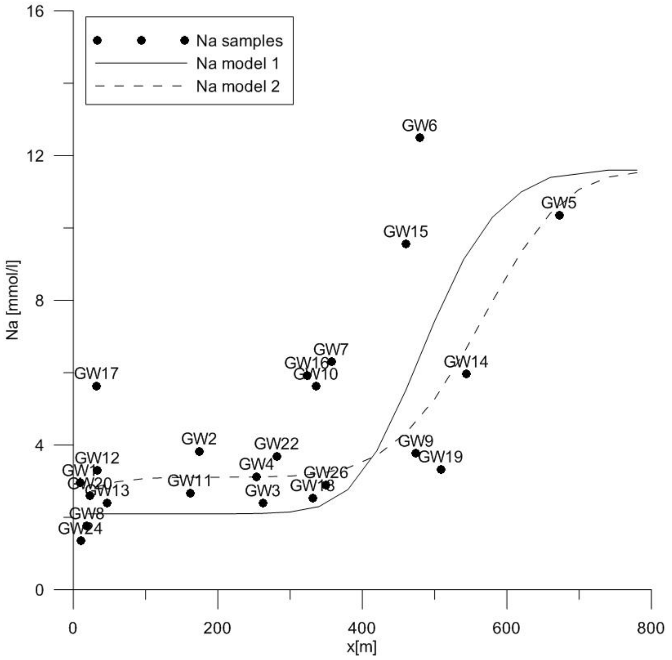

Figure 4.25: Sample values and model predictions for sodium in the study area based on chosen endmember species. Model time = 27 years

The model results helped us to explain the observed pattern, however the interpretations are quite different between the two models. For chloride as well as sodium, the predicted values by model 1 coincided well. This would mean that cation exchange capacity was indeed low and the groundwater flow was accurately schematized in the model. The results for model 2 coincided poorly with chloride showing that if no other processes occurred that affected the chloride concentrations, the groundwater flow assumed in model 2 was too high. Contrary to the poor chloride predictions, model 2 predicted the sodium concentrations almost as well as model 1. An explanation for this is that due to the high cation exchange capacity, sodium was retarded in the soil as explained by equation (25). This effect of retardation negated the higher groundwater flow in model 2 resulting in a similar sodium increase at a similar location on the streamline. The question therefore remained if no other processes affected the chloride concentrations. Assuming its conservative nature was correct, chemical reactions are impossible as an explanation. We did conclude in section 4.3.2 however that inundation of land near Nsooba channel had taken place and even though no effect of inundation was found in the diver data, small amounts of inundation water might leach into the aquifer decreasing the chloride concentrations such that the breakthrough-like pattern would actually be an artefact of inundation water. If both porosity and CEC were low, groundwater flow could indeed have been faster than assumed in model 1 and chloride and sodium could both have behaved conservatively, but would both have been affected by inundation. This could be a third option in line with the inundation water explanation.

The field results for calcium, magnesium and iron(II) (not shown) didn't show a correlation when plotted on a streamline. For calcium and magnesium, the concentrations in groundwater were probably not significantly elevated due to pit latrine input according to section 2.3.1. For iron(II), its availability in groundwater was primarily governed by redox conditions that were independent of distance to Nsooba channel.

The model and field results for potassium deviated from the previously described trends for the Cl^-, Na^+, Mg^{2+}, Ca^{2+} and Fe^{2+} components (figure 4.26). Potassium measured from samples in the field yielded high values compared to model predictions. This is in line with the enrichment that was observed earlier in section 4.4.4. and from section 2.3.1. Other than the dependency on input, the fate of potassium in groundwater remained elusive.

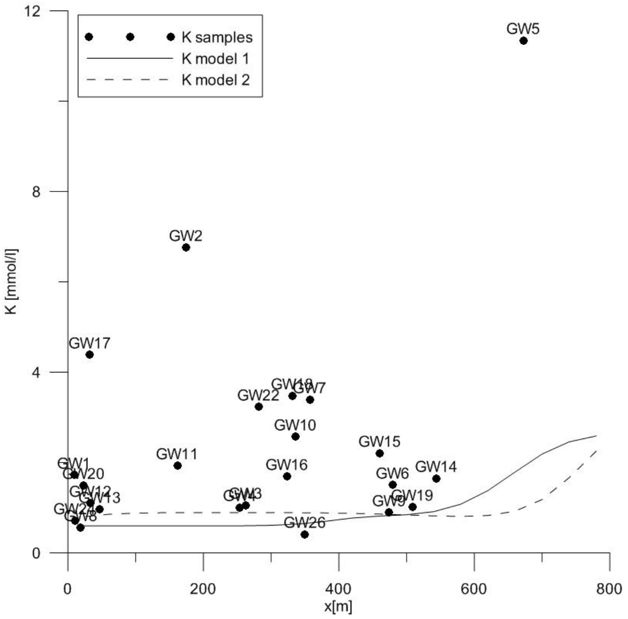

Figure 4.26: Sample values and model predictions for potassium based on chosen endmember species. Model time = 27 years

5. Discussion

The hydrological conditions of Bwaise were investigated in Kulabako et. al., (2007, 2008) and Nyenje et. al., (2012) as well as in this research. Comparison of the estimated flow velocity according to the Darcy equation for these three studies shows similar results where Nyenje et. al., (2012) reported an average value of 0.034 m/day, Kulabako et. al., (2008) reported 0.051 m/day and our study sits in between those values with 0.041 m/day with an assumed porosity of 0.3. Hydraulic conductivity yielded an average value of 3.43 m/day which is somewhat higher than the 2.3 and 1.7 m/day averages reported by Nyenje et. al., (2012) and Kulabako et. al., (2008) respectively, but overall we find these values to agree well. The fact that the Kulabako study yielded the highest flow velocity despite the lower hydraulic conductivity is most likely due to the increased steepness in topography found in the Bokasa and Kalimali areas of Bwaise. Porosity was not reported by Kulabako et. al., (2008) for the middle layer, but could also have caused the higher flow velocity. When we reduced our porosity to 0.15, a groundwater flow of 0.08 m/day was obtained which is markedly higher than the flow velocities obtained by all three studies, but since porosity has not been well documented for the middle layer we must consider the effects of its variation. The groundwater-surface water interactions showed the occurrence of flood events especially near the inflow transect of the study area. The data from this research do not give enough information to calculate exact volumes and locations of the floods. Additionally, to our knowledge it is unknown whether the smaller tertiary drains are also capable of overflowing. Observations done by Meijer (2011) during fieldwork in Bwaise confirm the occurrence of flooding during high intensity rainfall events.

Despite the occurrence of floods in the area, their effects on the groundwater levels were not registered by the divers. We can't conclude anything definite about the effects of inundation on the chemistry of the groundwater in Bwaise. We can however see that the chloride and sodium values in Nsooba channel from the work of Meijer (2011) were 2 mmol/l maximum during rainfall events which is much lower than polluted wells. If inundation did affect the groundwater chemistry sufficiently then polluted water could have been diluted near Nsooba channel. If inundation didn't affect groundwater chemistry then most likely the cation exchange capacity measured by Kulabako et. al., (2008) is erroneous. Laboratory errors were experienced during this study as well and it is not unlikely that reagents used in the analysis were impure either due to human error in preparation or due to pollution. From the history of Bwaise in section 2.3.1. it follows that the extent of housing remained fixed from approximately 1980 onwards. If one assumes that the greatest pollution input occurred from that point onwards, a flush time of 54 years with the peak of the breakthrough curve at 27 years coincides fairly well with the historical data available. The second and third model scenarios with a total flush time of 27 years, a delayed sodium presence and a reduction of chloride/sodium values due to inundation therefore also fits within historical data. It is however not possible to determine the exact variations of pollution input over time. It could for instance also be that Bwaise experienced stepwise development.

The analysis for geo-available metals yielded low results in general. For iron we found a value of 379.6 mg/kg. This compares fairly well to the values found by Kulabako et. al., (2008) in table 2.5. The weight percentage however is very low (0.04%) and it is unlikely that adsorption onto iron or aluminum complexes in the soil played a defining role in Bwaise. Meijer (2011) found a value of around 4000 mg/kg for iron in Nsooba channel sediments and these could therefore more effectively adsorb phosphorus by ligand exchange than the Bwaise soil. Nyenje et. al., (2012) found even lower values of 29 mg/kg iron in the middle layer at the solid waste and pit latrine site. An explanation for this may be the high sand percentage (73%) reported for the solid waste and latrine site. Soils with larger grain sizes are often reported to have a lower amount of sites available for sorption. Kulabako et. al., (2008) reported only 30% sand fraction for the middle layer which means smaller fractions are available to a greater extent. Our study showed a 65% sand value for the middle layer. Phosphorus sorption should therefore, based on soil texture, be more pronounced in the Bokasa and Kalimali zones compared to the Katoogo and St. Francis zones. Furthermore, the exact mechanism by which phosphorus is retained in soils is often complex where mediating substances like organic matter may promote or inhibit phosphate sorption depending on pH. Also, the effect of metal substitution in clay particles can facilitate positive edge sites available for phosphate sorption (de Mesquita Filho and Torrent, 1993). The mineralogy in Bwaise is as of yet insufficiently researched and insight into the nature of clay particles in Bwaise could improve our knowledge of adsorption. Kulabako et. al.,(2008) conclude based on CEC values that kaolinite should be well represented in the clay minerals of Bwaise. Additionally, from chapter 2, we have seen that both sorption and precipitation occur as a fast initial uptake followed by a more lengthy equilibration over time. This means that simply from dissolved or adsorbed concentrations of phosphate it is impossible to differentiate between sorption and precipitation. The phosphorus experiments in the Florida Keys by Corbett et. al., (1999) showed that a large amount of the injected phosphorus was adsorbed to the soil. Corbett et. al., related this to the high calcite content of the coastal aquifer. Jalali (2009) supports the view of calcite playing a major role in phosphorus adsorption, however they did not perform sorption experiments to show that this happens. Calcite has the potential to be a strong phosphorus adsorbent, unfortunately the calcite content of the soil in Bwaise is not exactly known. Young et. al., (2010) and Jayasingha et. al., (2011) report low nutrient concentrations in groundwater, but do not elaborate on the nature of the processes governing phosphate concentrations. Nitrate was generally accepted to be reduced. Young et. al., (2010) does mention that high retention times in an aquifer increase the capability for the removal of phosphorus as there is more time for phosphorus to be exposed to removal processes. This explanation was also invoked by Kulabako et. al., (2008) to explain higher phosphorus uptake by the soils at MW2 and MW3 sites relative to MW1 and MW4. This explanation does not hold for our research however, as the decreased hydraulic gradient in the Katoogo zone should produce increased removal of phosphorus relative to the St. Francis zone, but this was not measured. Additionally, no reason to assume macropore flow facilitated a short circuit in phosphorus transport in Bwaise was found even though Robinah draws upon this explanation for the observed lack of attenuation in the field relative to the adsorption experiments. The actual cause for the lack of attenuation in the field experiments is, according to us, still unexplained.

One of the ways this study expanded upon the knowledge already obtained from Bwaise is with the analyses of all cations and anions dissolved in groundwater. This allowed us to study the saturation indices of various minerals. It was shown in section 4.4.5 that the area dependent precipitation of hydroxyapatite and vivianite could regulate the phosphate values in Bwaise. Jalali et. al., (2009) reported that with calcium concentrations of 0.6 mmol/l, the SI for hydroxyapatite was found to be highly supersaturated for his research going up to 10 orders of magnitude. Our pH dependence shown in figure 4.23 shows that the average pH of 7.8 in the Jalali et. al., (2009) study may be the explanation for the high saturation index found. Other studies that reported significantly diminished phosphorus concentrations with respect to input did not include an analysis of saturation indices (Young et. al., 2010; Jayasingha et. al., 2011). The inhibitors for hydroxyapatite precipitation described by Cao et. al., (2007) could prevent the actual precipitation despite oversaturation. Magnesium has been found quite low in groundwater from Bwaise. Humic acid was not analyzed in this study, but given the high organic matter input due to pit latrine waste, dissolved humic acid may well be present in Bwaise. No inhibitors for vivianite precipitation were found in the literature.

From the results section, we concluded that the removal of nitrate and phosphate in the study area was significant relative to input by pit latrine pollution. One of the conclusions from the research by Meijer (2011) based on the inflow and outflow contaminant concentrations of Nsooba channel was that groundwater must have been a minor contributor to the water quality of Nsooba channel as there was almost no difference. Our research confirms this conclusion with orthophosphate values in groundwater mostly below 10 µmol/l. In relationship to the eutrophication standard proposed by Dodds et. al., (1998), groundwater did contain phosphorus concentrations in excess of the eutrophication standard and therefore does potentially contribute to the eutrophication of surface water bodies. The nature of this remaining orthophosphate in groundwater is not known though as the natural concentrations of orthophosphate in wetlands can be high due to the decay of organic material (section 2.2). The capacity for wetlands to retain nutrients has been found low according to Kansiime and Nalubega (1999), Kelderman et. al., (2007), Kanyiginya et. al., (2010)

6. Conclusions

From the geological data gathered, we confirmed the presence of three stratigraphic layers in the shallow aquifer system of Bwaise. The top layer was one of varying grain size and generally was linked to landfill material related to the reclamation of the wetland. The middle layer was a more sandy layer where the water table was also found and therefore we observed this to be the aquifer layer. After the initial encounter of the water table, typically it rose to a shallower depth indicating a system under pressure and therefore the nature of the aquifer was semi-confined. The bottom layer consisted of well consolidated material of finer grain size. This layer formed an effective seal separating the shallow water bearing layer from deeper aquifer systems.

The groundwater flow in Bwaise was found to be from Northeast to Southwest with an approximate gradient of 3 m/km, given that the hydraulic gradient was somewhat steeper in the St. Francis zone compared to the Katoogo zone of the research area. The average hydraulic conductivity was measured as 3.43 m/day by the use of slug tests and the subsequent groundwater flow was calculated to be 0.04 m/day assuming a porosity of 0.3 and 0.08 m/day with a porosity of 0.15. The study for the interaction between groundwater and surface water revealed that for the period of measurement, groundwater flow was largely towards Nsooba channel, except for brief reversals during high intensity rainfall events. From the moment the rainy season commenced, occurrences of flooding were registered. Diver data showed however that flooded water did not infiltrate to a great extent which meant that in the consideration of the water balance, it was not necessary to take flooding into account. The water balance for the aquifer yielded a system dominated by lateral subsurface flow as opposed to a rainfall dominated system. The closing error on the water balance was less than 10% which we found acceptable.

Our understanding of the possible effects of inundation was expanded by the phreeqc model outcome and the display of field values for chloride and sodium on flow path. The chloride and sodium values could be explained by a traditional breakthrough model where the groundwater flow was low and CEC was low. Inundation could however have decreased the chloride concentrations near Nsooba channel in case the porosity in the darcy equation was overestimated. CEC in the latter explanation could be higher than previously resulting in the significant retardation of sodium.

From the hydrochemical data and the analysis of EC, Cl^-, redox state and Stuyfzand parameters, it was concluded that 4 different classes of groundwater can be found in Bwaise. The most downstream transect of wells yielded unpolluted samples, in the Katoogo zone iron reducing polluted water was found, in the St. Francis zone nitrate reducing polluted water was found and along Nsooba channel, polluted water with variable concentrations for Cl^- and EC could be found. The nitrate concentrations in Bwaise were governed by a nitrate reduction process which removed all traces of nitrate from the groundwater when progressing downstream. Ammonium was significantly represented in groundwater with concentrations ussually above 1 mmol/l. Amonium values were lower still than input values which may be due to anaerobic ammonium oxidation playing a role here. Orthophosphate concentrations in groundwater (2-10 µmol/l) were found surprisingly low with respect to input concentrations (26.3 µmol/l). Both orthophosphate and ammonium presence in groundwater was similar despite the different groundwater classes identified.

Based on the low geo-available iron concentrations and relatively coarse grain size, it was concluded that adsorption on to metal hydroxides could not have played a major role in the study area. The study of saturation indices revealed however that hydroxyapatite had the potential to regulate orthophosphate concentrations in the St. Francis area and vivianite had the potential to do so in the Katoogo zone and Wakiso district. Combined, these two mineral phases were deemed the most likely control for orthophosphate in the entire research area, independently of the various other criteria for groundwater class.

Despite the significant reduction in orthophosphate values in groundwater, it was still found more than the eutrophication standard showing that if no dilution occurs, this groundwater still has a eutrophying effect on surface water.

7. Recommendations

Based on the findings in this study, the participating researchers would like to advise against the disposal of waste in tertiary drains as the soil of Bwaise is able to reduce the nutrient concentration to a great extent making it a healthier disposal route in terms of eutrophication risk. Additionally, the continued use of the pit latrines in slums residing over anaerobic aquifers is encouraged if the contents of the latrine are well contained and are only in contact with the soil system. We are aware that care needs to be taken with this advise as this study focused mainly on nutrient concentrations. The extent to which bacteria and viruses which can also be derived from pit latrines affect groundwater quality is as of yet unknown. The improvement of the current means of waste disposal in slums by the Kampala City Council could focus on the removal of waste from pit latrines as a service to the slum dwellers. A sewage connection would off course be ideal, however it is recognized that this service may as of yet be too expensive. Education on primary schools in slums could improve awareness amongst slum dwellers of the hygiene issues involved with pit latrine usage.

In terms of further research, x-ray diffraction analysis on the soil of Bwaise is advised in order to confirm or refute the current findings of hydroxyapatite and vivianite as joined controls on the orthophosphate concentrations in groundwater. Additionally, from the current body of data, the extent and magnitude of floods in Bwaise can be insufficiently quantified and therefore, the effects of the inundations on the groundwater chemistry are uncertain. Additionally, in order to establish a definitive distinction between adsorption and precipitation processes in sorption experiments a more mechanistic approach is advised such as the one recently introduced by Penn and Warren (2008). This method has been found able to distinguish between phosphate adsorption onto kaolinite (exothermic) and precipitation with aluminum (endothermic) based on reaction temperature during adsorption experiments.

References

Appelo C A J; Postma D (2005). Geochemistry, groundwater and pollution, 2^{nd} edition, CRC press London.

Argoss (2001). Guidelines to assessing the risk to groundwater from on-site sanitation. British Geological Survey Commissioned Report CR/01/142. BGS Keyworth, England.

Ateawung J N; Bashir I; Batelaan O (2010). A GIS based water balance study of Africa. Msc. Thesis at the University of Gent and University of Brussels, pp. 56

Van Beers (1958). The auger hole method.

Baross R; Isidoro D; Aragues R (2011). Long term water balances in La Violada irrigation district (Spain): I. Sequential assessment and minimization of closing errors. Agricultural Water Management, 102, pp. 35-45.

Berner R A (1981). Authigenic mineral formation resulting from organic matter decomposition in modern sediments. Fortschritte der Mineralogie, 59, pp. 117-135.

Bouwer H; Rice R C (1976). A slug test for determining hydraulic conductivity of unconfined aquifers with completely or partially penetrating wells. Water Resources Research, 12 (3), pp 423-428.

Bouwer H (1989). The Bouwer and Rice slug test – an update. Ground water, 27 (3), pp. 304-309.

Corbett D R; Kump L; Dillon K; Burnett W; Chanton J (1999). Fate of wastewater-borne nutrients under low discharge conditions in the subsurface of the Floride Keys, USA. Marine Chemistry, 69, pp. 99-115.

Cao X; Harris W G; Josan M S; Nair V D (2007). Inhibition of calcium phosphate precipitation under environmentally-relevant conditions. Science of the Total Environment, 383, pp. 205-215.

Cronin A A; Breslin N; Gibson J; Pedley S (2006). Monitoring source and domestic water quality in parallel with sanitary risk identification in Northern Mozambique to prioritise protection interventions. Journal of water and Health, 4(3), pp. 333-345.

De Mesquita Filho M V; Torrent J (1993). Phosphate sorption as related to mineralogy of a hydrosequence of soils from the Cerrado region (Brazil). Geoderma, 58, pp. 107-123.

Dodds W K; Jones J R; Welch E B (1998) Suggested classification of stream trophic state: distributions of temperate stream types by chlorophyll, total nitrogen, and phosphorus. Water Resources, 32, pp. 1455-1462.

Fitts C R; (2002). Groundwater Science. Academic press, pp. 450

Foppen J W; Kansiime F (2010). SCUSA: integrated approaches and strategies to address the sanitation crisis in unsewered slum areas in African mega-cities. Reviews in Environmental Science and Biotechnology, 8(4), pp. 305-311.

Freeze R A; Cherry J A (1979) Groundwater, Hemel-Hempstead: Prentice Hall international publishers, pp. 604.

Gelinas Y; Randall H; Robidoux L; Schmitt JP (1996). Well water survey in two districts of Conakry (Republic of Guinea), and comparison with the piped city water. Water Research, 30 (9), pp. 2017-2026

Griffioen J (2005). Extent of immobilisation of phosphate during aeration of nutrient rich, anoxic groundwater. Journal of Hydrology, 320, 359-369.

HACH (1997-2009). DR/890 colorimeter procedures manual. HACH company, 614 pp.

Haruna R; Ejobi F; Kabagambe E K (2005). The quality of water from protected springs in Katwe and Kisenyi parishes, Kampala city, Uganda. African health sciences, 5.

Hiradate S; Uchida N (2004). Effect of soil organic matter on pH-dependent phosphate sorption by soils. Soil Science and Plant Nutrition, 50, 65-675.

Holman I P; Whelan M J; Howden N J K; Bellamy P H; Willby N J; Rivas-Casado M; McConvey P; (2008). Phosphorus in groundwater – an overlooked contributor to eutrophication? Hydrological Processes, 22, pp. 5121-5127.

Holtan H; Kamp-Nielsen L; Stuanes A O (1988). Phosphorus in soil, water and sediment: an overview. Hydrobiologia, 170, pp. 19-34.

Hongve D (1997). Cycling of iron, manganese and phosphate in a meromictic lake. Limnology and Oceanography, 42, pp. 635-647.

Howard G; Stephen P; Barrett M; Nalubega M; Johal K (2003). Risk factors contributing to microbiological contamination of shallow groundwater in Kampala, Uganda. Water research, 37, 3421-3429.

Jalali M (2009). Phosphorous concentration, solubility and species in the groundwater in a semi-arid basin, southern Malayer, western Iran. Environmetal Geology, 57, pp. 1011-1020.

Jayasingha P; Pitawala A; Dharmagunawardhane H A (2011). Vulnerability of coastal aquifers due to nutrient pollution from agriculture: Kalpitiya, Sri Lanka. Water, Air and Soil pollution, 219, pp. 563-577.

Jensen D L; Boddum J K; Tjell JC; Christensen T H (2002). The solubility of rhodochrosite ($MnCO_3$) and siderite ($FeCO_3$) in anaerobic aquatic environments. Applied Geochemistry, 17, pp. 503-511.

Jetten M S M; Strous M; van de Pas-Schoonen K T; Schalk J; van Dongen U G J M; van de Graaf A A; Logemann S; Muyzer G; van Loosdrecht M C M; Kuenen J G (1998). The anaerobic oxidation of ammonium. FEMS Microbiology Reviews, 2, pp. 421-437.

Kiptum C K; Ndambuki J M (2012). Well water contamination by pit latrines: a case study of Langas. International Journal of Water Resources and Environmental Engineering, 4, pp. 35-43.

Kelderman P; Kansiime F; Tola M A; van Dam A (2007). The role of sediments for phosphorus retention in the Kirinya wetland (Uganda). Wetland Ecology Management, 15, 481-488.

Krapac I G; Dey W S; Roy W R; Smyth C A; Storment E; Sargent S L; Steele J D (2001). Impact of swine manure pits on groundwater quality. Environmental Pollution, 120, pp. 475-492.

Kulabako N R; Nalubega M; Thunvik R (2007). Study of the impact of land use and hydrogeological settings on the shallow groundwater quality in a peri-urban area of Kampala, Uganda. Science of the total environment, 381, pp. 180-199.

Kansiime F; Nalubega M (1999). Natural treatment by Uganda's Nakivubo swamp. Water Quality International, (Mar./Apr.), pp. 29-31.

Kanyiginya V; Kansiime F; Kimwaga R; Mashauri D A (2010). Assessment of nutrient retention by Natete wetland Kampala, Uganda. Physics and Chemistry of the Earth, 35, 657-664.

Katukiza A Y; Ronteltap M; Oleja A; Niwagaba C B; Kansiime F; Lens P N L (2010). Selection of sustainable sanitation technologies for urban slums — A case of Bwaise III in Kampala, Uganda. Science of the total environment, 409, pp. 52-62.

La Mer V K (1962). The solubility behavior of hydroxylapatite. Journal of colloid science, 66, pp. 973-978.

McGechan M B; Lewis D R (2002). Sorption of phosphorus by soil, part 1: Principles, equations and models. Biosystems Engineering, 82, pp. 1-24.

McNamara J P; Siegel D I; Glaser P H; Beck R M (1992) Hydrogeologic controls on peatland development in the Malloryville Wetland, New York (USA). Journal of Hydrology, 40, pp. 279-296.

Marshall B E; Falconer A C (1973). Eutrophication of a Tropical African Impoundment (Lake McIlwaine, Rhodesia). Hydrobiologia, 1-2, 109-123.

Massmann G; Tichomirowa M; Merz C; Pekdeger A (2003). Sulfide oxidation and sulfate reduction in a shallow groundwater system (Oderbruch aquifer, Germany). Journal of Hydrology, 278, pp. 231-243.

Meijer L (2011). Understanding the fate and transport of phosphorus in streams draining an unsewered slum in sub-Saharan Africa. Msc. Thesis in collaboration with UNESCO-IHE (Delft and University of Amsterdam (Amsterdam), pp. 109.

Mugisha P; Kansiime F; Mucunguzi P; Kateyo E (2007). Wetland vegetation and nutrient retention in Nakivubo and Kirinya wetlands in the Lake Victoria basin of Uganda, Physics and Chemistry of the Earth, 32, pp. 1359-1365.

Nicholson B J; Vitt D H (1994). Wetland devlopment at Elk Island National Park, Alberta, Canada. Journal of Paleolimnology, 12, pp. 19-34.

Nonner J C (2003). Introduction to hydrogeology. A.A.Balkema publishers, pp. 248

Nyaakana J B; Sengendo H; Lwasa S. Population (2004). Urban development and the environment in Uganda: the case study of Kampala city and its environs. Committee for International Cooperation in National Research in Demography. URL address: http://www.cicred.org

Nyenje P M; Foppen J W; Uhlenbrook S; Kulabako R; Muwanga A (2010). Eutrophication and nutrient release in urban areas of sub-Saharan Africa — A review. Science of the total Environment, 408, pp. 447–455.

Nyenje P M; Foppen J W; Uhlenbrook S; Kulabako R; Muwanga A (2012). Processes governing nutrient pollution in shallow aquifers underlying pit latrines and solid waste sites in slums. Personal communication, currently in review.

Okalebo J R; Gathua K W; Woomer P L (2002). Laboratory methods of soil and plant analysis: a working manual, 2nd edn. Tropical soil biology and fertility programme. Sacred Africa Publishers, Nairobi, Kenya, pp 88.

Parkhurst D L; Appelo C A J (1999) User's guide to PhreeQC (version 2) – A computer program for speciation, batch reaction, one-dimensional transport, and inverse geochemical calculations, pp. 326. URL address: wwwbrr.cr.usgs.gov.

Penn C J; Warren J G (2008). Investigating phosphorus sorption onto kaolinite ing Isothermal Titration Calorimetry. Soil Science Society of America Journal, 73, 560-568.

Postma D (1980). Formation of siderite and vivianite and the pore-water composition of a recent bog sediment in Denmark. Chemical Geology, 31, 225-244.

Qian J; Wang L; Zhan H; Chen Z (2011). Urban land-use effects on groundwater phosphate distribution in a shallow aquifer, Nanfei River basin, China. Hydrogeology Journal, 19, pp. 1431-1442.

Richardson C J; Qian S; Craft C B; Qualls R G (1997). Predictive models for phosphorus retention in wetlands. Wetlands Ecology and Management, 4, pp. 159-175.

Rivett M O; Buss S R; Morgan P; Smith J W N; Bemment C D (2008). Nitrate attenuation in groundwater: A review of biogeochemical controlling processes. Water Research, 42, pp. 4215-4232.

Robillard P D; Sharpe W E; and Wistock B R (2003). Nitrates in drinking water. Pennsylvania State University, Agricultural and Biological Engineering.

Reeve A S; Siegel D I; Glaser P H (1994). Geochemical controls on peatland pore water from the Hudson Bay lowland: a multivariate statistical approach. Journal of Hydrology, 181, pp. 285-304.

Schwindzer C R; Tomberlin T J (1982). Chemical and physical characteristics of shallow ground waters in northern Michigan Bogs, Swamps and Fens. American Journal of Botany, 69, pp. 1231-1239.

Sposito G (2008) The chemistry of soils, second edition. Oxford University Press, pp. 329.

Smith R L; Howes B L; Duff J H (1991). Denitrification in nitrate-contaminated groundwater: Occurrence in steep vertical geochemical gradients. Geochimica et Cosmochimica acta, 55, 1815-1825.

Sternbeck J (1996). Kinetics of rhodochrosite crystal growth at 25°C: the role of surface speciation. Geochimica et Cosmochimica Acta, 61, 785-793.

Stuyfzand, P.J. (1993). Hydrochemistry and hydrology of the coastal duune area of the western Netherlands. Ph.D. Thesis Vrije Universiteit, Amsterdam, The Netherlands, ISBN 90-74741-01-0.

Taylor R; Howard M (2000). A tectono-geomorphic model of the hydrogeology of deeply weathered crystalline rock: Evidence from Uganda. Hydrogeology journal, 8, pp. 279-294.

UBOS (2002). Census population size growth analytical report. Uganda Bureau of Statistics. URL address: http://www.ubos.org.

UN-HABITAT (2002). Sustainable urbanization - achieving agenda 21. URL address: http://www.unhabitat.org/pmss

UNEP (2002). African Environment outlook; past, present and future perspectives. URL address: http://www.unep.org/dewa/africa.

UNEP (2007). Africa Environment Outlook 2; chapter 4 - freshwater. URL address: http://www.unep.org/dewa/africa.

Wassen M J; Barendregt A; Bootsma M C; Schot P P (1988). Groundwater chemistry and vegetation of gradients from rich fen to poor fen in the Naardermeer (the Netherlands). Vegetation, 79, pp. 117-132.

Warah R (2003). The challenge of slums: Global report on human settlements. UN human settlements programme. URL address: www.globalpolicy.org/socecon/develop/africa/2003/03slums.htm

Wartel M; Skiker M; Auger Y; Boughriet A (1989). Interaction of manganese(II) with carbonates in seawater: Assessment of the solubility product of $MnCO_3$ and Mn distribution coefficient between the liquid phase and $CaCO_3$ particles. Marine Chemistry, 29, pp. 99-117.

WHO (2008) a. Guidelines for drinking water quality; volume 1 recommendations, 3rd edition. World Health Organization, Geneva.

WHO (2008) b. Water, Sanitation and hygiene. URL address: http://apps.who.int/ghodata/.

Appendix I

All groundwater level measurements in meter above sea level

x-coord	y-coord	Well	TOC [m.a.s.l.]	03/02/2011	11/02/2011	16/02/2011	25/02/2011	07/03/2011	16/03/2011	24/03/2011	02/04/2011
451058	38664	**GW1**	1139.43	1138.7	1138.45	1138.35	1138.25	***	1139.11	1138.91	1139.11
450946	38808	**GW2**	1139.647	1138.95	1138.96	1138.93	1138.86	1138.78	1139.00	1139.05	1139.15
450889	38892	**GW3**	1141.066	1140.35	1140.32	1140.27	1140.26	1140.23	1140.50	1140.43	1140.50
450837	38875	**GW4**	1141.517	1140.73	1140.50	1140.49	1140.56	1139.80	1140.82	1140.73	1140.77
450766	38890	**GW5**	1143.18	1141.60	1141.60	1141.56	1141.52	1141.34	1141.38	1141.52	1141.68
450854	38790	**GW6**	1139.255	1139.01	1138.95	1138.90	1138.88	1138.86	1139.05	1139.01	1139.05
450820	38724	**GW7**	1139.333	1138.42	1138.31	1138.25	1138.15	1138.07	1138.73	1138.61	1138.78
450916	38652	**GW8**	1139.381	1138.69	1138.60	1138.57	1138.52	1138.44	1138.98	1138.90	1139.12
450528	38796	**GW9**	1138.725	1138.10	1137.96	1137.89	1137.78	1137.72	1138.08	1138.23	1138.37
450429	38721	**GW10**	1138.503	**	**	1138.07	1138.03	1137.99	1138.01	1138.12	1138.27
450388	38616	**GW11**	1138.88	1137.72	1137.62	1137.62	1137.55	1137.49	1138.30	1138.00	1138.32
450511	38531	**GW12**	1138.798	1137.81	1137.69	1137.69	1137.63	1137.65	1138.24	1137.96	1138.30
450762	38531	**GW13**	1138.809	1138.33	1138.22	1138.14	1138.02	1137.93	1138.43	1138.45	1138.21
450474	38869	**GW14**	1139.184	1138.67	1138.56	1138.48	1138.40	1138.22	1138.54	1138.76	1138.90
450562	38780	**GW15**	1138.319	1138.16	1137.97	1137.88	1137.78	1137.61	1138.27	1138.27	1138.31
450676	38701	**GW16**	1138.959	1138.48	1138.40	1138.39	1138.33	1138.28	1138.48	1138.54	1138.67
450397	38539	**GW17**	1138.778	1137.89	1137.77	1137.73	1137.64	1137.57	1138.23	1138.02	1138.29
450315	38747	**GW18**	1138.284	1137.76	1137.68	1137.62	1137.55	1137.49	1138.16	1138.03	1138.18
450326	38865	**GW19**	1138.613	***	1138.32	1138.28	1138.20	1138.15	1138.31	1138.31	1138.50
450285	38542	**GW20**	1139.152	1137.65	1137.53	1137.50	1137.43	1137.37	1137.94	1137.79	1138.13
450393	38519	**GW21**	1139.081	1137.77	1137.63	1137.59	1137.57	1137.63	1137.98	1137.87	1137.94
450484	38682	**GW22**	1138.39	1137.92	1137.75	1137.68	1137.59	1137.49	1138.28	1138.20	1138.29
451058	38660	**GW23**	1139.505	1138.36	1138.32	1138.34	1138.30	1138.22	1138.68	1138.52	1138.72
450103	38554	**GW24**	1138.054	*	*	*	*	1137.29	1137.85	1137.46	1137.90
450116	38637	**GW25**	1138.025	*	*	*	*	1137.27	1137.87	1137.45	1137.89
450098	38775	**GW26**	1137.991	*	*	*	*	1137.42	1137.92	1137.63	1137.93
450575	38878	**SW**	1141.094	**	**	1140.01	1139.98	1139.96	1140.05	1140.09	**
450635	38860	**LS**	1141.111	**	**	1140.76	1140.47	1140.48	1140.47	1140.50	1140.50

* well was not yet installed at this time ** lock to the well would not open *** well run dry

Appendix II

	Analysis	Location	Equipment
Geology	Grain size	Makarere soil science lab	Sieves/hydrometer
	Geo-available metals	Utrecht Geochemistry lab	Spectro Ciros ICP-OES
Hydrology	Groundwater levels	Fieldwork	Tape measure
	Hydraulic conductivity	Fieldwork	Slug test
Chemistry	pH	Fieldwork	WTW pH 340i
	EC	Fieldwork	WTW EC3330i
	Temperature	Fieldwork	WTW pH 340i
	Alkalinity	Fieldwork	Hach field titration kit
	Nitrate	Fieldwork	HACH DR 890
	Orthophosphate	Fieldwork	HACH DR 890
	Ammonium	Fieldwork	HACH DR 890
	Dissolved cations	UNESCO-IHE lab	Thermo Scientific x-series 2 ICP-MS
	Dissolved anions	UNESCO-IHE lab	Dionex ICS-1000